

University of Mississippi

eGrove

---

Electronic Theses and Dissertations

Graduate School

---

2019

## Developing Zebrafish as an In Vivo Model to Screen Compounds for Anti-Cancer Activity in Human Breast Cancer

Trisha Dhawan

*University of Mississippi*

Follow this and additional works at: <https://egrove.olemiss.edu/etd>



Part of the [Pharmacology Commons](#)

---

### Recommended Citation

Dhawan, Trisha, "Developing Zebrafish as an In Vivo Model to Screen Compounds for Anti-Cancer Activity in Human Breast Cancer" (2019). *Electronic Theses and Dissertations*. 1598.

<https://egrove.olemiss.edu/etd/1598>

This Dissertation is brought to you for free and open access by the Graduate School at eGrove. It has been accepted for inclusion in Electronic Theses and Dissertations by an authorized administrator of eGrove. For more information, please contact [egrove@olemiss.edu](mailto:egrove@olemiss.edu).

DEVELOPING ZEBRAFISH AS AN IN VIVO MODEL TO SCREEN  
COMPOUNDS FOR ANTI-CANCER ACTIVITY IN HUMAN BREAST  
CANCER

A Dissertation  
presented in fulfillment of requirements  
for the degree of Doctor of Philosophy  
in the Department of BioMolecular Sciences  
Division of Pharmacology  
The University of Mississippi

by

Trisha Dhawan

December 2018

Copyright © 2018 by Trisha Dhawan

All rights reserved

## ABSTRACT

Breast Cancer (BC) is the most frequently diagnosed cancer; 1:8 women are at risk of developing BC in her lifetime. Cancer metastasis causes the majority of deaths in BC patients. Moreover, side effects of traditional chemotherapeutic drugs (TCD) impair the quality of life of these patients. Discovery and development of safe and effective new therapies is imperative for the treatment of BC and targeting metastasis. The goal herein is to further expand the applicability of transgenic zebrafish for *in vivo* xenotransplantation of human BC cells and to screen potential chemotherapeutics for toxicity and efficacy. For xenotransplantation, MCF-7, BT-474, and MDA-MB-231 BC cells were used to canvas the benign and malignant types of BC, respectively. Fluorescently-labeled MCF-7, BT-474, and MDA-MB-231 cells and the cytotoxic effect of TCD (doxorubicin, 4-hydroxytamoxifen, and paclitaxel) were determined for validation *in vitro* using cell viability assay. Test compounds (extracts of *Tinospora crispa* and potent microtubule inhibitors) were used to determine the cytotoxicity *in vitro*. Maximally tolerated concentration and no observed adverse effect level (NOAEL) of were determined in zebrafish following a waterborne exposure to concentrations (1-50  $\mu\text{M}$ ) of doxorubicin, 4-hydroxytamoxifen, paclitaxel, and curcumin and (10-800 nM) mertansine, ansamitocin P-3, and monomethyl auristatin E (MMAE) over 96 hours. NOAELs for paclitaxel, mertansine, ansamitocin P-3, and MMAE were 25, 400,

50, and 400 nM, respectively. Zebrafish were xenotransplanted with MCF-7, BT-474, and MDA-MB-231 cell lines to observe the effects of exposure to microtubule inhibitors on the proliferation of cancer cells. After xenotransplanting 50-100 BC cells/larva at 2 days post-fertilization, cell growth and migration were imaged at 1 and 5 days post-injection using fluorescent microscopy. Paclitaxel (25nM) significantly reduced the proliferation of MCF-7 cell xenografts compared to controls, confirming the use of this model for MCF-7 cell xenografts. Mertansine (10 and 200 nM) also significantly reduced the proliferation of MCF-7 cells. To our knowledge, this is the first study that used paclitaxel in BC xenografts even though it is a widely used chemotherapeutic in the treatment of BC. Additionally, NOAEL *in vivo* and cytotoxic effects of mertansine in zebrafish xenografts have not been studied before.

## **DEDICATION**

This journey of a thousand miles started with a single step.

Dedicated to Abhishek Upadhyay- for words will never be enough.

## **ACKNOWLEDGMENTS**

Filled with immense support, love, compassion, and guidance, the past five years have been so memorable because of many people. Firstly, my advisor, Dr. Kristie Willett, who I believe is a superwoman. I look up to her how she constantly works and aspire to be a small percentage of how she is, someday. She believed in my ideas and encouraged me constantly even when we didn't have the funding, and always welcomed me with a smile. I am beyond grateful for her constant support and guidance throughout this period. My committee members, Dr. Tracy Brooks, who held my hand without second thoughts and agreed to support this collaboration, trained me with cell culture techniques, and critical thinking. Dr. Asok Dasmahapatra, for his ever readiness to help and valuable feedback. Dr. Shabana Khan, for her mentoring, offering the workspace and supplies, and valuable feedback to improve my experiments. Dr. David Colby, who agreed to serve on my ORP committee, encouraged me to explore new ideas, and guided me when I needed help. I cannot thank Cammi Thornton, our lab manager, enough who was ever ready to troubleshoot, help, and never ever said no to anything. Dr. Sudeshna Roy for guiding me how to use Chemdraw software.

There is a whole host of faculty who I would like to thank for letting me use their microscopes. Dr. Vijayshankar Raman, Dr. Bradley Jones, Dr. Lainy Day, Dr. Babu Tekwani, Dr.

Jason Paris, and Dr. Nicole Ashpole. My experiments would never have completed without Dr. Ashpole's and Dr. Paris's microscope, I am very grateful to both for accommodating me amidst their lab work.

I would also like to thank the staff of BMS- Sherrie, who wears the brightest smile, Danielle and Candace, who are always there for the graduate students and make things easier for everyone in the department. Friends and colleagues in the School of Pharmacy, without whom the Friday nights wouldn't be so memorable.

I am forever grateful to my parents, who supported my decision of leaving India to pursue higher studies in a different continent, far far away from home. I am indebted to my dear friends, Sharon, Paramjeet, Gurpartap, Ishwadeep, Abhijeet, Suprabh, Shobhan, and Manjeet for their support throughout this period.

I also want to thank my parents in-law who supported my decision and encouraged me to continue my journey after marriage, and showered love and blessings on me.



## LIST OF ABBREVIATIONS AND SYMBOLS

4-OH-TAM	4-hydroxytamoxifen
ADC	Antibody drug conjugate
ALCL	Anaplastic large cell lymphoma
AUC	Area under the curve
BC	Breast cancer
BCSG1	Breast cancer specific gene 1
CF4	Fourth generation cross between casper and fli
CIPN	Chemotherapy induced peripheral neuropathy
CM-DiI	Chloromethyl-benzamidodialkylcarbicyanine
CYP1B1	Cytochrome P450 1B1
DNA	Deoxyribonucleic acid
DOX	Doxorubicin
DPF	Days post fertilization
DPI	Days post injection
EBCTCG	Early breast cancer trialists' collaborative group

ECM	Extracellular matrix
ER	Estrogen receptor
FITC	Fluorescein isothiocyanate
GDP	Guanine diphosphate
GTP	Guanine triphosphate
HER2	Human epidermal growth receptor 2
HPI	Hours post injection
IC50	Inhibitory concentration 50%
LUT	Look up table
MAP	Microtubule associated proteins
MED	Minimum effective dose
MMAE	Monomethyl auristatin
MTC	Maximally tolerated concentration
MTD	Maximum tolerated dose
MTS	(3-(4, 5-dimethylthiazol-2-yl)-5-(3-carboxymethoxyphenyl)-2-(4-sulfophenyl)-2h- tetrazolium
NOAEL	No observed adverse effect level
PR	Progesterone receptor
PTX	Paclitaxel

SERM	Selective estrogen receptor modulator
TAM	Tamoxifen
TGF- $\beta$	Transforming growth factor
TNBC	Triple negative breast cancer
TRITC	Tetramethylrhodamine isothiocyanate
VEGF	Vasculoendothelial growth factor

## TABLE OF CONTENTS

<b>ABSTRACT</b> .....	<b>II</b>
<b>DEDICATION</b> .....	<b>IV</b>
<b>ACKNOWLEDGMENTS</b> .....	<b>V</b>
<b>LIST OF ABBREVIATIONS AND SYMBOLS</b> .....	<b>VII</b>
<b>TABLE OF CONTENTS</b> .....	<b>X</b>
<b>LIST OF TABLES</b> .....	<b>XIV</b>
<b>LIST OF FIGURES</b> .....	<b>XV</b>
<b>CHAPTER I INTRODUCTION</b> .....	<b>1</b>
1.1 BREAST CANCER .....	1
<i>1.1.1 Metastasis</i> .....	2
<i>1.1.2 Tumor microenvironment</i> .....	5
<i>1.1.3 Traditionally used chemotherapeutics</i> .....	6
1.2 TRENDS IN BREAST CANCER DRUG DISCOVERY: .....	9
<i>1.2.1 Antibody Drug Conjugates (ADC)</i> .....	10

1.2.2 <i>Microtubule inhibitors as payloads:</i> .....	13
1.3 NATURAL PRODUCTS AS ANTI-CANCER COMPOUNDS.....	17
1.3.1 <i>Tinospora crispa</i> .....	18
1.4 XENOTRANSPLANT MODELS: .....	22
1.4.1 <i>Transgenic zebrafish as an anti-cancer drug screening model:</i> .....	23
1.4.2 <i>Patient derived xenografts</i> .....	25
1.4.3 <i>Advantages of using zebrafish vs. mouse for xenotransplantation:</i> .....	26
1.5 SPECIFIC AIMS .....	28
1.5.1 <i>Specific Aim 1- Establish anti-cancer efficacy and potential therapeutic index for test compounds in breast cancer cell lines:</i> .....	30
1.5.2 <i>Specific Aim 2- Demonstrate the maximally tolerated concentration (MTC) of anti-cancer compounds in vivo using zebrafish:</i> .....	30
1.5.3 <i>Specific Aim 3: Determine the efficacy and therapeutic index of the compounds in zebrafish embryos xenografted with human breast cancer cells.</i> .....	31
<b>CHAPTER II EXPERIMENTAL METHODS.....</b>	<b>32</b>
2.1 CELL CULTURE .....	32
2.1.1 <i>Labeling human breast cancer cells with fluorescent dye</i> .....	33
2.1.2 <i>Compounds</i> .....	33
2.1.3 <i>Cell Viability Assay</i> .....	33

2.2 ZEBRAFISH CULTURE.....	35
2.2.1 <i>Crossbreeding zebrafish</i> .....	36
2.3 MAXIMALLY TOLERATED CONCENTRATION (MTC) AND NO OBSERVED ADVERSE EFFECT LEVEL (NOAEL) IN ZEBRAFISH LARVAE .....	38
2.4 XENOTRANSPLANTATION.....	38
2.4.1 <i>Preparing cells for transplantation</i> .....	38
2.4.2 <i>Preparation of zebrafish for microinjection</i> .....	39
2.4.3 <i>Xenotransplant of CM-DiI labeled MCF-7, BT-474, and MDA-MB-231 cells in zebrafish larvae/embryos</i> .....	39
2.5 QUANTIFICATION OF BREAST CANCER CELL PROLIFERATION .....	40
2.5.1 <i>Preparation and mounting of xenotransplanted zebrafish for fluorescence microscopy</i> .....	40
2.5.2 <i>Imaging the xenotransplanted zebrafish larvae</i> .....	41
2.5.3 <i>Analysis of images obtained</i> .....	41
<b>CHAPTER III ZEBRAFISH AS AN IN VIVO SCREEN FOR COMPOUNDS WITH ANTI-CANCER ACTIVITY IN HUMAN BREAST CANCER .....</b>	<b>44</b>
3.1 RESULTS .....	44
3.1.1 <i>Determination of in vitro cytotoxicity in labeled vs unlabeled breast cancer cell lines</i> .....	44

3.1.2 Determination of NOAEL and MTC of test compounds in zebrafish: .....	50
3.1.3 Validation of transgenic zebrafish as a xenotransplant model for human breast cancer: .....	54
3.2 DISCUSSION .....	63
<b>CHAPTER IV FUTURE DIRECTIONS .....</b>	<b>72</b>
<b>BIBLIOGRAPHY .....</b>	<b>74</b>
<b>APPENDIX .....</b>	<b>86</b>
1.1 IN VITRO OPTIMIZATION .....	87
1.1.1 Transfection vs. Lypophilic dye .....	87
1.1.2 Effect of media on growth of different cancer cells: .....	87
1.1.3 Effect of Doxorubicin in zebrafish larvae .....	88
1.2 IN VIVO OPTIMIZATION .....	90
1.2.1 Preparation of agar coated petridish for microinjection: .....	90
1.2.2 Xenotransplant optimization .....	91
1.2.3 Microscopy optimization .....	94
1.3 QUANTIFICATION OF BREAST CANCER CELL PROLIFERATION VIA PCR .....	95
<b>VITA .....</b>	<b>99</b>

## LIST OF TABLES

<b>Table 1:</b> Mice vs. Zebrafish as xenotransplant models.....	28
<b>Table 2:</b> <i>Tinospora crispa</i> fractions tested in MCF-7 and MDA-MB-231 cells for cytotoxicity	47
<b>Table 3:</b> MTC and NOAEL determined for various anti-cancer compounds .....	53
<b>Table 4:</b> Percent incidence of deformities observed in larvae at MTC.....	54
<b>Table 5</b> Trial 1-Determination of metastatic behavior of MCF-7, BT-474, and MDA-MB-231 cells in zebrafish xenografts.....	57
<b>Table 8</b> IC50 values of microtubule inhibitors in literature .....	65
<b>Table 9:</b> RT-qPCR primers .....	97



## LIST OF FIGURES

<b>Figure 1:</b> Components of an antibody drug conjugate (ADC).....	12
<b>Figure 2:</b> Chemical structures of monomethyl auristatin e (MMAE), ansamitocin P-3, and mertansine.....	16
<b>Figure 3:</b> Chemical structures of various constituents of <i>T. crispa</i> tested for cytotoxicity in MCF-7 and MDA-MB-231 BC cells.....	20
<b>Figure 4:</b> From bench to bedside, overview of the process of patient derived xenograft drug discovery model.....	26
<b>Figure 5:</b> Layout of the xenograft experiments.....	31
<b>Figure 6:</b> Breast cancer cell lines used in the in vitro and in vivo experiments.....	32
<b>Figure 7:</b> Schematic representation of Casper and Tg(fli1a: EGFP) crosses.....	37
<b>Figure 8</b> Pictomicrograph showing xenografted larva at 5 dpi (A) and in (B) the cell counting procedure using graticules in blue, each at a distance of 100 microns away from the site the injection.....	43
<b>Figure 9:</b> Determination of potential sensitivity to CM-DiI in MCF-7 labeled and unlabeled cells after treatment with 4-OH-TAM and doxorubicin.....	46
<b>Figure 10:</b> Determination of cytotoxicity of <i>Tinospora crispa</i> fractions in MDA-MB-231 and	

MCF-7 cells.. .....	48
<b>Figure 11:</b> Determination of cytotoxicity of mertansine and paclitaxel in A) MCF-7, B) BT-474, and C) MDA-MB-231 cells. ....	49
<b>Figure 12:</b> Survival of zebrafish larvae after an exposure to different concentrations of doxorubicin, pravastatin, curcumin, and 4-OH-TAM (n=12) to determine the maximally tolerated concentration in the larvae. ....	50
<b>Figure 13:</b> Survival of zebrafish larvae after an exposure to different concentrations of potent microtubule inhibitors to determine the maximally tolerated concentration in the larvae (n = 12). ....	52
<b>Figure 14:</b> Survival of zebrafish larvae after an exposure of 10-100 nM of PTX and mertansine (n = 12). ....	53
<b>Figure 15:</b> Zebrafish larvae xenografted with the three BC cell lines.were imaged at 1 dpi.....	58
<b>Figure 16:</b> Zebrafish larvae xenografted with the three BC cell lines were imaged at 5 dpi.....	59
<b>Figure 17:</b> Trial 1 with MCF-7, BT-474, and MDA-MB-231 cells xenografted in zebrafish larvae. ....	60
<b>Figure 18:</b> Fold change in A) percentage of cells beyond 500 $\mu$ m, and B) in total number of cells in MCF-7 xenografted larvae treated with 25 nM Paclitaxel as compared with controls .....	61
<b>Figure 19:</b> Percent incidence of cells that traveled beyond A) 500 $\mu$ m and B) 1000 $\mu$ m in Trials 1, 2, and 3 in zebrafish larvae xenografted with MCF-7 cells at in Trials 1, 2, and 3 at 5 dpi.....	62
<b>Figure 20</b> Pictomicrographs of 4-day old zebrafish larvae after exposure to 12.5 $\mu$ M DOX for 24	

hours. Image acquired at 10x magnification using brightfield, FITC, and TRITC filters ..... 89

**Figure 21:** Percent incidence of larvae incubated at 34 for a period of 4 days for different parameters was evaluated. .... 91

**Figure 22:** Pictomicrographs of injection droplets in oil. A) Image of four consecutive injections acquired at 4x magnification. B) Image of injection acquired at 10 x magnification. C) Image of two injections acquired at 20x magnification using bright field..... 92

**Figure 23:** Timeline of the Xenotransplant Assay ..... 94

**Figure 24:** Elevation created using electrical tape on a coverslip for mounting anaesthetized zebrafish larvae for imaging under fluorescence microscope..... 95

**Figure 25:** Fold change in the expression of CYP1B1 in MCF-7, MDA-MB-231, and BT-474 cell lines. ....**Error! Bookmark not defined.**

# CHAPTER I

## INTRODUCTION

### 1.1 Breast Cancer

Breast cancer (BC) is the most frequently diagnosed cancer and represents 25% of all cancers detected in women worldwide. According to the American Cancer Society, it is estimated that approximately 266,120 women will be diagnosed, and over 41,400 women are estimated to succumb to this disease in the United States in 2018. One in eight women is at a risk of developing BC in her lifetime (Siegel et al., 2018). BC incidence rose from 1980s and declined in early 2000s. The five-year survival rates have increased from 75% to over 90% from 1975 to 2011. Considerable progress has been made in the last several decades in the treatment of BC with the identification of breast cancer intrinsic subtypes. Leading to a change in classification from ductal, inflammatory or invasive to expression of molecular features from a biopsy for estrogen receptor (ER), progesterone receptor (PR), and the human epidermal growth receptor 2 (HER2) protein. BC is classified on the basis of molecular signatures as ER positive (ER+), PR positive (PR+), or HER2 protein positive (HER2+). Approximately 70% of BC is ER/PR+, and 20% of BC is HER2+. BC can be positive for two or three receptors at a time or it can be negative for all three. This latter scenario is known as triple negative BC (TNBC) (Perou et al. 2000). ER/PR+ BC is responsive to treatment with tamoxifen (TAM), HER2 protein positive BC is amenable to treatment with Trastuzumab, and therapy options for TNBC are limited to traditional

chemotherapy. Doxorubicin (DOX) and paclitaxel (PTX) are also used to treat later stage and more aggressive ER+ and HER2+ BC, and thus are applicable to all cases of BC (Ades et al., 2017). The poor prognosis of breast cancer is due to the subsequent formation of metastasis in approximately 30-50% of patients even when they are treated with chemotherapy and endocrine adjuvant therapies at early stages of BC (Lin 2013; Roche and Vahdat 2011; Martin et al. 2017).

### 1.1.1 Metastasis

Metastasis is the spread of breast cancer to other locations in the body and is a highly dynamic process (Mansel et al. 2007). Majority of the deaths in breast cancer patients are due to the metastasis to different organs, and not the primary tumor itself (Weigelt et al. 2005). Metastatic BC is also classified as stage IV breast cancer and patients suffering from stage IV BC have similar treatment options available as other stages of BC. Currently, there are no therapeutic agents for the prevention of metastasis and BC is considered incurable once it reaches a metastatic stage. The approaches for treating metastatic cancer are palliative in nature (Roche and Vahdat 2011).

The link between motility of the cancer cells and the development of metastasis was first suggested by Rudolf Virchow, a German scientist (David 1988). The BC metastasis process, as reviewed by Scully et al., involves multiple sequential steps and tumor cells must complete all these steps for successful metastasis (Scully et al. 2012). Metastasis initially occurs by invasion into surrounding host tissue. The tumor cells disrupt the cell-to-cell adhesions and cell adhesion to extracellular matrix (ECM). Cell-to-cell adhesion is largely mediated by the cadherin family and in BC metastasis (Li and Feng 2011). Integrins, transmembrane receptors on the components of ECM, are responsible for the adherence of tumor cells to ECM (Mego et al., 2010). Transport of

tumors from the primary tumor site to distal organs occurs at a single-cell level or collectively in a number of cells after intravasation into the blood circulation or lymphatic vessels (McSherry et al. 2007). The collective migration occurs in intermediately or highly differentiated lobular carcinomas of the breast. However, in poorly differentiated tumors, due to abnormalities in the structure and function of the intercellular adhesion proteins, the coordinated cell migration may change to single cell migration. The presence of intercellular junctions is vital for the collective migration of cancer cells; hence they circulate as emboli in the blood or lymphatic vessels after invasion (McSherry et al. 2007). The tumor cells then endure cell cycle arrest and adhere to capillary beds in the target organs, occasionally for long periods of time, before tumor cells extravasate the parenchyma of the target organ whereby they proliferate and develop angiogenesis (Hunter et al., 2008). It is critical that the tumor cells simultaneously evade immunosurveillance and apoptosis to survive as tumor cells are undergoing these steps (Fidler, et al., 1978; Hunter et al., 2008). Metastasis cannot occur until there is a favorable microenvironment making tumor microenvironment a critical factor for this process (Scully et al. 2012).

Novel anti-cancer drugs are rarely used in metastatic cancer settings, which is a challenge in clinical settings as drug candidates are tested in patients with metastatic disease. Neoadjuvant therapies in patients with localized cancer are being evaluated to prevent cancer metastasis; to determine if the neoadjuvant therapies are helpful in eliminating the disseminated cancer cells which lead to formation of metastases. Therefore, for novel anti-cancer drug discovery, it is important to simulate conditions which promote the normal proliferation and migration of cancer cells for a robust and efficient model. The established in vitro models must have in vivo complements in order to gain insights in the molecular mechanisms as well as to elucidate

multicellular interactions involved with tumor progression (Vittori et al. 2015). Mouse models are traditionally used for screening anti-cancer compounds but have certain disadvantages that limit their use to study metastasis. It is difficult to assess early stage metastasis, the metastatic process is a long process in mice, and sacrificing the animal is essential to study tumor lesions (Zhao et al. 2015). Although it is difficult to simulate the metastatic process entirely in zebrafish, certain stages of metastasis can be studied. It was observed that tumorigenic human gastrointestinal cells metastasize when xenotransplanted in zebrafish and non-tumorigenic tissues do not metastasize (Marques et al. 2009). The clinical behavior of tumor cells is also conserved in zebrafish as demonstrated by glioblastoma cells injected in the brain and yolk sac which did not metastasize beyond the surrounding brain tissue (Lal et al. 2012). The transgenic zebrafish, being transparent, affords us the opportunity to study tumor metastasis in vivo using high resolution microscopy, and to observe the in vivo growth patterns of human cancer cell lines in terms of invasiveness and response to cytotoxic compounds. Moreover, in zebrafish, the rapid process of metastasis can be observed in as soon as two days post injection (Yang et al. 2013). Using targeted disruption of proteins and molecules, inhibition of metastasis can be studied in zebrafish. For example, inhibition of PDK1/PLC $\gamma$ 1 complex using 2-O-Bn-InsP5, a small molecule inhibitor, reduced the metastasis of MDA-MB-231 BC cells in 2 dpf zebrafish embryos. The zebrafish embryos were injected at different sites including duct of Cuvier and perivitelline cavity, and significantly reduced dissemination of tumor cells was observed as compared to controls (Raimondi et al. 2016). Similar significant reduction in dissemination of MDA-MB-231 cells was also seen when v-integrin was knocked down in MDA-MB-231 and by chemically inhibiting v-integrin using GLPG0187, suggesting the involvement of v-integrin in metastasis (Y. Li et al. 2015).

### 1.1.2 Tumor microenvironment

The presence of a conducive microenvironment for tumor cell proliferation and malignant progression is critical for the development of metastases (Psaila et al. 2007). The tumor microenvironment consists of fibroblasts, immune cells, mural cells of the blood and lymph vessels, along with the ECM and endothelial cells, and the malignant cells interact with these cells at the primary as well as the metastatic sites (Folkman and Kalluri 2004; Kalluri and Zeisberg 2006; Fidler et al. 2007). These multiple types of cells secrete cytokines, growth factors, and proteases that may be involved in the invasion and metastasis of BC primary tumors (McSherry et al. 2007). The transformation of “in situ” breast cancer to metastatic form is a result of these interactions (Coghlin and Murray 2010). The metastatic cascade is complex, and this complexity is attributed by the tumor cell biology as well as the entire organism in which the tumor dwells. There is limited literature on the microenvironment in zebrafish, however it is possible to study the key tumor microenvironment factors in a zebrafish xenograft model. The hematopoietic stem cell niche is proposed to be a factor in housing cancer cells to bone marrow. The caudal hematopoietic tissue in zebrafish is the area of embryonic hematopoiesis and thought to be composed of a bone marrow hematopoietic stem cell niche. Sacco et al injected multiple myeloma cells, fluorescently labeled, in the intracardiac region of 2 dpf Casper zebrafish and found tumor cells localized in hematopoietic tissue within 30 minutes of injection (Sacco et al. 2016). Another group injected multiple tumor cells in the duct of Cuvier found the cancer cells localized in the caudal hematopoietic tissue area. They discovered a novel mechanism of formation of the metastatic niche and that the site of formation of micrometastasis is determined by the physiological migration of neutrophils, and an interplay between VEGF and neutrophils (He et al.



2012). These studies point to the relevance of zebrafish in studying the role of hematopoietic niche in metastasis. Zebrafish larvae provide the opportunity to observe the behavior of grafted tumor cells by high resolution in vivo imaging techniques and rapid analysis of metastatic behavior of human tumor cells (Tobia et al. 2013). Our goal is to employ the transgenic zebrafish xenotransplantation model to identify cytotoxic compounds that can be used in the treatment of all the BC subtypes.

### **1.1.3 Traditionally used chemotherapeutics**

The available treatment options for BC include a) surgery, b) radiation therapy, c) chemotherapy and d) targeted therapy to cell receptors. a) Surgery and b) radiation are invasive methods and are more localized, but not feasible for metastasis treatment. The current gold standard for treating early stage breast cancer patients is breast-conserving surgery (BCS) with adjuvant radiotherapy (Franceschini et al. 2015). c) Chemotherapeutic drugs, on the other hand, are potent cytotoxic agents with different mechanisms of action depending on the type of solid tumor being treated. Tamoxifen (TAM), DOX, and PTX are the most widely used drugs depending on the type of BC. DOX and TAM are the first line treatment for ER/PR+ BC, are associated with marked toxicities and long-term adverse events such as lymphedema, neurotoxicity, and chemotherapy induced peripheral neuropathy (CIPN) which impair the quality of life of these patients (Hershman et al. 2011). For TNBC, there are no specific treatment options available to deal with the metastasis, which is the main cause of death in the patients, as the metastasis spreads and forms micrometastasis in bones and other organs. However, DOX along with daunorubicin is the first line of treatment for patients suffering for this type of BC. As in other types of BC subtypes, in TNBC patients as well, there is a development of resistance and they stop responding

to the treatment (Ades, Tryfonidis, and Zardavas 2017) pointing to an urgent need for efficient therapeutics with minimal side effects.

Tamoxifen (TAM) is the first line of treatment for ER/PR+ BC, a selective estrogen receptor modulator (SERM), which acts as an antagonist for estrogen receptor in breast tissues (Rivenbark et al. 2013). Tamoxifen, a nonsteroidal triphenylethylene derivative, is a competitive inhibitor of estrogen binding at the ER and blocks estrogen action on the BC cells expressing these receptors. Upon binding to the ER, tamoxifen induces the synthesis of cytosine transforming growth factor- $\beta$  (TGF- $\beta$ ) and inhibits the proliferation of these cells by negatively regulating the autocrine system (V. C. Jordan 1993; Sawka et al. 1986). Although, with adjuvant therapy, a 35% decrease in the BC is seen in patients treated with tamoxifen, patients develop resistance to tamoxifen and stop responding to the treatment. Based on the findings of several trials of five years of TAM treatment versus no treatment, TAM increased the incidence of endometrial cancer in postmenopausal women who had not undergone hysterectomy before trial entry. The overall life-table calculations for older women suggest in 15 years a 2-3% risk of endometrial cancer if they used adjuvant TAM, and if they use TAM for 10 years that would put them at an additional risk of 2% in 15 years. However, this risk is lower in premenopausal women (Early Breast Cancer Trialists' Collaborative Group (EBCTCG) et al. 2011; Davies et al. 2013).

Doxorubicin (DOX) is an anthracycline drug extracted from *Streptomyces peuceotius* in the 1970s and is a routinely used antineoplastic agent in the treatment of various cancers such as breast, ovarian, lung, gastric, thyroid, non-Hodgkin's and Hodgkin's lymphoma (Thorn et al. 2011). DOX acts mainly by intercalating the DNA and disrupting the topoisomerase-II-mediated

DNA repair leading to DNA damage and cell death. Another proposed mechanism of action of DOX is the formation of reactive oxygen species upon oxidation to semiquinone which gets converted back to DOX leading to formation of free radicals which damage the DNA, proteins and triggers apoptotic cell death pathways in cancer cells (Doroshov 1986; Gewirtz 1999). However, the use of doxorubicin is limited by cardiotoxicity and doxorubicin resistance in patients (Thorn et al. 2011). In most cancer treatments DOX is rarely administered in isolation but with other chemotherapeutic compounds such as taxanes or trastuzumab. Moreover, co-treatment with trastuzumab or taxanes also results in cardiotoxicity (Gianni et al., 2007). A combination of taxanes and anthracyclines are now widely used as standard first line treatment in advanced stages of breast cancer as this combination showed better response rates than standard anthracycline based treatment (Ghersli et al. 2005).

Taxanes (paclitaxel and docetaxel) are widely used to treat breast cancer, especially the metastatic anthracycline-resistant breast cancers. Taxanes are associated with adverse side effects which include myalgias, peripheral neuropathy, and skin reactions. CIPN, a distal sensory neuropathy, is marked by pain, numbness, tingling, and a decrease in the functional capacity in the extremities. The other side effects associated with taxanes include ataxia, paresthesia, impairment of joint position sense, and a loss in tendon function (Hershman et al. 2011; De Laurentiis et al. 2008). Randomized trials of taxanes as adjuvant therapy for breast cancer indicated a range of 15-23% grade 2 and 3 neuropathy based on the NCI (National Cancer Institute) Common Terminology Criteria. A grade 2 neuropathy results in mild symptoms affecting functioning whereas grade 3 neuropathy greatly affects routine activities. A study conducted to evaluate the prevalence and severity of symptoms after adjuvant paclitaxel treatment with median months since

last treatment with PTX was 12 months was conducted in 50 women. The study found that 80% of the patients who received taxane-based adjuvant chemotherapy for treatment of early stage breast cancer experienced neuropathy symptoms up to 2 years after completing the treatment (Hershman et al. 2011).

As patients with TNBC cannot be treated using hormone or targeted therapy, there are limited treatment options and chemotherapy is the mainstay. Recent research has identified potential new targets for breast cancer drugs. There are five major areas where targeted therapies are being extensively studied: a) monoclonal antibodies, b) tyrosine kinase receptor inhibitors, c) small molecules targeting molecule-drug conjugates, d) antisense and siRNA approaches, and e) antibody drug conjugates (ADCs). These drugs are currently being evaluated in the treatment of TNBC as single or combination therapy to discover and develop effective therapies for improving the rate of survival, and the quality of life of patients during cancer treatment and post-cancer.

## **1.2 Trends in breast cancer drug discovery:**

Targeted therapies aim molecular targets and pathways which are vital for cancer cell proliferation. These may be VEGF (vascular endothelial growth factor), tyrosine kinases, epidermal growth factor receptor (EGFR), androgen receptor, poly (ADP-ribose) polymerase (PARP). By targeting these molecular targets and pathways that the cancer cells depend on to proliferate and metastasize, researchers have been able to identify and develop compounds that cause selective cytotoxicity in cancer cells with minimized damage to host cells (Nagini 2017). The other aspect of targeted therapies is to explore natural products to identify potent anti-cancer compounds. However, effectiveness of novel anti-cancer compounds is limited by a lack of

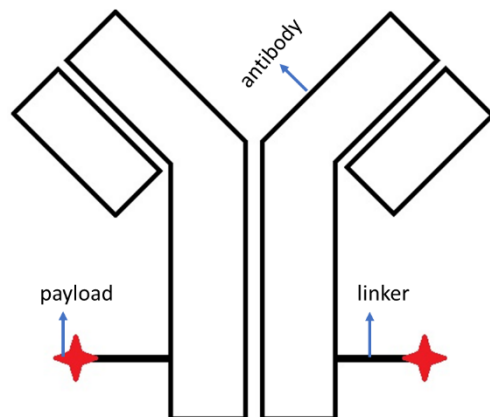
selectivity for tumor cells, and potent anti-cancer compounds need to be used close to their maximally tolerated dose (MTD) to achieve a therapeutic effect that is clinically effective. In many cancer types, a standard modality is to administer a combination of drugs which have different mechanisms of action as well as their toxicity profiles do not overlap, thereby improving antitumor activity by exhibiting an additive or synergistic anti-cancer effect (Chari et al. 2014). However, such regimens render systemic toxicity in the patient and are effective only a small proportion of cancers. To overcome the issue of limited clinical efficacy, antibody drug conjugates (ADC's) were developed. ADC's combine two approaches of targeted therapy- identification of specific molecular markers expressed by tumor cells called antigens, using antibodies that target the antigens as vehicles for selective drug delivery to the tumor cell, and linking the cytotoxic drug to the cytotoxic drug without causing chemotherapeutic damage to non-target tissues (Doronina et al. 2003; Chari et al. 2014).

### 1.2.1 Antibody Drug Conjugates (ADC)

Antibody drug conjugates comprise mainly of three components a) antibody, b) linker, and c) cytotoxic drug or payload as shown in Figure 1.

**Antibody-** Monoclonal antibodies have been used as targeted therapies in cancer because cancer cells express specific molecular markers such as CD33 on malignant blast cells in patients suffering from acute myeloid leukemia (Linenberger 2005), CD30 positive Hodgkin/Reed-Steinberg cells in Hodgkin lymphoma and CD30 positive large anaplastic lymphoid cells in systemic anaplastic large cell lymphoma (ALCL) (van de Donk and Dhimolea 2012), and HER2 positive breast cancer cells (Gutierrez and Schiff 2011) are responsible for the progression and

survival of the tumor cells. These tumor-associated antigens should be minimally expressed by normal human tissues. The antibody should be well internalized by receptor-mediated endocytosis and the target antigen should not be downregulated by the ADC (Perez et al. 2014; Panowski et al. 2014). The rate of internalization of the ADC in the cancer cell is a poorly understood process and is affected by factors like epitope on the target antigen, high interstitial tumor pressure, downregulation of the antigen, and presence of kinetic and physical barriers that diminish the cytotoxic payload uptake (Mack et al. 2014; Perez et al. 2014). The antibodies used can be human, humanized, and chimeric or mouse. However, the most commonly used antibodies include human IgG isotypes. Once part of the ADC, the antibodies can retain their original properties and activate immune functions and still act as signal modulators or receptor inhibitors (Xie et al. 2004). Currently, there are four approved ADC's for cancer treatment which are gemtuzumab ozogamicin (anti-CD33), brentuximab vedotin (anti-CD30), trastuzumab emtansine (anti-HER2), inotuzuman ozogamicin (anti-CD22) for acute myelogenous leukemia, anaplastic large cell lymphoma/Hodgkin's lymphoma, HER2+ breast cancer, and acute lymphoblastic leukemia respectively (Doronina et al. 2003; Gualberto 2012; Dhillon 2014).



**Figure 1:** Components of an antibody drug conjugate (ADC).

**Linker-** The pharmacokinetics, therapeutic index, and efficacy of the ADC is dependent on the linkers. Ideally, a linker should be stable and prevent the release of the cytotoxic drug before reaching the target, thus preventing off-target toxicity. The linker should be able to release the drug once the ADC is internalized. The drug-antibody ratio (DAR) is also critical because attaching too few drug molecules may lead to a decrease in the efficacy and attaching too many drug molecules may make the ADC unstable. This may lead to altered pharmacokinetics, increased plasma clearance, reduced half-life that leads to an increased systemic toxicity (Perez *et al.*, 2014). Currently, the licensed ADCs are produced with nonspecific conjugation to lysine residues and non-canonical amino acid incorporation or modification of peptide tags (Zhou, 2017). Linkers may be cleavable or non-cleavable. Cleavable linkers (acid sensitive, lysosomal protease-sensitive, or glutathione-sensitive) increase the possibility of bystander effect (Panowski *et al.*, 2014). For screening different antibodies and linkers for the ADC's, it is important to consider the difference in pharmacodynamics and pharmacokinetics when the ADC exposure is waterborne. This also applies to solubility of compounds in DMSO or other suitable solvents for waterborne exposures

and the concentration of these solvents as hydrophobic compounds or high molecular weight compounds cannot be administered in a waterborne exposure.

**Drug or cytotoxic payload:** There are two classes of compounds being extensively used in the design of payloads, and these compounds and their derivatives are being studied as ADC in a number of clinical trials for various solid and liquid tumors. The two classes of compounds are microtubule inhibitors and DNA intercalators. The first generation of ADCs used classical chemotherapy drugs like doxorubicin and methotrexate and offered the benefit of well-known cytotoxic profile. Studies showed that the actual concentration of the cytotoxic payload in the tumor cells was minimal with only 1-2% of the administered dose reaching the tumor cells. Therefore, the cytotoxic payload used must be highly potent and effective at nanomolar and picomolar concentrations (Teicher and Chari, 2011). Since then, extensive research has been conducted in the design and selection of payloads, antibodies, and linkers. To optimize the therapeutic index of the drug, tumor selectivity is improved to either increase the maximally tolerated dose (MTD) or to increase the potency of the cytotoxic drug thereby decreasing the minimum effective dose (MED)(Chari et al. 2014).

### 1.2.2 Microtubule inhibitors as payloads:

Major dynamic structural component of a cell that is vital in the development, reproduction, division, and in maintaining the shape of the cell, microtubules are polymers of  $\alpha$  and  $\beta$  tubulin heterodimers. Microtubules exhibit complex polymerization dynamics which determine and regulate their biological functions. The microtubules are polymerized by a mechanism known as nucleation-elongation wherein a short microtubule nucleus is formed followed by lengthening of



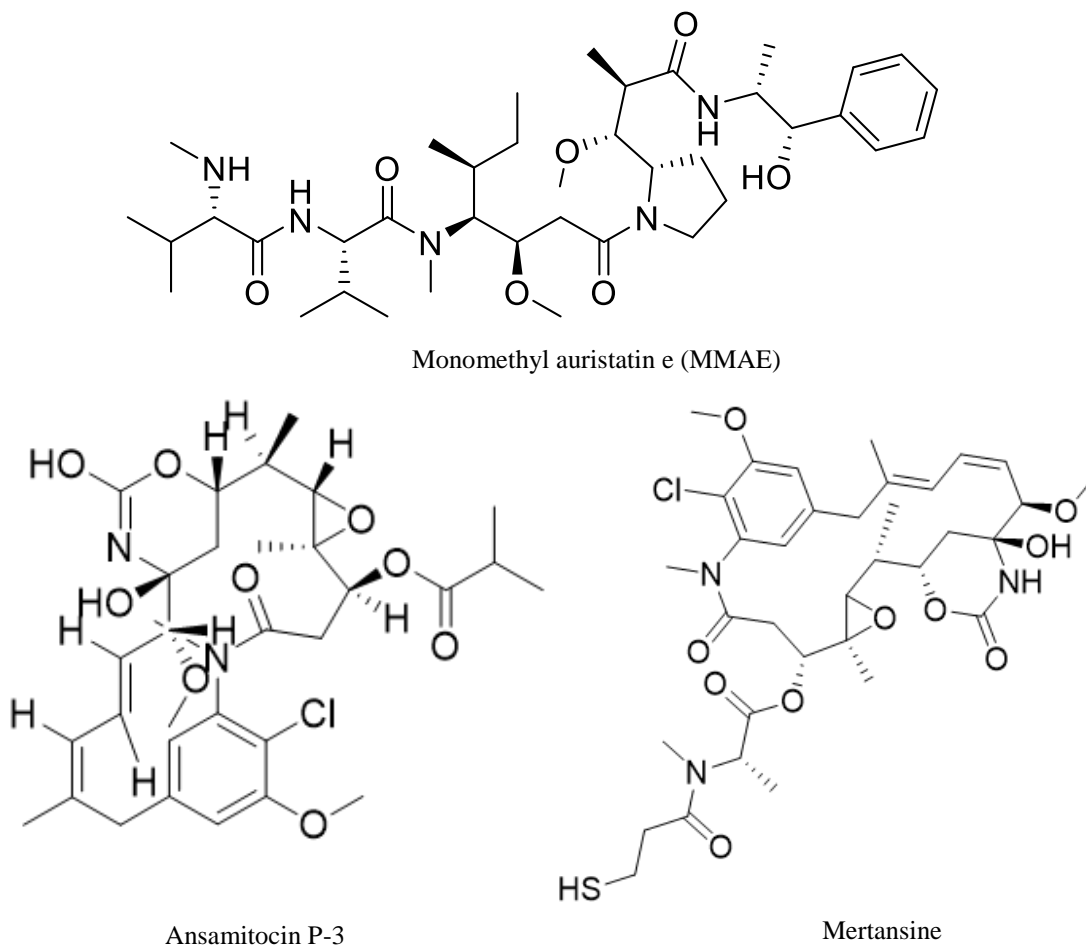
the microtubule at each end with a reversible and noncovalent addition of tubulin dimers (Jordan, 2002). The complex polymerization dynamics are possible with the binding of tubulin to guanine triphosphate (GTP) whereby energy is released by hydrolysis of (GTP) to guanine diphosphate (GDP) and  $P_i$  at the growing end of microtubules, leaving a microtubule core consisting of tubulin with stoichiometrically bound GDP. Until the tubulin subunit dissociates from the microtubule, GDP remains non-dissociable and non-exchangeable. There are two dynamic behaviors of microtubules, “treadmilling” and “dynamic instability”. In treadmilling, there is a net growth of one end of the microtubule and a net shortening of the other end. Dynamic instability involves switching of phases between rapid growth and shortening of the microtubule ends, and these transitions are regulated by the presence or absence of the region of tubulin-GDP at the microtubule end. Growth of a microtubule continues as long as it maintains a stabilizing cap of tubulin-GTP or tubulin-GDP- $P_i$  at its end, and the loss of this cap results in depolymerization of the microtubule (Jordan *et al.*, 1993; Wilson and Jordan, 1995). Microtubule ends, known as plus and minus ends, are not equivalent. The plus end is kinetically more dynamic than the minus end. Both ends can elongate or shorten, but changes in length at the plus end are much larger than the minus end. Microtubules endure lengthy periods of slow lengthening, short periods of quick shortening, and periods of pause. Both treadmilling and dynamic instability occur in living cells and are excellently regulated by microtubule associated proteins (MAP) and by drugs (Wilson and Jordan, 1995). Microtubules are believed to be a major target for anti-cancer drug discovery (Wilson and Jordan, 1995; Jordan *et al.*, 1998; Pasquier and Kavallaris, 2008) and compounds that target microtubules, microtubule stabilizers and destabilizers, are widely investigated in anti-cancer drug discovery (Pasquier and Kavallaris, 2008).

### 1.2.2.1 Microtubule inhibitors

*Taxol*, a mitotic inhibitor, was isolated from the bark of *Taxus brevifolia* (northwest Pacific Yew Tree) in 1967. It is produced by a fungal endophyte when grown on semisynthetic media, first isolated from the phloem tissue of the Pacific Yew Tree (Stierle, Strobel and Stierle, 1993). Bristol-Myers Squibb commercially developed this fungal endophyte under the trademark Taxol and generic name Paclitaxel (PTX). PTX arrests cells by stabilizing spindle microtubules during mitosis (Schiff and Horwitz, 1980; Wilson and Jordan, 1995). PTX has high affinity for microtubules, leads to an increase in microtubule polymerization in vitro, boosts both nucleation and elongation phases, and it decreases critical tubulin subunit concentration. PTX polymerized microtubules are very stable and resist depolymerization by lower temperatures (4 °C) and calcium, induces self-assembly of tubulin into microtubules at 0 °C in the absence of GTP, MAP's, and at alkaline pH (Aparajitha and Priyadarshini K, 2012). Although PTX is potent chemotherapeutic drug, multidrug resistance developed by tumor cells and restricted drug access to the growing tumor cells caused by immune vascularization, tissue hypoxia, reduction in blood flow are limitations to tumor responsiveness (Vredenburg *et al.*, 2001). Targeted therapies to overcome these limitations are required which can utilize existing potent drugs and their derivatives for effective anti-cancer activity.

Maytansinoids and auristatins are two largest classes of potent microtubule inhibitors which are presently utilized as a “payload” of ADC's in clinical trials (Beck *et al.*, 2017). We selected three compounds belonging to the microtubule inhibitor class- maytansinoids and auristatins to test their maximally tolerated concentration in vivo, and their effect on BC cell proliferation. These compounds are highly potent and reported IC<sub>50</sub> values in various solid tumors

is in the picomolar and nanomolar ranges.



**Figure 2:** Chemical structures of monomethyl auristatin e (MMAE), ansamitocin P-3, and mertansine.

*Dolastatin 10*, a linear peptide, was isolated from *Dolabella auricularia*, a shell-less marine mollusk found in the Indian Ocean. Dolastatin 10 and its derivatives are microtubule inhibitors and inhibit the binding of tubulin-GTP, causing a blockage of microtubule dynamics (Pettit et al. 1998). Auristatins, fully synthetic analogues of dolastatin 10, were identified by SAR studies based on dolastatin 10 (Otani *et al.*, 2000). Auristatins block the assembly of tubulin and cause a cell

cycle arrest in the G2/M phase. They are a commonly used cytotoxic payload and comprise of the majority of payloads in ADCs being investigated. For our studies, we selected monomethyl auristatin e (MMAE), Figure 2, to determine the MTC in larvae over a period of 96 hours. Bretuximab vedotin is an approved ADC for the treatment of anaplastic large cell lymphoma/Hodgkin's lymphoma.

*Maytansinoids* are another class of potent tubulin inhibitors. They are isolated from the Ethiopian shrub *Maytenus ovatus* by Kupchan et al. in 1972 (Kupchan *et al.*, 1972). Maytansine was one of the first compounds found to kill cancer cells with IC<sub>50</sub> values in the picomolar range and was found to be more cytotoxic than doxorubicin, methotrexate, and 5-fluorouracil. Maytansine attaches to tubulin with high affinity for tubulin located at microtubule ends. The binding of maytansine to tubulin leads to cytological changes in which chromosomes are scattered at random in the arrested cells in metaphase and leads to the formation of multinucleated or large cells (Cassady *et al.*, 2004). Maytansine inhibits microtubule assembly by binding to tubulin and have KD~ 1µmol/L. Mertansine is a semisynthetic analog of maytansine (Kupchan *et al.*, 1972), small molecular weight of 737.5 Da cytotoxic agent (Xie *et al.*, 2004). The intercellular target of mertansine is tubulin, and it inhibits the polymerization of tubulin in cancer cells (Xie *et al.*, 2004).

### **1.3 Natural products as anti-cancer compounds**

Natural products continue to play a highly significant role in drug discovery and development process. Natural compounds have a long and successful history in anticancer drug discovery (Newman and Cragg, 2012). Natural products, owing to their chemical diversity and biological activities, are attractive candidates for anticancer drug discovery. The National Center

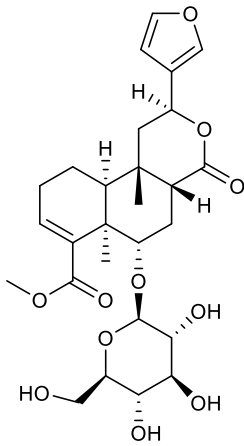
for Natural Products Research at The University of Mississippi is one of the largest natural product research institutions in the country and has an extensive library of novel compounds isolated from plants and other natural sources. Our initial approach was to test novel compounds with unknown anti-cancer activity to develop this model as a medium-throughput anti-cancer drug screening tool.

### 1.3.1 *Tinospora crispa*

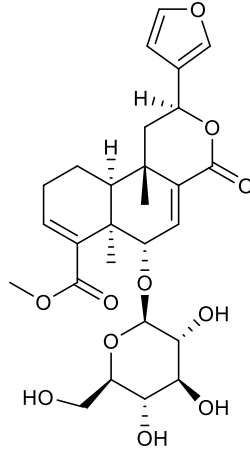
*Tinospora crispa* is a herbaceous vine found in Asian and African rainforests and mixed deciduous forests (Pathak et al. 1995). Traditionally, this medicinal plant has found use as folk prescription in Asian countries like Malaysia, Indonesia, Thailand, and the Philippines for treating hypertension, diabetes, urinary disorders, fever, malaria, internal inflammation, rheumatism, appetite stimulation, and maintaining good health (Kongsaktrakoon et al.1984) (Rahman *et al.*, 1999) (Pathak et al. 1995). Phytochemically, *T. crispa* is composed of diverse secondary metabolites. More than 65 compounds have been isolated and identified such as alkaloids, flavonoids, and flavone glycosides, lactones, sterols, triterpenes, diterpenes and diterpene glycosides, and nucleosides. Clerodane-type furanoditerpenoids are the characteristic compounds of *T. crispa* (Ahmad et al. 2016). Borapetoside A, borapetoside B, borapetol A, borapetol B, tinoturbride, tinocrisposide, N-formylanondine, N-formylnornuciferine, N-acetyl nornuciferine and picrotoxin are some of the chemical constituents isolated from *T. crispa* (Pathak et al. 1995). Investigative studies have been performed by different groups of researchers to identify the active constituents of *T. crispa* extracts responsible for diverse activities such as anti-inflammatory, anti-diabetic, and anti-cancer activity as described below.

Abood et. al. evaluated crude ethanol extracts of *T. crispa* along with its isolated fractions

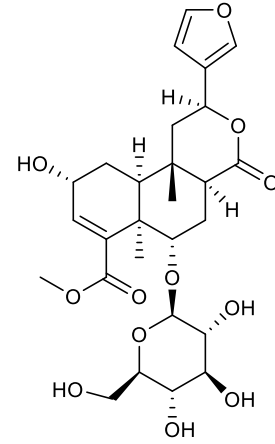
for potential anti-inflammatory activity and observed that the ethanolic extract and its subsequent fractions stimulated the murine macrophages from blood (RAW264.7) proliferation in a dose dependent manner. The ethanol extract and its fractions increased RAW264.7 at a dose of 25-800  $\mu\text{g/mL}$ , and improved intracellular expressions of cytokine INF- $\gamma$ , IL-6, and IL-8. The ethyl acetate fraction was found to be the most active of all the fractions tested, with significant increase in intracellular expression of cytokines in RAW264.7 macrophages (Abood, Fahmi and Abdulla, 2014). Methanolic and aqueous extracts of *T. crispa* stem reduced the secretion of macrophage colony stimulating factor (M-CSF), vascular cell adhesion molecule (VCAM-1), and intracellular cell adhesion molecule (ICAM-1) in TNF- $\alpha$  stimulated human umbilical vein endothelial cells (HUVECs) (Kamarazaman, Amorn and Ali, 2012). *T. crispa* aqueous extract in doses of 50, 100, and 150 mg/kg significantly inhibited the development of edema in a foot pad thickness experiment, exhibiting similar results to ibuprofen (Hipol, Cariaga and Hipol, 2012).



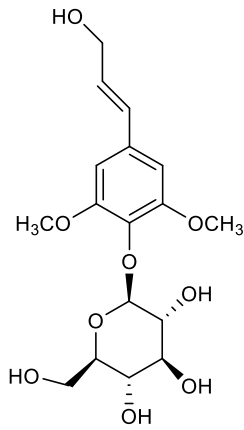
Borapetoside C



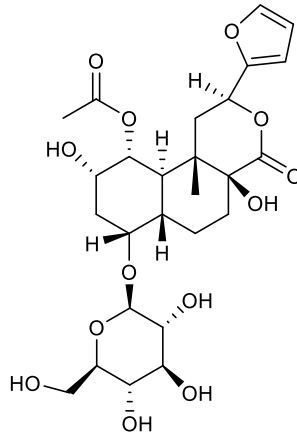
Borapetoside F (AP-3-29-3TC)



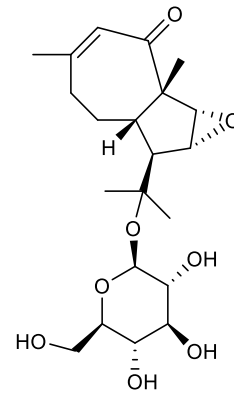
Borapetoside B (AP-2-60-2Tc)



Syringin (AP-2-47-5Tc)



Tinosineside A (AP-1-42-4 Ts)



Tinocordifolioside (AP-1-39-8 Ts)

**Figure 3:** Chemical structures of various constituents of *T. crispata* tested for cytotoxicity in MCF-7 and MDA-MB-231 BC cells

Although numerous compounds have been reported from *T.crispa*, few have been evaluated for cytotoxic activity and the active compounds responsible for cytotoxicity in cancer cells still need to be identified. Iqbal et al. reported  $IC_{50} > 10\mu M$  for borapetoside A, B, C and D in PC-3 cancer cells (human prostate) and normal 3T3 (mouse fibroblast) cell line (Choudhary *et al.*, 2010). Mantaj et al. reported selective inhibition of the expression of STAT3 and STAT3 target genes cyclin D1, fascin and bcl-2 and thus, significant toxicity against STAT3-dependent MDA-MB 231 breast cancer cell line by crispene E, a furanoditerpenoid isolated from the hexane fraction of *T. crispera* (Mantaj *et al.*, 2015). The methanolic and other polar fractions of *T. crispera* have been reported to show cytotoxic activity in different cell lines. Froemming observed a dose dependent cytotoxic effect in methanolic extract of *T.crispa* on MDA-MB-231 and MCF-7 cancer cell lines with an  $IC_{50}$  value of 44.8 and 33.8  $\mu g/mL$  (Mantaj *et al.*, 2011). Zulkhairi et. al. studied cytotoxic effects of various extracts of *T. crispera* in different cancer cells such as breast, ovarian, and hepatic cancer cells. The aqueous crude extract of *T. crispera* stem showed  $IC_{50}$  values of 107  $\mu g/mL$  in MCF-7 cells, 165  $\mu g/mL$  in HeLa cells, 100  $\mu g/mL$  in Caov-3 cells, and 165  $\mu g/mL$  in HepG2 cells. They observed significant cytotoxicity of the crude aqueous extract in comparison with cisplatin and tamoxifen, the traditionally used chemotherapeutic drugs. The major components with anti-cancer activity still need to be investigated (Zulkhairi et al. 2008). The evidence of anti-proliferative activity in cancer cells owing to the active chemical constituents, such as diterpenoids and alkaloids, encouraged us to investigate the anti-cancer potential of various *T. crispera* extracts uninvestigated in MCF-7, and MDA-MB-231 breast cancer cell lines. For our project, we tested compounds (Figure 3) isolated from *T. crispera* by Abidah Parveen in the National



Center for Natural Product Research. As some of these compounds have not been tested before for in vitro cytotoxicity, we tested these compounds using cytotoxicity assays to determine the anti-cancer activity of various fractions in MCF-7 and MDA-MB-231 BC cell lines.

#### **1.4 Xenotransplant models:**

Mouse models are traditionally used as “gold standard” for cancer screening (Patel et al. 2014; Agorku et al. 2016; Tovar et al. 2017; Radloff et al. 2008; Jung 2014). Advantages of using a mouse model for xenograft study include a large number of orthotopic tissues for xenotransplantation, availability of wide range of transgenic mice including humanized, severe combined immunodeficient (SCID); and a higher conservation of genes, molecular pathways, and organ systems with human beings (Veinotte et al. 2014). However, this model has several drawbacks that limit its choice for running rapid anti-cancer drug screening assays. These drawbacks include but are not limited to: mice are expensive; the number of pups produced per clutch is small, a dedicated facility is required along with personnel which adds up to the costs of housing and maintaining these animals. Moreover, tumors take longer (6-8 weeks) to develop in mice; it is difficult to monitor tumors grown in non-transparent animals, substantial amounts of test compounds are required for administering in mice, and the number of cells required to xenotransplant is in the range of  $\sim 10^6$ /animal. Lastly, the number of animals used per experiment is limited to a small number due to these reasons. There is a need to explore other animal models to overcome the shortcomings of the mouse model that offer rapid, reproducible, and robust outcomes as an alternative xenotransplantation studies.

#### 1.4.1 Transgenic zebrafish as an anti-cancer drug screening model:

For our project, using transgenic *Casper/fli* zebrafish as an alternative to the conventional mouse model for treating breast cancer, we expect to develop an efficient model to screen the vast array of natural compounds available at the University of Mississippi Natural Products Center. This screen would enable us to contribute to the discovery of efficacious and safe compounds with anti-cancer properties. The ultimate goal of this project is to find and establish the potential of new therapeutic compounds for breast cancer that are safe and effective to augment the disease.

Zebrafish have become an attractive and widely used animal model for various diseases including gastrointestinal disorders such as inflammatory bowel disease (Fleming *et al.* 2010), alcoholic liver disease (Lin *et al.*, 2015); brain disorders such as depression (Fonseka *et al.*, 2016), and neurodevelopmental disorders such as autism spectrum disorder (Meshalkina *et al.*, 2018); muscular dystrophies (Li *et al.*, 2017), cardiomyopathy (Gu *et al.*, 2017), infectious diseases as described in a book section by Sullivan *et al.* (Sullivan *et al.*, 2017); and continues to be explored as a model organism in a whole host of other diseases.

Zebrafish have 70% similarity with human genes that encode proteins, which make zebrafish an excellent model to study human diseases related to gene dysfunction (Howe *et al.*, 2013). This points to high conservation of molecular mechanisms involved in normal and disease conditions, and compounds targeting these molecular mechanisms can be closely translated to the context of human physio-pathogenesis (Okuda *et al.*, 2016). Comparison of zebrafish and human genomes reveal stark conservation in sequence and function of proto-oncogenes, angiogenic factors, tumor suppressor, cell cycle, and extracellular matrix proteins (Zon *et al.*, 2013). In

addition to the genetic similarities, zebrafish offer practical and logistical advantages as an animal model. These include high fecundity, rapid ex-vivo development of the embryos, small size, and transparency of the embryo-larval zebrafish.

Existing zebrafish models have demonstrated human cancer cells, including breast cancer, can grow, divide, metastasize, and induce angiogenesis similarly to rodent xenograft models (Marques *et al.*, 2009). Moreover, the fish can be easily handled, maintained in small volumes of water, transferred into multiwell plates, and pose as a noninvasive cancer model to study the exposure-dependent effects on cancer progression using high resolution microscopy (Parng *et al.*, 2002; Wehmas *et al.*, 2016). Zebrafish embryos lack an active, fully functional adaptive immune system until ~28 days which allows implantation of human cells without rejection (Lam *et al.*, 2004). Easy handling, low costs, and rapidness are unparalleled by other vertebrate organisms and make it a promising system in primary tumors (Marques *et al.*, 2009). Cancer cells interact with their microenvironment and the whole organism to form cancers. Therefore, the cancer models established in vitro must have in vivo complements in order to gain insights in the molecular mechanisms as well as elucidating multicellular interactions involved with tumor progression (Vittori *et al.*, 2015). Xenografts of various human tumors in zebrafish have been studied over the past decade. These xenograft models include tumors of ovaries, lung, breast, prostate, skin, leukemia, melanoma.

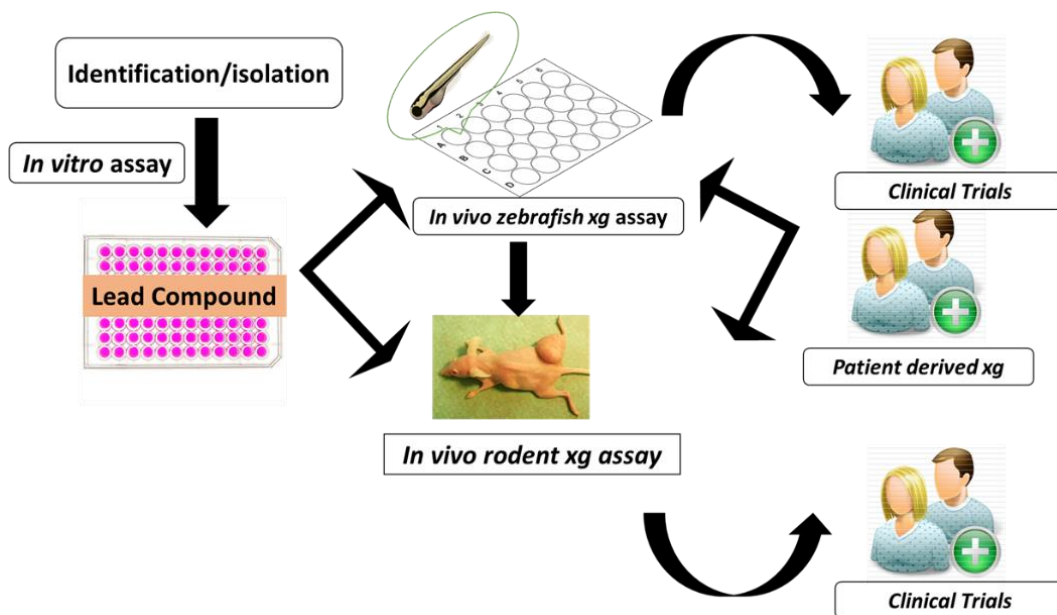
For optimal visualization of red fluorescence labeled cancer cells we used a cross between Tg(*fli1a*:EGFP), a transgenic zebrafish line that exhibits a green fluorescent vasculature by expressing EGFP under *fli1* promoter (Lawson and Weinstein, 2002; Stoletov *et al.*, 2007), and

optically transparent *Casper* zebrafish embryos, developed by White et al. in 2008 (White *et al.*, 2008a). The crossing procedure is described in the methods section.

#### 1.4.2 Patient derived xenografts

More recently, zebrafish have been employed to xenograft tumor cells derived from patients to test combination therapies against resistant tumor types which are difficult to treat with a single conventional therapeutic. Patient derived xenografts (PDX) offer an advantage over traditional models of pre-clinical development of oncologic drugs and provide the advantage of evaluating the drug sensitivity in patients (Cassidy et al. 2015). Figure 4 is an illustration of the processes involved in developing drugs from bench to bedside. PDX in zebrafish have been successfully performed by different groups in clinical settings. PDX also offers the opportunity to explore molecular events involved in tumor angiogenesis and metastasis, and eventually personalized treatment (Gaudenzi *et al.*, 2017). So far, researchers have only been able to establish PDX in zebrafish successfully and the dosing is the next step. Neuroendocrine, breast, leukemia and other cancers have been successfully xenotransplanted in the zebrafish embryos. These assays are fast (3-7 days) and would provide substantial information for a clinician and aid in the determination of tailored therapy for the patient (Deveau et al. 2017). Recently, Karkampouna et al. xenografted human hepatocellular carcinoma cells (HCC) in zebrafish, mice, and ex vivo to determine the expression of CRIPTO, a cell surface protein belonging to TGF- $\beta$  family that is highly expressed in various human cancers, and performed drug response assays in them (Karkampouxna et al. 2018). The HepG2 cells expressing CRIPTO were xenografted in zebrafish to determine the potential of the cells to migrate and develop tumor foci; combination therapy using doxorubicin and sorafenib, standard drugs for HCC treatment, was tested targeting CRIPTO

in ex vivo tumor cultures. Similar xenograft experiments using zebrafish are being widely performed in clinical settings to determine new molecular targets as well as to determine best dosing regimen specifically for the patient.



**Figure 4:** From bench to bedside, overview of the process of patient derived xenograft drug discovery model.


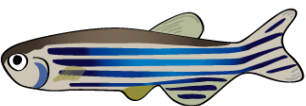
### 1.4.3 Advantages of using zebrafish vs. mouse for xenotransplantation:

Zebrafish provide an alternative platform for a cancer model that can be traditionally accomplished in mouse models (Yen *et al.*, 2014). The comparison between zebrafish and mice as xenograft models is summarized in Table 1. Additionally, morpholino injections in zebrafish embryos can be utilized to induce a transient block in the translation of gene function and gene inactivation, and this technique is fast and easy as compared to generating knock-out mice. Using morpholinos, the role of genes involved in angiogenesis can be studied in targeted drug discovery of novel therapeutic agents (Tobia *et al.*, 2013). Evaluation of metastasis formation in currently

used mouse models take several weeks as compared to zebrafish, where metastasis is observed as early as one day post injection (dpi). The zebrafish tumor xenograft model therefore is sensitive and allows observation of single cells and their daughter cells in vivo (Marques *et al.*, 2009). Moreover, the physiological responses to pharmacologically active compounds in zebrafish embryo are comparable to mammalian systems (Zon and Peterson, 2005). Zebrafish embryos provide an environment that mimics the human body, including hormones and nutrition. Also, as compared to the conventional mouse animal model that requires a dedicated animal facility, develops tumor slowly, in our proposed model it is feasible, less tedious and inexpensive to xenotransplant 12-30 embryos/treatment group with cancer cells and to study the tumor growth and progression in each treatment group. The availability of various tissue-specific fluorescent reporter transgenic lines along with transparency of zebrafish has enabled high resolution in vivo analysis of tumor cell progression. It also enables us to observe the interactions between host tumor microenvironment and the tumor cells (Feitsma and Cuppen, 2008; Binder and Zon, 2013).

Even with numerous advantages rendering zebrafish as an excellent model for xenotransplantation, there are limitations of using this model. For example, the lack of an adaptive immune system in zebrafish embryos limits the investigation of the role of the immune system in cancer pathogenesis and drug response (Deveau *et al.* 2017). Zebrafish provide a platform to xenograft tumor cells orthotopically, the organs that are not present in fish such as breasts, lungs, joints, limbs, and prostate glands. It is also important to note that the drugs that can be tested in zebrafish larvae are limited by their characteristics such as molecular weight, solubility, stability and bioavailability since the exposures are waterborne (Brown *et al.*, 2017).

**Table 1:** Mice vs. Zebrafish as xenotransplant models.

		
<b>Duration of experiment</b>	2-4 months	3-6 days
<b>Cost</b>	\$45-60	\$1-2
<b>Maintenance costs</b>	\$1-3/mouse	Cents/tank
<b>Number of cells required for xenografting</b>	~10 <sup>6</sup> /mouse	100-200/larva
<b>Cancer cell tracking</b>	Tumor mass	Single cells
<b>Visualization frequency</b>	End point of experiment	Everyday
<b>Histology</b>	Individual organs	Whole fish

## 1.5 Specific Aims

The goal of this project was to develop transgenic zebrafish as an in vivo animal model to screen anti-cancer compounds for treatment of human breast cancer. The zebrafish larvae developed for this study is a fourth-generation cross between *Casper* and *fli* strains (CF4), possesses a transparent body with fluorescence tagged vasculature. The transparent body allows for visualization of BC cells (labeled with red fluorescent dye) which can be traced, and the effects of anti-cancer compounds on the tumor cells can also be observed. Our central hypothesis was to establish the value of our transgenic *Casper/fli* zebrafish, using DOX, PTX, 4-hydroxytamoxifen (4-OH-TAM), known chemotherapeutic agents used widely as a first line therapy in estrogen-

dependent/independent breast cancer subtypes. For this, anti-cancer efficacy and potential therapeutic index for test compounds in breast cancer cell lines was first established (Aim 1), subsequently, we described the maximally tolerated concentration of anti-cancer compounds in vivo using zebrafish larvae (Aim 2), and in our final aim 3, we determined the efficacy and therapeutic index of the compounds in zebrafish larvae xenografted with human breast cancer cells (Aim 3).

Our experimental approach was accomplished in three aims utilizing in vitro assays and in vivo assays. Briefly, three types of BC cells lines were used- Estrogen Receptor positive (ER+, MCF-7), human epidermal growth factor 2 protein positive (HER2+, BT-474), and triple negative (TNBC, MD-MBA-231) for the evaluation of safety and selectivity of compounds. The in vitro assays were followed by in vivo assays to determine the maximally tolerated concentration of the extracts and fractions, and the toxic effects, if any, associated with these compounds. The larvae were exposed to a range of concentration of different compounds and the maximally tolerated concentration was determined over a period of 96 hours. The concentration range determined was subsequently administered to xenotransplanted zebrafish larvae to determine the anti-cancer potential in an in vivo setting.

The focus of our work was to establish the transgenic zebrafish as a xenograft model using traditionally used chemotherapeutic compounds and then with compounds that have not been tested in zebrafish xenografts before. The establishment of this model will offer an opportunity for us to screen more novel compounds in zebrafish larvae. We will conduct the following three specific aims to establish the transgenic zebrafish xenograft model.



### **1.5.1 Specific Aim 1- Establish anti-cancer efficacy and potential therapeutic index for test compounds in breast cancer cell lines:**

Hypothesis: The effect of the compounds tested (DOX, PTX, Curcumin, *T. crista*, and 4-OH-TAM) on the viability in cell lines (MCF-7, BT-474, and MDA-MB 231 unlabeled and labeled with CM-DiI) will be comparable, and the CM-DiI labeled cells do not have sensitivity to the compounds related to the dye.

Approach: Test effect of cytotoxic compounds in MCF-7, BT-474, and MDA-MB 231 cells labeled with CM-DiI and evaluate if CM-DiI affects the cellular response to chemotherapeutic agents and establish that the agents work as expected. For the latter outcome, 4-OH-TAM should demonstrate a measure of inhibited cell growth in ER+ MCF-7 cells and DOX and PTX should inhibit the growth of all cell lines.

### **1.5.2 Specific Aim 2- Demonstrate the maximally tolerated concentration (MTC) of anti-cancer compounds in vivo using zebrafish:**

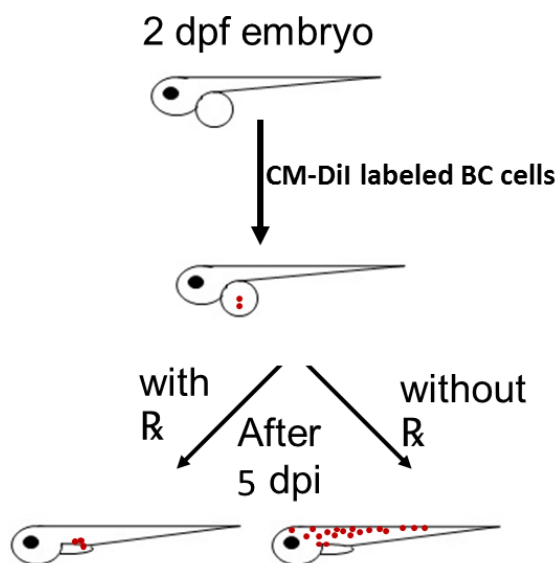
Hypothesis: Maximally tolerated concentration (MTC) of chemotherapeutic drugs in the zebrafish is comparable to the dose equivalent administered in humans.

Approach: Expose 3-day post fertilization (3 dpf) larvae to a range of concentrations of known cytotoxic and test compounds to determine maximally tolerated concentration (MTC) that causes minimal toxicity evaluated as phenotypic developmental defects in the zebrafish. Freshly made doses administered every 24 hours and the phenotypic defects observed over a period of 96 hours. This proposal was approved by IACUC, protocol number- 16-007.

### 1.5.3 Specific Aim 3: Determine the efficacy and therapeutic index of the compounds in zebrafish embryos xenografted with human breast cancer cells.

Hypothesis: BC tumor burden will be reduced by exposing the zebrafish to the anti-cancer compounds DOX, PTX, and 4-OH-TAM and novel test compounds screened in Specific Aim 1.

Approach: Inject the CM-DiI labeled BC cells in zebrafish embryos and exposed them to the safe dose-range of compounds determined in Specific Aim 2 to determine the anti-cancer efficacy of each compound by counting and comparing the number of cells in each larva using fluorescence microscopy at 1 day post injection and at 5 days post injection. The layout for this experiment and the timepoints are illustrated in Figure 5.



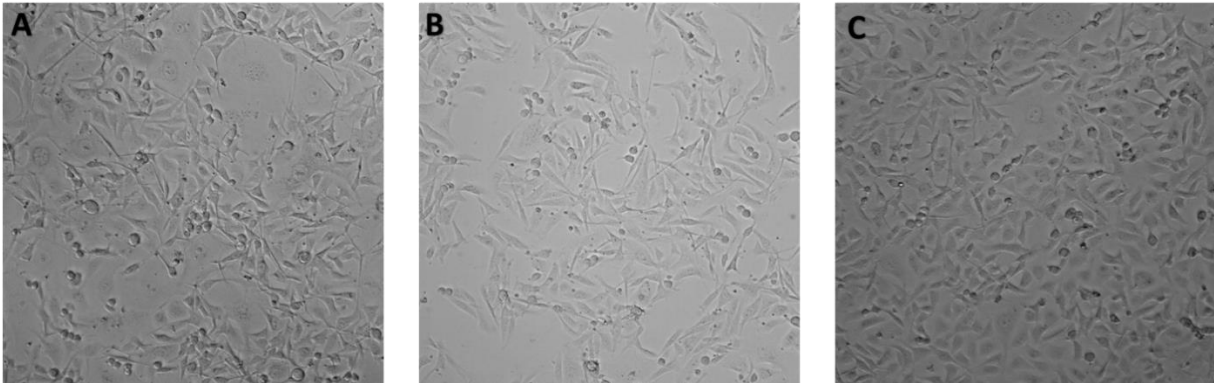
**Figure 5:** Layout of the xenograft experiments. Larvae will be injected with fluorescently labeled BC cells at 2 days post fertilization, imaged at 1 day post injection (dpi), and treatment will begin at 1 dpi. The treatment continued for 96 hours and on 5 dpi, the larvae were imaged again to determine the change in number of cancer cells

## CHAPTER II

### EXPERIMENTAL METHODS

#### 2.1 Cell Culture

Cells were cultured and maintained according to the instructions by ATCC (Manassas, VA). MCF-7 (ATCC® HTB-22™, provided by Dr. Tracy Brooks), MDA-MB 231 (MDA-MB-231 (ATCC® HTB-26™, provided by Dr. Shabana Khan), and BT-474 (ATCC® HTB-20™, ATCC) cells (Figure 6) were maintained in DMEM media (Life Technologies, CA) supplemented with 10% fetal bovine serum (FBS) (Life Technologies, CA) and 1% penicillin/streptomycin antibiotics (Sigma-Aldrich, MO) at 37 °C in humid conditions with 5% CO<sub>2</sub>. Cells were maintained in exponential growth phase until needed for experimental procedures.



**Figure 6:** Breast cancer cell lines used in the in vitro and in vivo experiments. MCF-7 (A), MDA-MB-231 (B), and BT-474 (C) were maintained in DMEM media, imaged at 10x magnification

### **2.1.1 Labeling human breast cancer cells with fluorescent dye**

Chloromethyl-benzamidodialkylcarbocyanine dye (CM-DiI) (ThermoFisher Scientific, CA) is a lipophilic dye that intercalates the plasma membrane of a cell and is reported to be expressed by daughter cells for several generations. MCF-7, BT-474, and MDA-MB 231 were labeled with CM-DiI according to the manufacturer's instructions. Briefly, CM-DiI was dissolved in DMSO (final concentration: CM-DiI: 4.8  $\mu\text{g/ml}$ , DMSO: 0.4%). Cells were incubated with CM-DiI cell-labeling solution directly diluted into phosphate-buffered saline (PBS) (2  $\mu\text{L}$  of labeling solution per mL of medium) for 4 min at 37 °C, followed by 15 min at 4 °C. The cells were then centrifuged at 4000 rpm (2670 x g) for 3 minutes to remove unincorporated dye and rinsed twice with PBS.

### **2.1.2 Compounds**

The compounds used were doxorubicin and tamoxifen (provided by Dr. Tracy Brooks), 4-hydroxytamoxifen (Sigma Aldrich), mertansine (CAS no 139504-50-0, Abovchem), ansamitocin P-3 (CAS no. 66547-09-9, Carbosynth), monomethyl auristatin E (CAS no 474645-27-7, Advanced ChemBlocks Inc), and curcumin (provided by Dr. Shabana Khan), paclitaxel (Sigma Aldrich). Stock solutions of 10 mM were made using DMSO for doxorubicin and curcumin, ethanol for 4-hydroxytamoxifen, and tamoxifen, and 1 mM stocks were made for mertansine, ansamitocin P-3, MMAE and paclitaxel. The stocks were stored in aliquots at -20 °C.

### **2.1.3 Cell Viability Assay**

The MTS [(3-(4, 5-dimethylthiazol-2-yl)-5-(3-carboxymethoxyphenyl)-2-(4-sulfophenyl)-2H-tetrazolium] assay was used to determine the cell viability using colorimetric analysis. The

basis of this assay is that tetrazolium is reduced by the NAD(P)H dehydrogenase enzyme in viable cells. A colored formazan dye is formed upon reduction which can be detected from its absorbance between 490-500 nm (Mosmann, 1983). Breast cancer cells were trypsinized from flasks, centrifuged at 4000 rpm (2670 x g) for 5 minutes and resuspended in DMEM. After counting the cells, they were diluted with trypan blue in a ratio of 1:10. Trypan blue aids in determining the number of dead cells as it is not absorbed by viable cells. The cells were then seeded at a density of  $5.0 \times 10^3$  cells per well in a 96 well plate.

Cells were allowed to attach overnight, and test compounds were diluted over a 5-6 log range from a high dose of 100  $\mu$ M in case of traditional chemotherapeutic drugs; and 100 nM in case of potent microtubule inhibitors, added to the cell plate and allowed to incubate for 24, 72, or 96 hours. At the end of the time point, 20  $\mu$ L of a solution of 2 mg/mL MTS and 5% PMS (phenazine methosulfate) (Promega, CA) was added to each well. The plate was incubated at 37  $^{\circ}$ C for 2-4 hours, and absorbance read on a Bio-Tek spectrophotometer (Bio-Tek Instruments, VT) at 490 nm. Absorbance was converted into percent cell viability by first subtracting the absorbance of the compounds and then normalizing to control cell growth. All experiments had internal biological triplicates. GraphPad Prism 5.0 was used to determine the  $IC_{50}$  of each compound by non-linear regression with curve fit using dose response-inhibition equation ( $\log[\text{inhibitor}]$  vs. response) with variable slope. For statistical analysis, two-tailed, unpaired t-test with Welch's correction (not assuming equal variances) was used at 95% confidence interval. Anti-cancer efficacy was evaluated by the  $IC_{50}$  in unlabeled and CM-DiI labeled MCF-7, BT-474, and MDA-MB-231 cells, and for test compounds in the cell lines.

## 2.2 Zebrafish culture

The transgenic Tg(*flila*:EGFP)<sup>y1</sup> zebrafish was generously gifted by Dr. Robert Tanguay (Oregon State University) and roy<sup>a9</sup>; mitfa<sup>w2</sup> Casper zebrafish was purchased from Zebrafish International Resource Center (ZIRC), catalog ID: 1689. Zebrafish were raised according to IACUC protocol #14-020 and housed in clean, restricted access facility in Aquatic Habitats Flow-through System (Aquatic Habitats, Florida). The light cycle for zebrafish was set to 14: 10 hours light: dark (dark 22:00 -08:00) to simulate natural breeding conditions.

The parameters for zebrafish water were set between a range of 26-30°C for temperature; pH 7.4-8; conductivity was adjusted using Instant Ocean salt at 60 ppm. The adult zebrafish were fed twice daily with Gemma 300 micro food. Larvae at age 5 dpf were fed Gemma 75 micro twice daily, and larvae at 30 dpf were fed Gemma 175 micro twice daily. For collecting eggs, mature zebrafish were spawned once a week in a spawning trap tank in the ratio of 1:1 male to female. Approximately two hours after the onset of the light cycle, the eggs were collected from the spawning tank. The eggs were washed, dead and unfertilized eggs removed, and added into a petridish containing zebrafish embryo water (sterilized deionized water, pH 7.4-7.7, 60 ppm Instant Ocean). The eggs were incubated at a temperature of 28°C and the light cycle was set to 14:10. Subsequently, the dead embryos were removed, and embryo water was replaced as required until the larvae were 5 dpf, at which point they were transferred in a regular tank in the zebrafish system. For xenotransplant experiments, the eggs collected from F3 crosses were incubated at 34°C.

### 2.2.1 Crossbreeding zebrafish

The Tg(*fli1a*:EGFP) transgenic zebrafish expresses the enhanced green fluorescent protein throughout their life owing to the *fli1a* promoter in their endothelial cells. Casper transgenic zebrafish, on the other hand, possess *roy*<sup>a9</sup>; *mitfa*<sup>w2</sup> genes in their homozygous recessive allelic form. The *roy*<sup>a9</sup> gene imparts transparency while the *mitfa*<sup>w2</sup> gene makes them devoid of pigment (White *et al.*, 2008b). For optimal imaging of the fluorescently labeled cancer cells in the fish, it was imperative that the fish were transparent, lacked pigment, and had the EGFP labeled vasculature. This ensured no interference of the inherent pigment of the zebrafish larvae in capturing images of the CM-DiI labeled BC cells in the xenografted fish. The Tg(*fli1a*:EGFP) and Casper transgenic lines were maintained and bred independently, and subsequently spawned together to obtain the hybrid transgenic embryos. The hybrid lines were maintained and bred to stock for experiments. The crossing technique was optimized by Dr. Faisal Albaqami. We repeated his methods and obtained Casper X Tg(*fli1a*:EGFP) crosses. Briefly, adult Tg(*fli1a*:EGFP) males and Casper females were spawned in a ratio of 1:1 in the breeding tanks. The eggs were collected, washed, and dead ones were removed. Eggs were maintained in a petridish containing zebrafish embryo water. These embryos were representative of the first generation (F1) crosses. The F1 crosses possessed heterozygous dominant wildtype and recessive mutated forms of *roy*<sup>a9</sup>; *mitfa*<sup>w2</sup> genes as a result of equal distribution of parent alleles. As a result, the F1 zebrafish expressed the EGFP under the *fli1a* promoter and appeared similar to Tg(*fli1a*:EGFP) and all embryos express green fluorescence in their vasculature. All the embryos were screened at 1 dpf for fluorescence and the strong EGFP expressing embryos were selected to be raised. These embryos, upon maturation, were spawned among themselves similarly, in the ratio of 1 male to 1 female and the

eggs were collected. The eggs collected from the F1 spawning were the F2 generation. F2 crosses expressing the EGFP were selected at 2 dpf and raised. The F2 crosses possessed EGFP, but there were different phenotypes owing to inheritance patterns as shown in Figure 7. The F2 transgenic embryos were raised, and upon reaching adulthood, bred to obtain the third generation (F3), and the procedure was repeated to obtain F4 offspring. All zebrafish experiments for this research were done using F4 offspring that possessed recessive mutated forms of *roy*<sup>a9</sup>; *mitfa*<sup>w2</sup> genes and expressed EGFP under *fli1a* promoter.

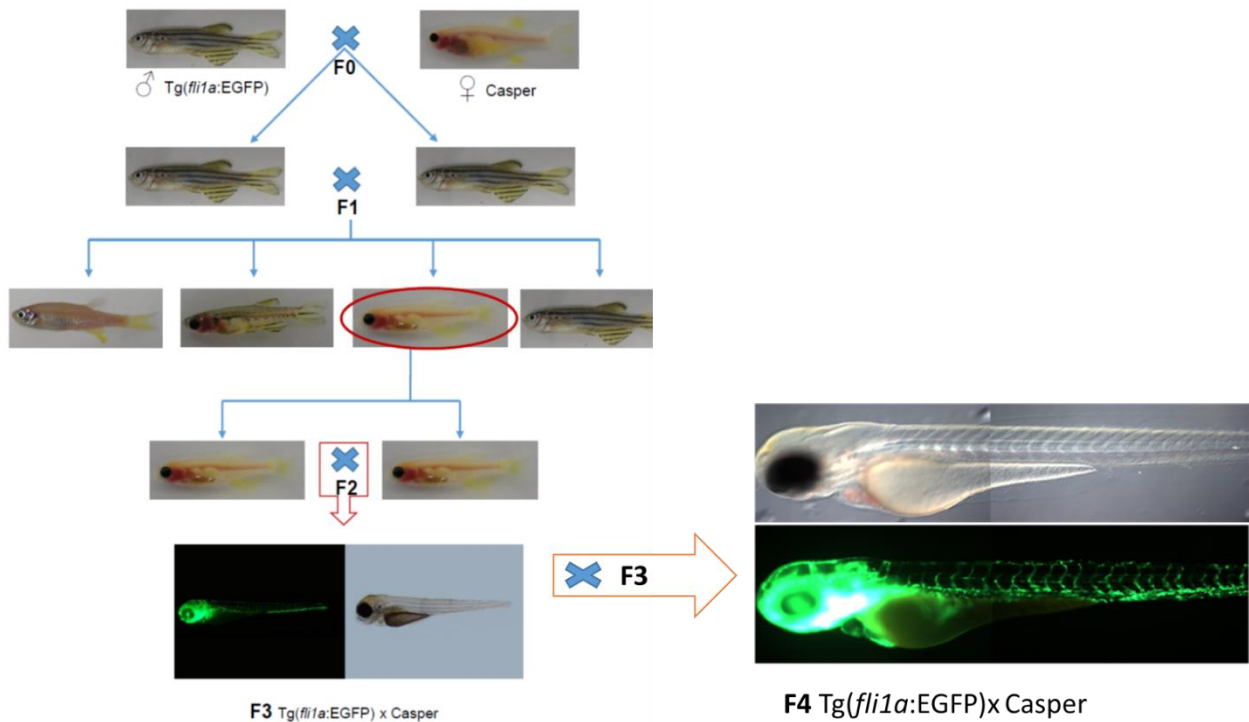


Figure 7: Schematic representation of Casper and *Tg(fli1a:EGFP)* crosses as described in Dr. Faisal Albaqami's dissertation (2016).



## **2.3 Maximally tolerated concentration (MTC) and no observed adverse effect level (NOAEL) in zebrafish larvae**

Maximally tolerated concentration (MTC) is the highest concentration at which the survival of the zebrafish larvae at the end of a 96-hour exposure was more than 80%, and no observed adverse effect level (NOAEL) is the concentration of compound at which deformities (curved body axis, yolk sac, and pericardial edema) were not observed in larvae exposed for a period of 96 hours. Zebrafish larvae aged 3 days post fertilization (dpf) were exposed to different concentrations of the test compounds for 96 hours to determine MTC in the exposed larvae. Each treatment group comprised of 12 larvae and corresponding controls treated with embryo water. Every 24 hours, the larvae were observed under a microscope to determine survival and for any visible phenotypic defects. Ultimately based on MTC and NOAEL, an optimal concentration of each compound that did not cause any overt developmental defects or toxicity in the fish was determined.

## **2.4 Xenotransplantation**

### **2.4.1 Preparing cells for transplantation**

Cells (MCF-7, BT-474, and MDA-MB-231) were prepared for transplantation using labeling procedure as described in 2.1. The pellet was resuspended in 300  $\mu$ L serum free DMEM. The labeled cells (100-200) were injected in zebrafish embryos within 2 hours to avoid clumping of cells.

## **2.4.2 Preparation of zebrafish for microinjection**

The F3 adult zebrafish were spawned two days before the microinjection. Eggs were collected the next morning, dead ones removed, and incubated at 34°C. At 1 dpf, the eggs were examined for fluorescence and the embryos expressing EGFP were selected. At 2 dpf, the embryos were anaesthetized using 0.02% tricaine methanesulfonate and oriented them in the dorsal position in a petridish coated with agarose gel. The borosilicate capillaries were pulled using Sutter Instrument P-20 ( pull = 20, velocity = 50, time = 200, pressure =200, and heat = ramp +21°C) as suggested by Wehmas et al (Wehmas *et al.*, 2016).

## **2.4.3 Xenotransplant of CM-DiI labeled MCF-7, BT-474, and MDA-MB-231 cells in zebrafish larvae/embryos**

Xenotransplantation of the breast cancer cells in 2 dpf zebrafish embryos using a protocol similar to the procedure described previously (Haldi *et al.*, 2006). The number of labeled cancer cells/mL were approximately  $1 \times 10^6$ . This pellet was resuspended in 300  $\mu$ l of serum-free DMEM and 4-5  $\mu$ l of this suspension was added to a pulled needle using Eppendorf capillary tips. Five  $\mu$ l of the labeled cell suspension was added to each needle. The needle was then inserted in the orifice of the micromanipulator and trimmed using forceps. The tip of the pulled needle was then trimmed using forceps to allow a droplet of approximately 5 nL to be injected into each fish. The number of cells in each droplet was counted and the diameter of the droplet measured to determine the number of cells/injection. The optimization procedure is described in Appendix I. The total number of cells/injection were calculated to be about 100-200 in a droplet with a radius of 160  $\mu$ m. Borosilicate needles were used to microinject CM-DiI labeled MCF-7, BT-474, and MDA-MB-

231 cells in the yolk sac of 2 dpf zebrafish embryos. The microneedle was positioned at a 45-degree angle to inject approximately 50 nL of the cell suspension into the yolk-sac of the larvae; 100-200 cells per larva were injected, approximately  $n = 60$  larvae were injected for each experiment.

## **2.5 Quantification of breast cancer cell proliferation**

### **2.5.1 Preparation and mounting of xenotransplanted zebrafish for fluorescence microscopy**

At 1 dpi, the xenotransplanted zebrafish larvae were anaesthetized in a 0.02% tricaine solution and then mounted in 110  $\mu$ L of 0.8% low melt agarose in tricaine in 48 well plates. The agarose gel was allowed to cool down before adding anaesthetized larvae in each well. The larvae were positioned using a pipette tip in a lateral position to image the yolk sac. The imaging was done at 1 dpi to identify the fish with cancer cells and remove the ones that did not have cancer cells or were deformed. After imaging the larvae and selecting the ones with the tumor cells at 1 dpi, the larvae were exposed to different concentrations of each compound with 20-30 larvae/treatment (approximately 30 larvae were injected for each treatment group, but at 1 dpi some of them died, had edemas, or did not have cancer cells and were eliminated from further evaluation) in 48 well plates. The larvae were exposed to the compounds at concentrations determined from the in vitro  $IC_{50}$  values and the in vivo MTC and NOAEL assays in water for 96 hours in 48 well plates. The effect of these compounds on the malignant cells was then observed as the distance traveled by the cancer cells from the site of injection after treatment with the compounds. In Trial 1, MCF-7, BT-474, and MDA-MB-231 xenografted larvae were treated with

10 nM mertansine (n = 12) for comparison of metastatic behavior in three cell lines. Subsequently, in Trial 2, MCF-7 xenografts were treated with 10 nM mertansine and 25 nM PTX in three independent experiments (n = 6-19). In Trial 3, MCF-7 xenografts were then treated with 200 nM mertansine in three independent experiments, and MDA-MB-231 xenografts were treated with 200 nM mertansine and 25 nM PXT in two independent experiments. The xenografted fish were exposed to the selected concentration of compounds for 96 hours starting at 1 dpi, observed every 24 hours for morphological changes and mortality, and the dose refreshed. After the 96-hour dosing period, living larvae were imaged similarly at 5 dpi to determine the proliferation and metastasis of cancer cells and the effect of treatment on the number of cancer cells.

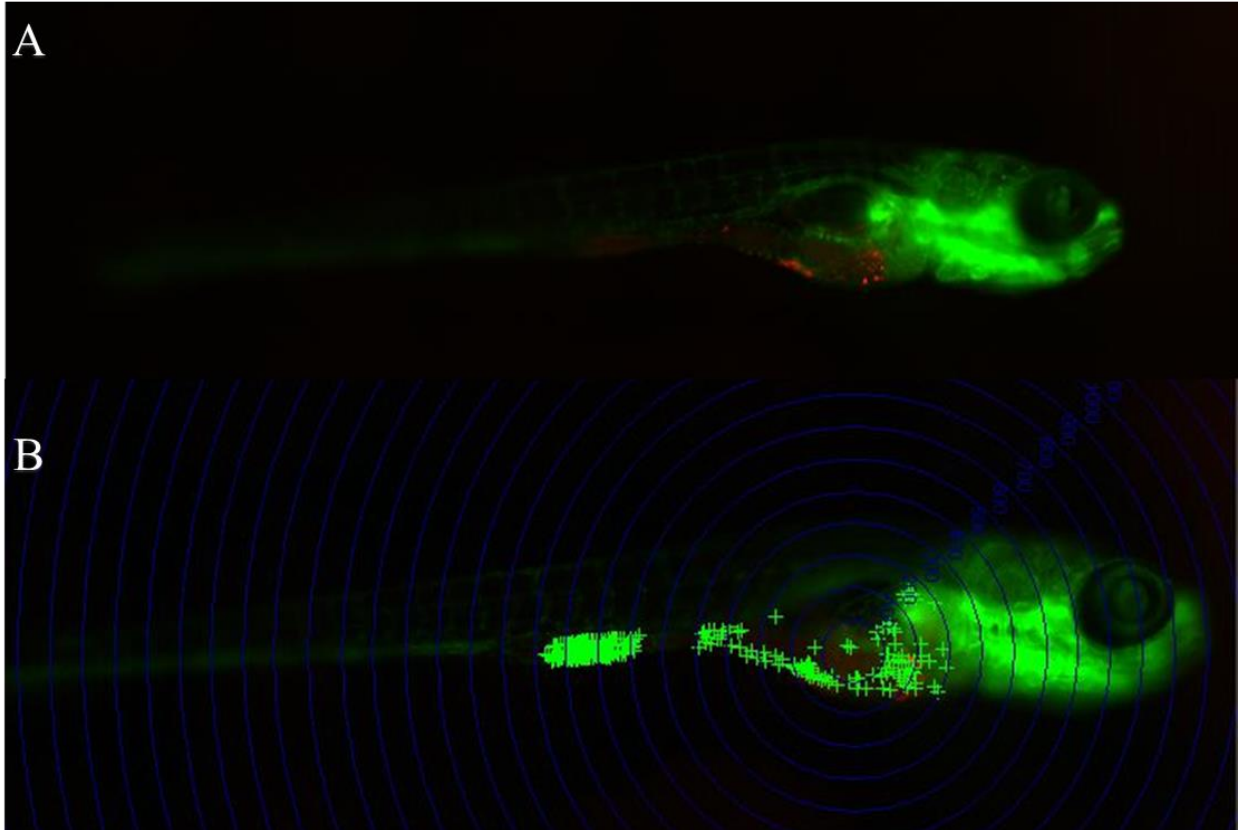
### **2.5.2 Imaging the xenotransplanted zebrafish larvae**

The xenotransplanted larvae were imaged using Nikon Eclipse Ti2 microscope using triggered tetramethylrhodamine isothiocyanate (TRITC) (excitation wavelength 550 nm and emission wavelength 580 nm) and fluorescein isothiocyanate (FITC) (excitation wavelength 494 nm and emission wavelength 518 nm) acquisition, where both TRITC and FITC wavelengths were emitted simultaneously. The exposure times used for TRITC and FITC filters were 200 milliseconds with 100% and 50%, intensities respectively. We obtained z-stacks of the fish using triggered FITC and TRITC settings and 10x + 1.5x objective was used. Each z-stack was 15  $\mu$ m thick. The images were acquired using NIS Elements software (Nikon).

### **2.5.3 Analysis of images obtained**

The fluorescent images were analyzed by selection of every second z-stack slice. The TRITC look up table (LUT) was adjusted to eliminate background and autofluorescence, and was

kept at the same LUTs for the entire fish. The site of injection was determined, and graticules (concentric circles starting at the site of injection then moving out, 100 microns apart) were centered on the site of injection. Each circle moving out from the site of injection was 100  $\mu\text{m}$  away along the entire length of the fish as shown in Figure 8. Next, cells were manually counted using only the TRITC filter image. The number of cells were counted from each selected z-frame and in every 100  $\mu\text{m}$  ring. The percent incidence of the number of cells that traveled beyond distances of 500, 1000, 1500, 2000, and 2500 nm from the site of injection were calculated. Data was analyzed using GraphPad Prism 5.0 and Two-way ANOVA was performed to determine statistical significance using Sidak's multiple comparisons.



**Figure 8** Pictomicrograph showing xenografted larva at 5 dpi (A) and in (B) the cell counting procedure using graticules in blue, each at a distance of 100 microns away from the site the injection. The green plus sign indicates each individual breast cancer cell. Number of cells in each graticule were manually counted.

## CHAPTER III

# ZEBRAFISH AS AN IN VIVO SCREEN FOR COMPOUNDS WITH ANTI-CANCER ACTIVITY IN HUMAN BREAST CANCER

### 3.1 Results

#### 3.1.1 Determination of in vitro cytotoxicity in labeled vs unlabeled breast cancer cell lines

To determine if the breast cancer cell lines that were labeled with CM-DiI possessed different sensitivity to standard chemotherapeutic compounds as compared to the unlabeled cells, MCF-7 and MB-231 cells were plated and treated with a log dose range for 72 hours. Figure 9 shows the treatment of MCF-7 cells with DOX and 4-OH-TAM. The  $IC_{50}$ s of doxorubicin and 4-OH-TAM in labeled and unlabeled cells were  $0.33 \pm 0.41 \mu\text{M}$  and  $0.47 \pm 0.038 \mu\text{M}$ , and  $27.48 \pm 0.52 \mu\text{M}$  and  $28.80 \pm 0.71 \mu\text{M}$ , respectively. A significant difference in the  $IC_{50}$ s of labeled vs parental cell lines was neither observed, for 4-OH-TAM ( $n = 3$ ,  $p = 0.0578$ , two-tailed unpaired t-test) nor for DOX ( $n = 3$ ,  $p = 0.2288$ , two-tailed unpaired t-test)

*Tinospora crispa* extracts (Table 3) were tested in both labeled and unlabeled MCF-7 and MDA-MB-231 cells at concentrations ranging up to 100 mg/mL (Figure 10). Only data from the unlabeled experiments is shown. No cytotoxic effects were observed at any concentration of the ten extracts.

Next, the potent microtubule inhibitors, mertansine, ansamitocin P-3, and MMAE were tested in vitro in MCF-7, BT-474, and MDA-MB-231 labeled and unlabeled cells (results shown in Appendix I) in multiple batches and repetitions to encompass a wide range of concentrations. Initially, it was challenging to get a stable solution of PTX, and it required multiple attempts and repetitions to achieve a stable solution where PTX did not precipitate out of solution. The ultimate concentration of PTX that was stable in DMSO was 1 mM and the freshly prepared stock was stored at -20°C in aliquots. Mertansine and PTX IC<sub>50</sub> values in MCF-7 cells were 0.120 ± 0.02 μM and 0.39 ± 0.06 μM, respectively. For MDA-MB-231 cells, the IC<sub>50</sub> values for mertansine and PTX were 0.09 ± 0.02 μM and 0.26 ± 0.04 μM, respectively. In BT-474, the IC<sub>50</sub>s were 0.11 ± 0.03 μM and 0.57 ± 0.1 μM, respectively (Figure 11). Mertansine was most cytotoxic in MDA-MB-231 cells with an IC<sub>50</sub> value of 0.09 μM whereas PTX was most toxic in MCF-7 cells.



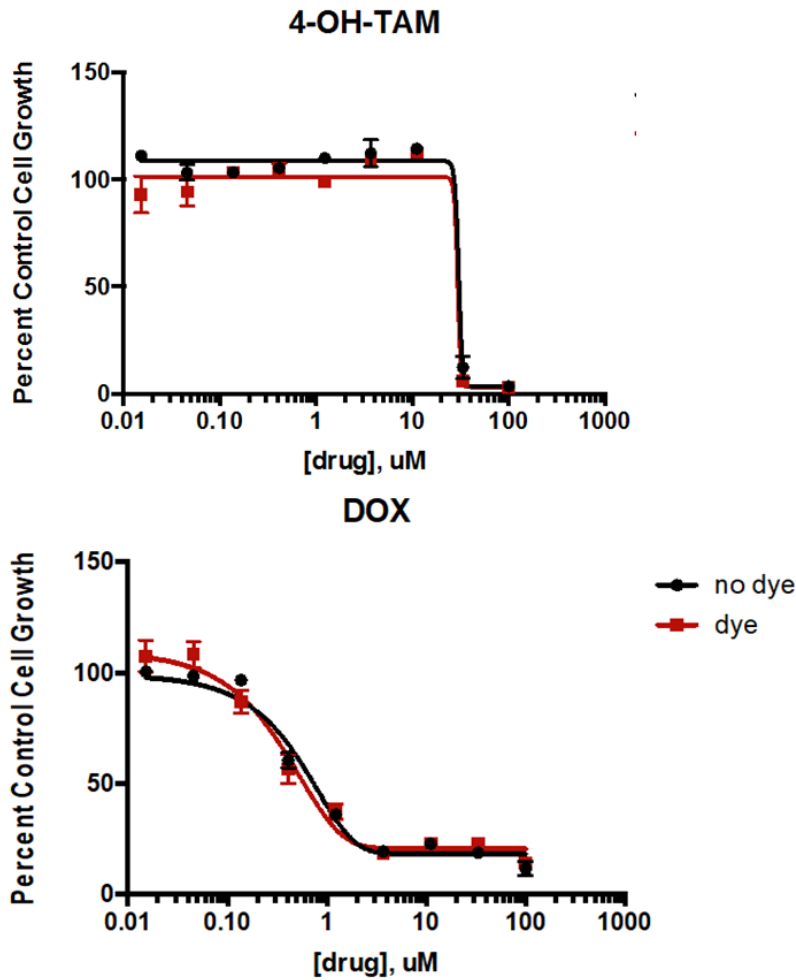
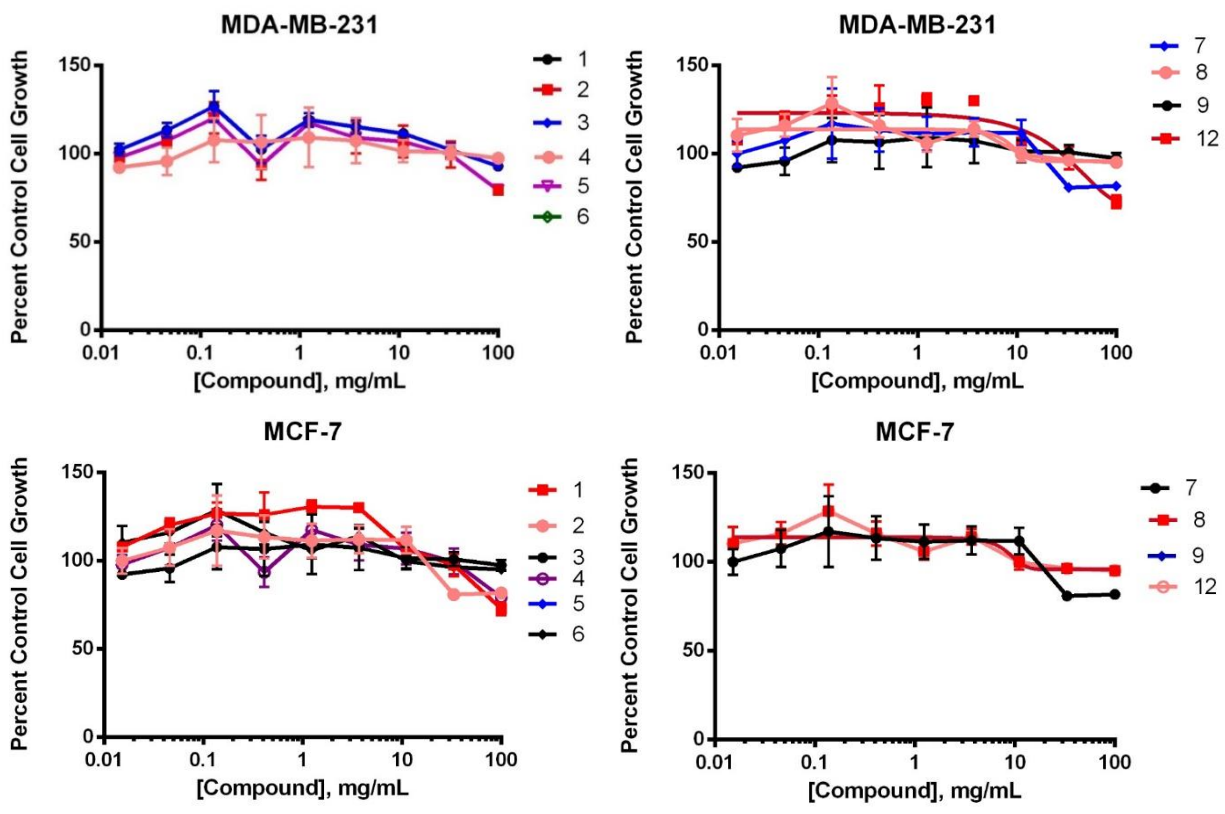


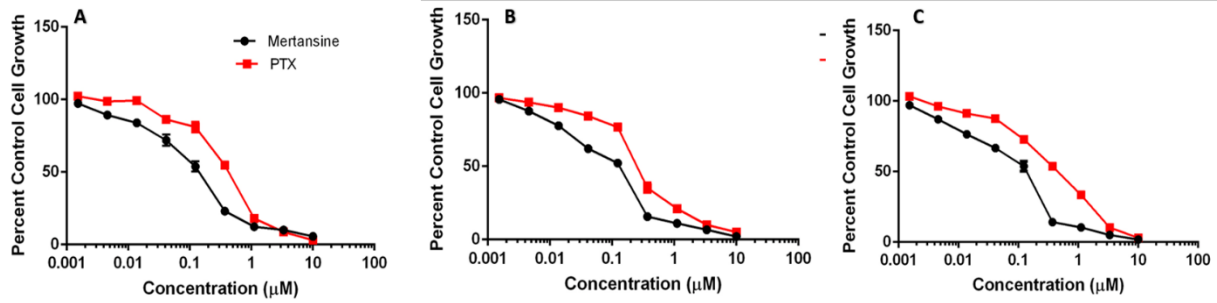
Figure 9: Determination of potential sensitivity to CM-DiI in MCF-7 labeled and unlabeled cells after treatment with 4-OH-TAM and doxorubicin. The cells, in triplicate wells, were exposed to drugs for a period of 72 hours. No statistically significant difference was found in the IC<sub>50</sub>'s of labeled vs unlabeled cells in response to the treatment tested using a two-tailed unpaired t-test with Welch's correction without assuming equal variance at 95% confidence

**Table 2:** *Tinospora crispa* fractions tested in MCF-7 and MDA-MB-231 cells for cytotoxicity

<b>Compound 1</b>	AP-3-39-3TC
<b>Compound 2</b>	<i>T. Crispa</i> methanolic extract
<b>Compound 3</b>	Tinosineside A (AP-1-42-4 Ts)
<b>Compound 4</b>	AP-TC-But
<b>Compound 5</b>	<i>T. Crispa</i> ethyl acetate fraction
<b>Compound 6</b>	<i>T. Crispa</i> chloroform fraction
<b>Compound 7</b>	Borapetoside E (AP-3-29-3Tc)
<b>Compound 8</b>	Borapetoside B (AP-2-60-2Tc)
<b>Compound 9</b>	Borapetoside F
<b>Compound 12</b>	Syringin (AP-2-47-5Tc)

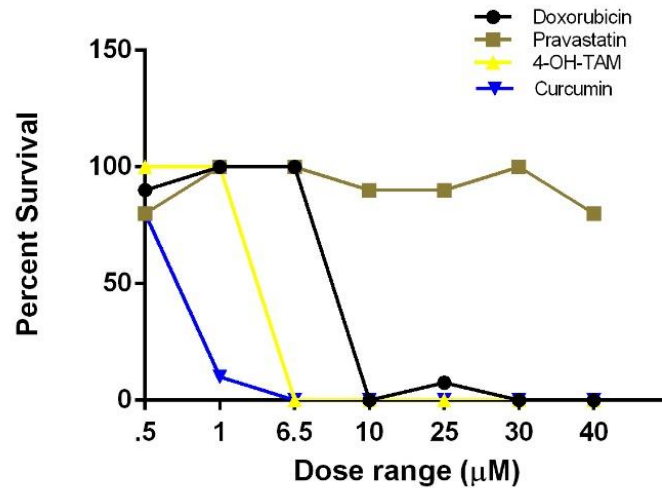


**Figure 10:** Determination of cytotoxicity of *Tinospora crispa* fractions in MDA-MB-231 and MCF-7 cells. The cells, in triplicate wells, were exposed to *Tinospora crispa* fractions (see Table 3 for fractions corresponding to legend numbers) for a period of 72 hours. No toxicity was observed in either cell line upon treatment with these compounds for a period of 72 hours.



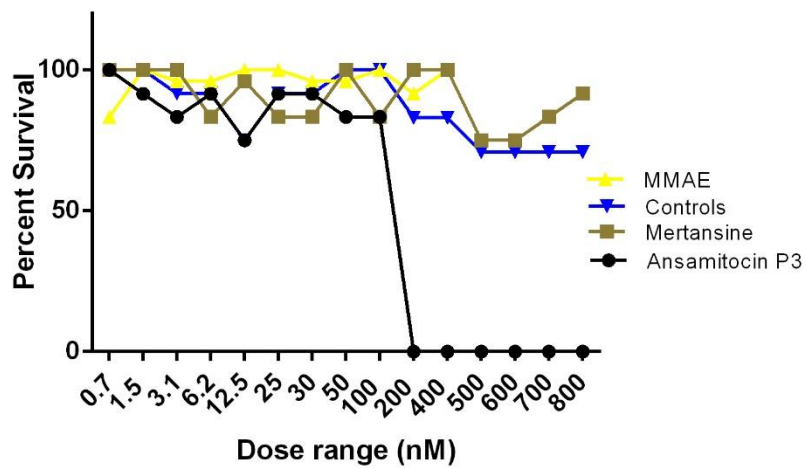
**Figure 11:** Determination of cytotoxicity of mertansine and paclitaxel in A) MCF-7, B) BT-474, and C) MDA-MB-231 cells. The cells, in triplicate wells, were exposed to different concentrations of mertansine and paclitaxel for a period of 24 hours

### 3.1.2 Determination of NOAEL and MTC of test compounds in zebrafish:

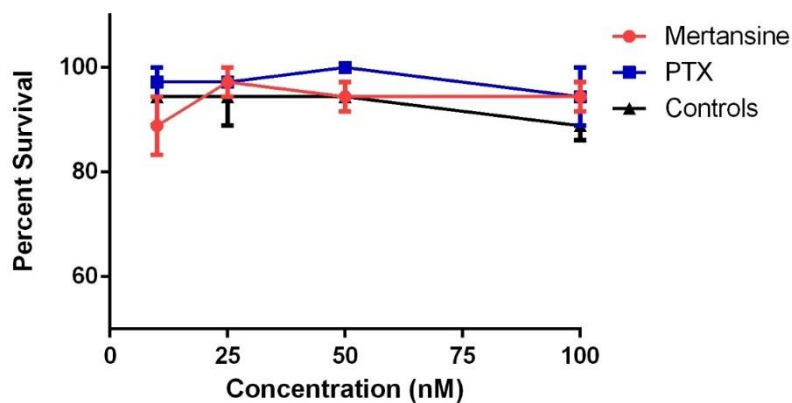


**Figure 12:** Survival of zebrafish larvae after an exposure to different concentrations of doxorubicin, pravastatin, curcumin, and 4-OH-TAM (n=12) to determine the maximally tolerated concentration in the larvae. The exposure started at 3 days post fertilization (dpf), doses were renewed every 24 hours up to 96 hours and the deformities were also noted.

Three-day old zebrafish larvae were plated in 48 well plates, one fish per well, and were dosed with varying concentrations of compounds for a period of 96 hours. The test chemical was re-administered every 24 hours and the larvae were observed for any deformities. The percent incidence of deformities observed at MTC in mertansine, ansamitocin P-3, MMAE and PTX are listed in Table 4. The MTC and the NOAEL were determined after the end of the exposure and a concentration lower than MTC was used as treatment for the xenotransplanted larvae. Observed MTCs for doxorubicin, 4-OH-TAM, PTX, curcumin, pravastatin, mertansine, ansamitocin P-3, and MMAE are listed in Table 3 below. For MMAE, 83% and 91% of the larvae survived at concentrations of 700 and 800 nM, but higher incidences of deformities were noted at these concentrations. For mertansine and PTX, the MTC was determined from three independent experiments (Figure 14), and we selected 25 nM for PTX, and 10 and 200 nM mertansine as the therapeutic concentration in our xenograft experiments.



**Figure 13:** Survival of zebrafish larvae after an exposure to different concentrations of potent microtubule inhibitors to determine the maximally tolerated concentration in the larvae (n = 12). The exposure started at 3 days post fertilization (dpf), doses were renewed every 24 hours up to 96 hours and the deformities were also noted.



**Figure 14:** Survival of zebrafish larvae after an exposure of 10-100 nM of PTX and mertansine (n = 12).

**Table 3:** MTC and NOAEL determined for various anti-cancer compounds

Compound	MTC	NOAEL
Doxorubicin	6.5 $\mu$ M	NM
Curcumin	0.5 $\mu$ M	NM
Pravastatin	40 $\mu$ M	NM
Paclitaxel	100 nM	25 nM
Mertansine	800 nM	400 nM
Monomethyl auristatin E	800 nM	400 nM
Ansamitocin P-3	100 nM	50 nM



**Table 4:** Percent incidence of deformities observed in larvae at MTC

Compound	Percent incidence of deformity observed at MTC	
	Yolk sac/Pericardial edema	Curved body axis
Mertansine	30	60
MMAE	50	90
Ansamitocin P-3	45	65
Paclitaxel	40	50

### **3.1.3 Validation of transgenic zebrafish as a xenotransplant model for human breast cancer:**

Three sets of trials (Table 6) aimed at answering questions about the validation of zebrafish as a xenotransplant model were performed. In the first experimental group, Trial 1, the metastatic behavior of MCF-7, BT-474, and MDA-MB-231 cells in vivo was observed at 1 and 5 dpi (Figure 15 and 16, respectively). Counting and analysis of cancer cells in the xenografts at 1 dpi showed in only a few zebrafish larva the cancer cells traveled beyond 600 micrometers from the site of injection (Figure 15). The larvae were then randomly distributed into control and treatment groups (n = 12), and treated with 10 nM mertansine. As it was observed that not many cells in either of the three experimental groups traveled beyond a distance of 500-600 micrometers from the site of injection at 1 dpi, it would be worthwhile to assess the total number of cells in each xenograft at 5 dpi, as well as to determine the number of cells that traveled beyond the 500  $\mu$ m distance mark as this was the farthest distance traveled by the cells in any of the three xenograft experimental groups. At 5 dpi, the total number of cells in the larvae as well as the percent incidence of cancer cells that traveled a beyond 500 micrometers from the site of injection in each larva at 5 dpi was determined in control and treatment groups. The effect of treatment on distance travelled by the

cancer cells from the site of injection in larvae xenografted with the three different cell types xenotransplanted was evaluated. Comparison of the total number of cells between the three BC xenograft experimental groups suggests that there was no significant difference in the metastatic potential of MCF-7, BT-474, or MDA-MB-231 cells or in the percent incidence of cells that traveled beyond 500  $\mu\text{m}$  in the three cell lines in Experiment 1 ( $n = 12$ , One-way ANOVA) (Figure 17).

For MCF-7 xenografts, in 25 nM PTX treated larvae in two of three experiments in Trial 2, a 50-60% decrease (Figure 18) in the fold change of percentage of cells beyond 500  $\mu\text{m}$  from the site of injection and in fold change in total number of cells as compared with controls was observed. This decrease was consistent with the overall significant reduction of percentage of cell that traveled beyond 1000  $\mu\text{m}$  in PTX treated group (Figure 19 (B)) ( $n = 6-10$ , One-way ANOVA,  $p < 0.05$ ). For MDA-MB-231 xenografts, in 25 nM PTX treatment groups, there was a 10-20% decrease in the fold change in percentage of cells beyond 500  $\mu\text{m}$  and fold change in total number of cells as compared to controls. A 55% decrease in the total number of cells was also observed in the 25 nM PTX group as compared to controls. However, a significant reduction of the percent incidence of cells beyond 500 and 1000  $\mu\text{m}$  in PTX treated larvae was not observed. These data point to effectiveness of 25 nM PTX in MCF-7 and MDA-MB-231 xenografts.

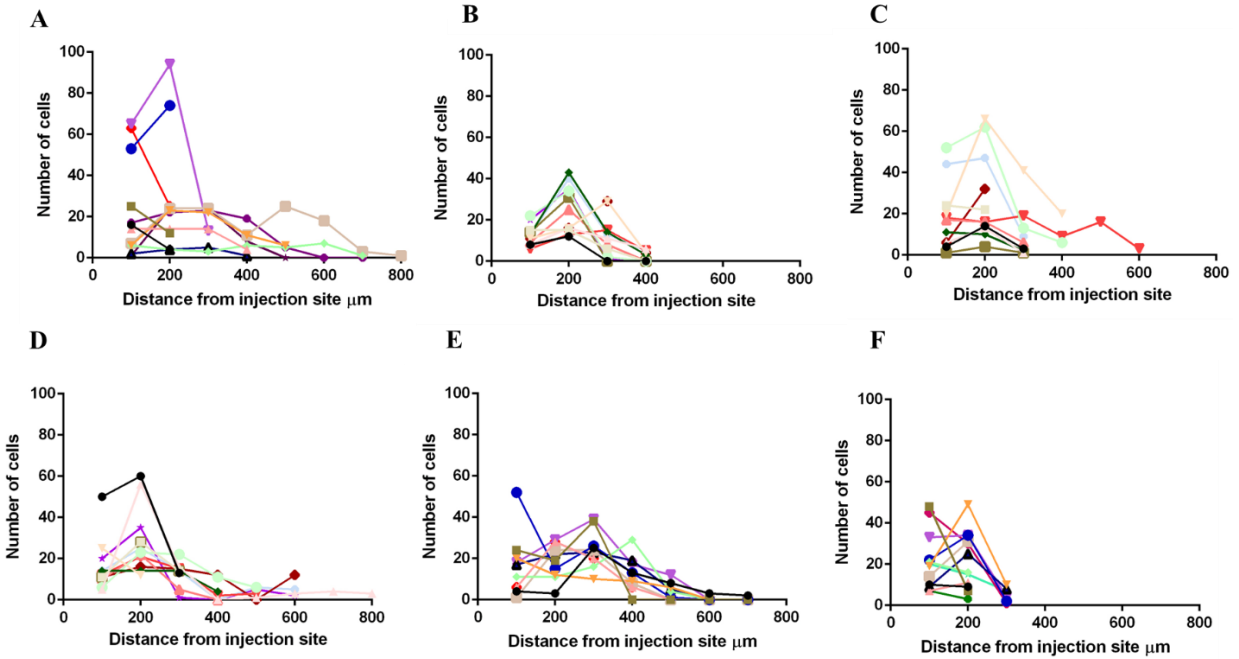
For MCF-7 xenografts treated with 10 nM mertansine, a 50-60% reduction in fold change in percentage of cells beyond 500  $\mu\text{m}$  and 20-30% decrease in fold change in total number of cells as compared to controls was observed in three out of four experiments. Also, a significant reduction in tumor burden beyond 500 and 1000  $\mu\text{m}$  from the site of injection was observed in the

10 nM mertansine treatment groups (Figure 19) (n= 6-13, One-way ANOVA,  $p < 0.05$ ). In MDA-MB-231 xenografts in the 10 nM mertansine treatment group, approximately 10% reduction was observed in the fold change in percentage of cells beyond 500  $\mu\text{m}$  and fold change in total number of cells as compared to controls. However, 10 nM mertansine was not effective in reducing tumor burden in MDA-MB-231 xenografts as compared to controls.

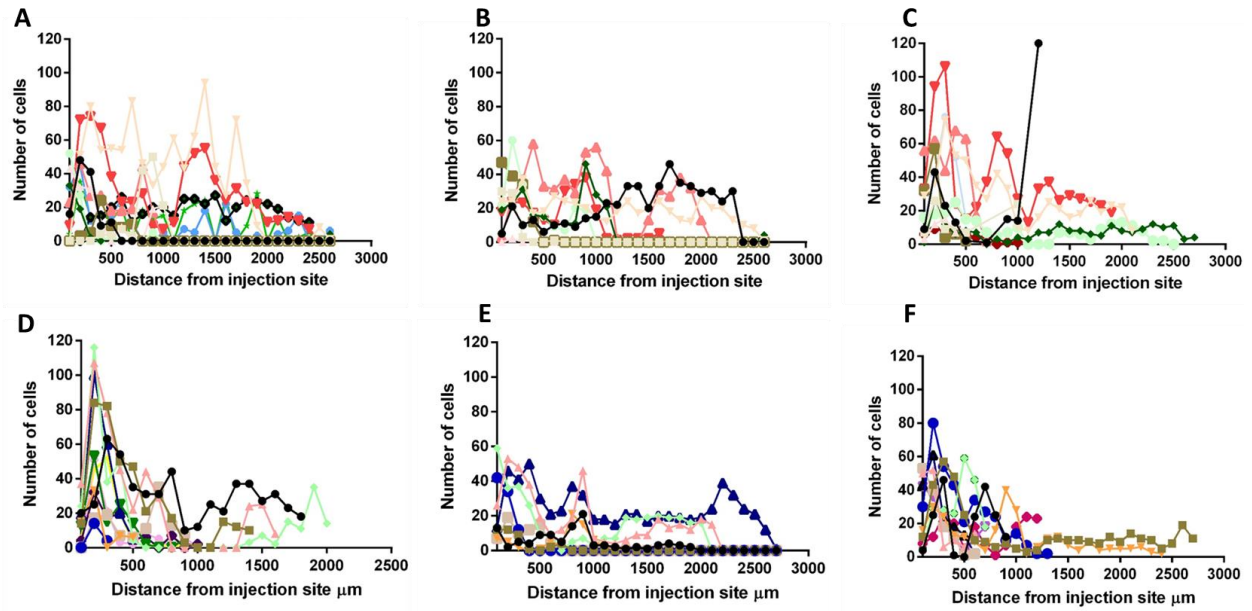
For MCF-7 xenografts treated with a higher concentration of mertansine, 200 nM, it was observed that a 20-60% decrease in the fold change in percentage of cells beyond 500  $\mu\text{m}$  and 40-50% decrease in fold change in total number of cells as compared to controls was observed in four experiments. Overall, a 75% reduction in the fold change in percentage of cells beyond 500  $\mu\text{m}$  was observed in 200 nM mertansine groups. Interestingly, a significant reduction in the total number of cells, percent incidence of cells beyond 500  $\mu\text{m}$ , and 1000  $\mu\text{m}$  was observed in the three experiments with 200 nM mertansine treatments (Figure 19) (n= 4-15, One-way ANOVA,  $p < 0.05$ ). In MDA-MB-231 xenografted larvae treated with 200 nM mertansine, there was a 10% reduction in tumor burden beyond 1000  $\mu\text{m}$  as compared to controls but it was not significant (n = 22, One-way ANOVA).

**Table 5** Trial 1-Determination of metastatic behavior of MCF-7, BT-474, and MDA-MB-231 cells in zebrafish xenografts

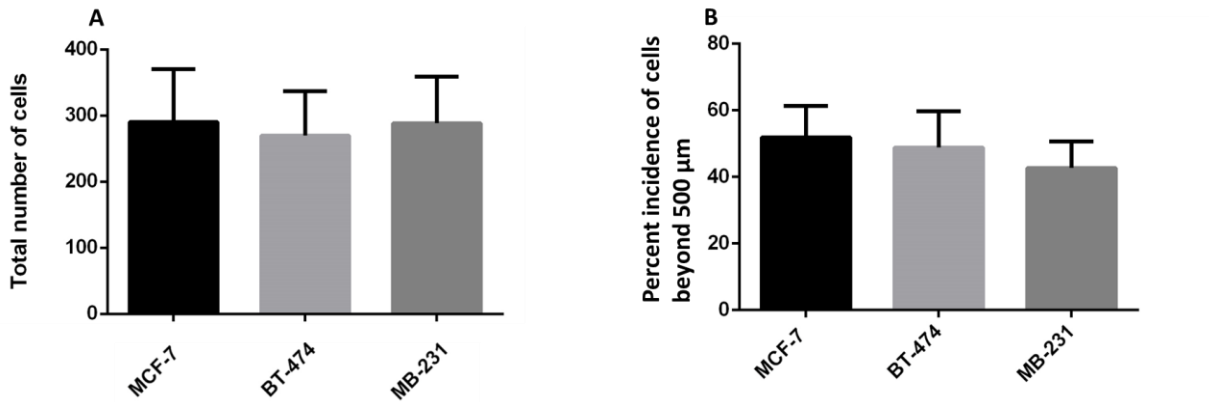
	<b>Exp 1 (MCF-7)</b>		<b>Exp 2 (MDA-MB-231)</b>		<b>Exp 3 (BT-474)</b>	
	<b>Ctrl</b>	<b>Mert (10 nM)</b>	<b>Ctrl</b>	<b>Mert (10 nM)</b>	<b>Ctrl</b>	<b>Mert (10 nM)</b>
Average total number of cells	290±80	208±60	288±67	209±75	202±70	147±80
Total number of fish at 5 DPI/ Total number at 1 DPI	12/20	12/20	12/20	12/19	12/22	12/21



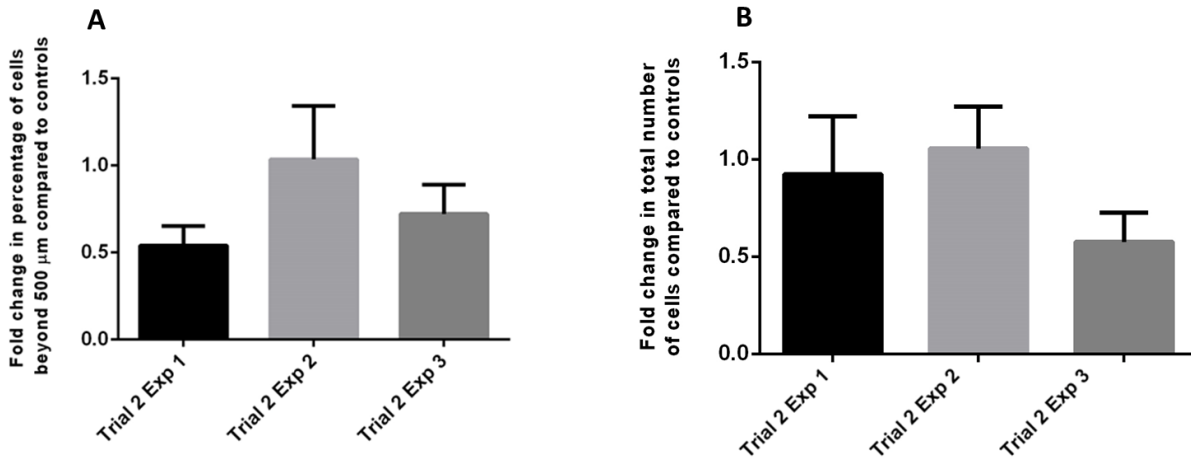
**Figure 15:** Zebrafish larvae xenografted with the three BC cell lines were imaged for detection of cancer cells at 1 dpi and randomly sorted into control and treatment groups. The images for larvae that survived until 5 dpi in both control and treatment groups were then analyzed for the distance traveled by cancer cells from the site of injection in each larva at 1 and 5 dpi. Distance traveled by MCF-7 cells in A) control group and D) treatment group, BT-474 cells in B) control group and E) treatment group, and MDA-MB-231 cells in C) control group and F) treatment group.



**Figure 16:** Zebrafish larvae xenografted with the three BC cell lines were imaged at 5 dpi. Distance traveled by MCF-7 cells in A) control group and D) treatment group, BT-474 cells in B) control group and E) treatment group, and MDA-MB-231 cells in C) control group and E) treatment group.

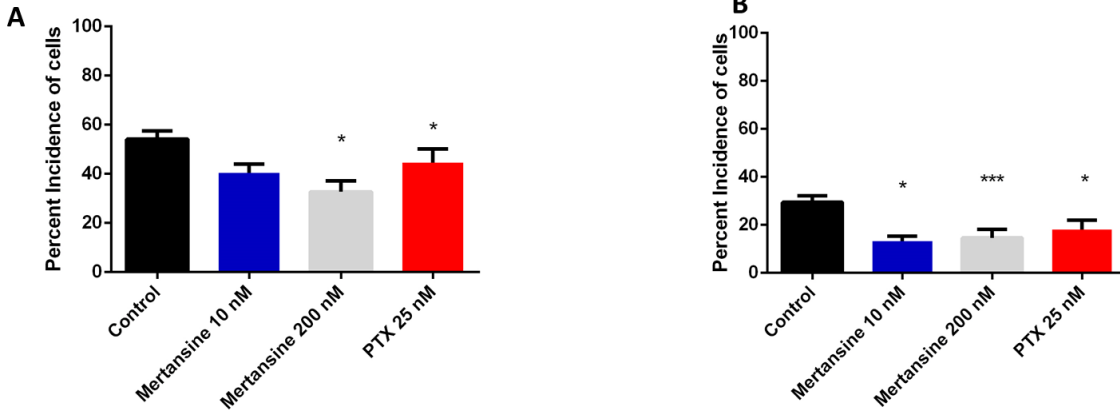


**Figure 17:** Trial 1 with MCF-7, BT-474, and MDA-MB-231 cells xenografted in zebrafish larvae. A) Total number of cells in MCF-7, BT-474, and MDA-MB-231 xenografts in the control group at 5 dpi (n = 12). B) Percent incidence of cells beyond 500  $\mu\text{m}$  from the site of injection in MCF-7, BT-474, and MDA-MB-231 xenografts in the control group at 5 dpi (n = 12).



**Figure 18:** Fold change in A) percentage of cells beyond 500  $\mu\text{m}$ , and B) in total number of cells in MCF-7 xenografted larvae treated with 25 nM Paclitaxel as compared with controls in each of three experiments. N = 9-15





**Figure 19:** Percent incidence of cells that traveled beyond A) 500  $\mu\text{m}$  and B) 1000  $\mu\text{m}$  in Trials 1, 2, and 3 in zebrafish larvae xenografted with MCF-7 cells at in Trials 1, 2, and 3 at 5 dpi. Data analyzed using one-way ANOVA, \*( $p < 0.05$ ) and \*\*\*( $p < 0.0001$ ) ( $n = 4-13$ ).

## 3.2 Discussion

We hypothesized that zebrafish larvae xenografted with human breast cancer cells and treated with traditionally used chemotherapeutics would exhibit a decrease in the number of cancer cells throughout the body of the zebrafish larvae as compared to the untreated controls. Three different breast cancer cell lines which encompass the three subtypes of breast cancer- ER/PR+ (MCF-7), HER2+ (BT-474), and TNBC (MDA-MB-231) were used. The characteristics that define these subtypes include, but are not limited to, their metastatic potential which attributes aggressiveness to the breast cancer cells. Zebrafish xenografts of human breast cancer represent an interplay between tumor and host cells, and the subsequent upregulation or downregulation of molecular signals facilitate migration of the tumor cells to different organs in the host. Our model offers the opportunity to study molecular mechanisms that are involved in the metastatic processes and to understand the role of key players.

The fluorescence of cancer cells is vital in the screening studies as it makes visualization and tracking of cancer cells in vivo feasible using live animals under a fluorescence microscope. Determining if the CM-DiI dye labelling makes the cells differentially sensitive to test compounds was important as it could affect the interpretation of the results. We did not find any significant difference in the  $IC_{50}$  values when labeled and unlabeled breast cancer cells were treated with the test compounds (Figure 9). Similarly, in order to determine if the labeled cells behaved differently or if there were artifacts produced by the dye, Ghotra et al. (2012) transfected PC3 prostate cancer cells with mCherry, and injected zebrafish larvae with labeled CM-DiI as well as mCherry labeled

PC3 cells. They did not find any significant changes in the migration pattern of the tumor cells in the two groups (Ghotra *et al.*, 2012). Our results from the in vitro cytotoxicity studies also indicate that CM-DiI is a reliable tool to label and observe the metastatic patterns and in determining anti-cancer potential of established and test compounds in vitro, and literature supports its use in vivo. Potent microtubule inhibitors used in this study-mertansine, ansamitocin P-3, and MMAE were tested in all three BC cell lines to determine their cytotoxicity. IC<sub>50</sub> values for mertansine and MMAE are not available for MCF-7, BT-474, and MDA-MB-231 cell lines in the literature. The IC<sub>50</sub> values for these compounds are listed in Table 7.

**Table 6** IC<sub>50</sub> values of microtubule inhibitors in literature

	<b>Mertansine</b>	<b>MMAE</b>	<b>Ansamitocin P-3</b>
<b>IC<sub>50</sub> in vitro (literature)</b>	1.10 nM SK-Br-3 and KB (Wayne C. Widdison <i>et al.</i> , 2006)	0.1 nM H3396 breast carcinoma (Doronina <i>et al.</i> , 2006)	<ul style="list-style-type: none"> <li>• 0.02 nM MCF-7</li> <li>• 0.150 nM MDA-MB-231 (Venghateri <i>et al.</i>, 2013)</li> </ul>
<b>IC<sub>50</sub> values (our results)</b>	<ul style="list-style-type: none"> <li>• 0.120 ± 0.02 μM MCF-7</li> <li>• 0.09 ± 0.02 μM MDA-MB-231</li> <li>• 6.7 ± 2.6 μM BT-474</li> </ul>	<ul style="list-style-type: none"> <li>• 0.150 ± 0.02 μM MCF-7</li> <li>• 0.050 μM MDA-MB-231</li> <li>• 0.04 ± 0.01 μM BT-474</li> </ul>	<ul style="list-style-type: none"> <li>• 0.095 ± 0.03 μM MCF-7</li> <li>• 0.07 μM MDA-MB-231</li> <li>• 0.049 ± 0.01 μM BT-474</li> </ul>

The NOAEL of different compounds, standard chemotherapeutics used in BC treatment, and test compounds with potential anti-cancer activity, was determined in zebrafish larvae for a period of 96 hours starting at 3 dpf (Table 4). The NOAEL and MTC provide a range of safe dosing concentrations that can be used in the xenograft assays. In most published xenograft studies using zebrafish, the xenografted larvae are dosed with a range of concentrations of known or test compounds to determine the cytotoxic effect on the tumor cells. In our study, we first determined the safe dosing range in un-injected larvae before treating the xenografts. This, in addition to the in vitro IC<sub>50</sub> values, provides us with a wide range of concentrations for exposure in the xenografts. We used 25 nM for PTX, and 10, and 200 nM for mertansine in the xenografts as concentrations observed as NOAEL. In mice, PTX is administered i.v./i.p. or in the tail at a concentration of 10 mg/ml in a solution of cremophor (Ma *et al.*, 2015) whereas in humans, for treatment of metastatic breast cancer, concentration up to 175 mg/m<sup>2</sup> is administered over three hours every three weeks.

In patients who are prone to hypersensitivity reactions, dexamethasone (20 mg) is administered as premedication to PTX (Quock *et al.*, 2002). To our knowledge, mertansine, MMAE, and ansamitocin P-3 have not been tested in zebrafish previously for toxicity.

Zebrafish has been extensively used as a xenograft model for different hematologic and solid human tumors as summarized by Drabsch (Drabsch *et al.* 2017). The zebrafish xenograft model presents numerous advantages such as requirement of small spaces for housing, inexpensive cost of breeding, EGFP labeled vasculature that makes visualizing angiogenesis feasible, ease of xenografting hundreds of animals per experiment, and live microscopy of the entire organism. Few limitations are still to be considered when using this model system. One of the limitations include incubation temperature, which is different for human cells (37°C) and zebrafish larvae (28°C). To overcome the difference in temperature, an optimal temperature was determined (34°C) which does not affect the growth of cancer cells or of the zebrafish larvae but is lower than normal human body temperature. The lack of an immune system should be considered when performing the xenograft assays as in a clinical setting immune cells have a key role in both facilitating as well as in eliminating tumor cells.

The xenograft experiments were performed in three different settings to compare the effect of PTX and low and high concentrations of mertansine. The zebrafish were injected with MCF-7, BT-474, and MDA-MB-231 cells (n = 12) and treated with 10 nM mertansine (as determined from the IC<sub>50</sub> from the initial MTS assay) in Trial 1. The rationale behind Trial 1 was to determine if the metastatic potential of the three BC cell lines was also represented *in vivo*. No significant differences in the migration pattern of the three cell lines were found to suggest a difference in the

migration pattern between these cell lines. Similar results for MCF-7 and BT-474 cells xenografts were observed by Eguiara et al., where xenografted single cells derived from BT-474 mammospheres, and parental cells from monolayer cultures to observe the migration pattern between the two types. They observed higher migration potential in xenografts with mammospheres and a weak metastatic potential of the monolayer culture cells, which is consistent with what we observed (Eguiara *et al.*, 2011). However, another group found the BT-474 to be more metastatic as compared to MCF-7 cells in xenografts (Ghotra *et al.*, 2012). This points to a need for understanding the factors that may be involved in the migration of cells in the xenografts. Firstly, the experimental factors such as site of injection, number of cells injected, incubation temperature, are all to be considered for the migration of cells in the xenografts. Eguiara et al, similar to us, injected the BT-474 in the yolk sac of the zebrafish at 2 dpf and the xenografts were incubated at 28 as well as 34°C. The only difference was that they injected approximately 500 cells in each larva. Ghotra et al., on the other hand used the same incubation temperature of 34°C, injection site yolk sac, and ~100 cells/larva. It is worthy to note that even with 500 cells, the monolayer BT-474 did not show high metastatic potential ((Eguiara *et al.*, 2011), whereas ~100 cells showed high metastatic potential under the same setting for Ghotra et al. Therefore, the number of cells injected can be ruled out to be a factor involved in the aggressiveness of the tumor. Other factors such as tumor microenvironment, may also be involved in the metastasis of the cells in vivo. Even with an investigation of the various molecular factors that may be involved in tumor cells migration in the xenografts, such as VEGF and neutrophils ((He *et al.*, 2012), in metastasis of tumor cells to hematopoietic tissues in melanoma xenografts as early as 30 minutes post injection, the role of zebrafish tumor microenvironment is not well described in the literature and needs

further investigation.

In these experiments, two different methods of analyzing the data were used to determine reduction in tumor burden in treatment groups versus controls. In one method, data was normalized to controls to determine the fold change in tumor cells, and in the second method, the percentage of cells beyond 500 and 1000  $\mu\text{m}$  were normalized with the total number of cells within that one larva. The 10 and 200 nM mertansine were found to be effective in significantly reducing the tumor burden in MCF-7 xenografts whereas the same results were not observed for MDA-MB-231 xenografts. This may be due to less sensitivity of MDA-MB-231 cells to mertansine, although a 10% reduction in tumor burden was observed in both treatment groups beyond 500 and 1000  $\mu\text{m}$  for 10 and 200 nM mertansine, respectively, this change was not significant. Moreover, an increase in total number of cells was observed in the MDA-MB-231 xenografts treated with 200 nM mertansine as compared to controls. Higher concentrations of mertansine need to be tested to determine efficacy in MDA-MB-231 xenografts.

For MCF-7 xenografts treated with 25 nM PTX, a significant reduction in tumor burden was observed in MCF-7 xenografts, when tested using different methods for analysis. This indicates an effective positive control for MCF-7 xenografts. In MDA-MB-231 xenografts, a reduction in tumor burden was observed in the two experiments with PTX treatment, however, this reduction was not statistically significant as compared to controls. This may also point to less sensitivity of MDA-MB-231 cells to PTX as observed with mertansine treatment. Treatment with higher concentration of PTX is required to further confirm efficacy in the MDA-MB-231 xenografts.

To the best of our knowledge, PTX has not been tested in zebrafish xenografted with breast cancer cell lines even though it is one of the most commonly used chemotherapeutics for the treatment of breast cancer in humans. Jung et al (2012) tested different concentrations of PTX in zebrafish xenografted with oral carcinoma cells (YD10B and HSC-2) and two colon cancer cell lines (HCT116 and DLD-1) to observe the effects of PTX on cancer cell dissemination and found effectiveness at 100 nM PTX (Jung *et al.*, 2012). In addition to PTX, other standard chemotherapeutic drugs that have been tested for validation of the zebrafish xenograft model using other human tumor cells include use of rapamycin, (mTOR inhibitor- inhibits lymphangiogenesis in zebrafish and mammals) to determine inhibition of lymphangiogenesis, an important step in tumor metastasis; as a positive control to screen compounds with potential inhibition of lymphangiogenesis (Astin *et al.*, 2014).

A significant decrease in both the overall number of cells as well as the distance traveled by the MCF-7 cancer cells from the site of injection in the zebrafish xenografts treated with PTX was observed. The treatment of the xenografts with mertansine (10 and 200 nM) demonstrated a higher survival in the xenografts and a reduction in the total number of cells as well as a decline in the number of cells that proliferated and traveled larger distances in the zebrafish from the site of injection in the yolk sac to the trunk and tail regions. These results aid us in the validation of the zebrafish xenograft model for the screening of anti-cancer compounds for human breast cancer.

The determination of concentration of the compounds for exposure in xenografts was dependent on many factors. The original hypothesis was to use a concentration that was higher than the IC<sub>50</sub> values, and between the range determined from the MTC and NOAEL observations.



However, for PTX, 25 nM (NOAEL) was used, which is lower than the IC<sub>50</sub> for PTX. Poor solubility of PTX in water was a major drawback for the zebrafish exposures, resulting in use of a low concentration stock solution (4 mM) from which smaller dilutions were made and aliquots were used to make fresh doses every day for the exposures. However, at 50 and 100 nM concentrations, higher incidences of deformities were observed in the larvae, and NOAEL was observed at 25 nM which is indicative of interference of PTX at concentrations higher than 50 nM to interfere with the molecular mechanisms in zebrafish. A reduction in tumor burden in both MCF-7 and MDA-MB-231 xenografts at 25 nM further suggests that the effect of PTX that may be due to the effective uptake of the compound from water by the larva. PTX, due to its poor water solubility, is administered in mice and humans in a Cremophor solution (polyethyleneglycerol tricinoate) and dehydrated ethanol, and is diluted in 0.9% (w/v) sodium chloride to make a final concentration of PTX of 0.3 and 1.2 mg/ml. The pharmacokinetics of PTX are known to be non-linear and the it is likely that Cremophor contributes to the nonlinearity. A typical injection of 2, 10, and 20 mg/kg in mice and 2 and 10 mg/kg in humans in Cremphor showed similar levels of Cremophor in patients as compared to mice indicating the role of Cremophor in non-linear pharmacokinetics of PTX (Willyard, 2018). It is important to note the involvement of vehicles such as Cremophor in the pharmacokinetics of drugs while extrapolating the effective concentrations of potent chemotherapeutic compounds administered as pharmaceutical formulations.

Mertansine is more potent than PTX, and because of this reason it is being extensively investigated in the development of antibody drug conjugates. The high potency of mertansine makes it toxic and it has an insufficient therapeutic window (Helft *et al.*, 2004). The solution is the

development of ADC's with the goal to achieve effective and targeted cancer cell cytotoxicity without the substantial toxicity mertansine would upon administration as a single agent. The monoclonal antibodies bind to the target tissue in a selective manner to reduce the intrinsic toxicity to the host tissues and results in an accumulation of the payload in the target tumor tissue (Xie *et al.*, 2004). Cantuzumab mertansine (huC242-DM1) is an approved ADC with four molecules of mertansine as the payload, humanized monoclonal antibody huC242 (specifically binds to the extracellular domain of tumor- associated carbohydrate antigen CanAg (for cancer antigen), a glycoform of MUC1, which is strongly expressed in many different solid tumors such as pancreatic, colorectal, biliary, gastric, uterine, bladder, and non-small cell lung cancers (Baeckström *et al.*, 1991; Xie *et al.*, 2004), and linked by disulfide bonds (Xie *et al.*, 2004). The zebrafish xenograft model can be utilized to study the efficacy of ADC's with different combinations of antibodies and linkers with potent payloads in a short-term assay, aiding in rapid screening of ADC combinations. This represents a rapidly growing area of drug development and approximately 12 ADC's have been approved by FDA in the past decade alone and different ADC combinations are currently being investigated in clinical trials for various cancers. Using a zebrafish xenograft to screen the different components for targeted delivery in breast cancer could provide important insights to molecular interactions and efficacy for drug development.

## **CHAPTER IV**

### **FUTURE DIRECTIONS**

Our study successfully developed a xenotransplantation model for the screening of anti-cancer compounds. Potent microtubule inhibitors that have been studied for decades, were tested in zebrafish larvae xenografted with human breast cancer cell lines. Mertansine, ansamitocin P-3, and MMAE have not been tested in zebrafish for developmental toxicity or in vivo anti-cancer treatment. With the establishment of the xenograft model, we can now study the effects of ansamitocin P-3 and MMAE and other components of ADCs in zebrafish xenografted with MCF-7, BT-474, and MDA-MB-231 cell lines to determine the response of these cell lines to these compounds.

The other two components of the ADC- the linkers and the antibodies will be tested, first in zebrafish larvae, and subsequently in xenografts. These studies present their own set of challenges owing to larger molecular weight of antibodies and the compatibility of humanized and mouse antibodies with zebrafish. This would be a unique opportunity to observe the efficacy of various combinations of antibodies and linkers. In several cancer patients, the cancer cells develop resistance to conventional therapies and the patient stops responding to treatment. Zebrafish xenografts of tumors derived from patients, PDX, are excellent models in the drug discovery field and for development of precision medicine as these assays are quick, short, and are useful in predicting the anti-cancer efficacy of novel test compounds, and the responses to conventionally

used chemotherapeutic drugs in case the tumors develop resistance. In clinical settings, zebrafish PDX model offers the advantage of using a large number of larvae which helps in ruling out variance in animals, the number of cells required are also less (~200/larva), and the amount of compound required for the treatment is also low aiding in efficient medium throughput assays. Zebrafish as a PDX model for multiple myeloma (Lin *et al.*, 2016) was shown to exhibit similar responses to standard chemotherapeutic drugs used for multiple myeloma (MM) bortezomib and lenalidomide, and four novel compounds in dexamethasone resistant and dexamethasone sensitive cell lines (MMIR and MMIS, respectively) and subsequently tested the response in patient derived xenografts from two newly diagnosed and four relapse MM patients. This study validated the use of zebrafish for PDX using primary MM cells. Zebrafish PDX for different solid and hematologic tumors presents a research field with enormous potential for exploration and development of novel anti-cancer compounds for fast detection of effective therapies tailored for individual patients.

In this study we were able to develop a human breast cancer zebrafish model based on the skeleton established by the work of one of the previous graduate students, Dr. Faisal Albaqami, and for the first time in our lab, we were able to quantify, by counting, the proliferation of breast cancer cells *in vivo*.

## **BIBLIOGRAPHY**

Abood, W., Fahmi, I. and Abdulla, M. (2014) 'Immunomodulatory effect of an isolated fraction from *Tinospora crispa* on intracellular expression of INF- $\gamma$ , IL-6 and IL-8', BMC.

Ades, F., Tryfonidis, K. and Zardavas, D. (2017) 'The past and future of breast cancer treatment—from the papyrus to individualised treatment approaches', *ecancermedicalsecience*, 11, p. 746. doi: 10.3332/ecancer.2017.746.

Agorku, D. J. et al. (2016) 'Depletion of Mouse Cells from Human Tumor Xenografts Significantly Improves Downstream Analysis of Target Cells', *Journal of Visualized Experiments*, (113). doi: 10.3791/54259.

Ahmad, W., Jantan, I. and Bukhari, S. N. A. (2016) 'Tinospora crispa (L.) Hook. f. & Thomson: A Review of Its Ethnobotanical, Phytochemical, and Pharmacological Aspects', *Frontiers in Pharmacology*. *Frontiers*, 7, p. 59. doi: 10.3389/fphar.2016.00059.

Aparajitha, K. U. and Priyadarshini K (2012) 'Paclitaxel Against Cancer: A Short Review', *Paclitaxel Against Cancer: A Short Review*. *Med chem*, 27(2). doi: 10.4172/2161-0444.1000130.

Astin, J. W. et al. (2014) 'An in vivo antilymphatic screen in zebrafish identifies novel inhibitors of mammalian lymphangiogenesis and lymphatic-mediated metastasis.', *Molecular cancer therapeutics*. American Association for Cancer Research, 13(10), pp. 2450–62. doi: 10.1158/1535-7163.MCT-14-0469-T.

Baeckström, D. et al. (1991) 'Purification and characterization of a membrane-bound and a secreted mucin-type glycoprotein carrying the carcinoma-associated sialyl-Lea epitope on distinct core proteins.', *The Journal of biological chemistry*, 266(32), pp. 21537–47.

Beck, A. et al. (2017) 'Strategies and challenges for the next generation of antibody–drug conjugates', *Nature Reviews Drug Discovery*, 16(5), pp. 315–337. doi: 10.1038/nrd.2016.268.

Binder, V. and Zon, L. I. (2013) 'High throughput in vivo phenotyping: The zebrafish as tool for drug discovery for hematopoietic stem cells and cancer', *Drug Discovery Today: Disease Models*. Elsevier Ltd, 10(1), pp. e17–e22. doi: 10.1016/j.ddmod.2012.02.007.

Brown, H. K. et al. (2017) 'Zebrafish xenograft models of cancer and metastasis for drug discovery', *Expert Opinion on Drug Discovery*, 12(4), pp. 379–389. doi: 10.1080/17460441.2017.1297416.

Cassady, J. M. et al. (2004) 'Recent Developments in the Maytansinoid Antitumor Agents', *CHEMICAL & PHARMACEUTICAL BULLETIN*. The Pharmaceutical Society of Japan, 52(1), pp. 1–26. doi: 10.1248/cpb.52.1.

Cassidy, J. W., Caldas, C. and Bruna, A. (2015) 'Maintaining Tumor Heterogeneity in Patient-Derived Tumor Xenografts.', *Cancer research*. Europe PMC Funders, 75(15), pp. 2963–8. doi:

10.1158/0008-5472.CAN-15-0727.

Chari, R. V. J., Miller, M. L. and Widdison, W. C. (2014) 'Antibody-Drug Conjugates: An Emerging Concept in Cancer Therapy', *Angewandte Chemie International Edition*. WILEY-VCH Verlag, 53(15), pp. 3796–3827. doi: 10.1002/anie.201307628.

Choudhary, M. I. et al. (2010) 'cis-Clerodane-Type Furanoditerpenoids from *Tinospora crispa*', *Journal of Natural Products*. American Chemical Society and American Society of Pharmacognosy, 73(4), pp. 541–547. doi: 10.1021/np900551u.

Coghlin, C. and Murray, G. I. (2010) 'Current and emerging concepts in tumour metastasis', *The Journal of Pathology*, 222(1), pp. 1–15. doi: 10.1002/path.2727.

David, H. (1988) 'Rudolf Virchow and Modern Aspects of Tumor Pathology', *Pathology - Research and Practice*, 183(3), pp. 356–364. doi: 10.1016/S0344-0338(88)80138-9.

Davies, C. et al. (2013) 'Long-term effects of continuing adjuvant tamoxifen to 10 years versus stopping at 5 years after diagnosis of oestrogen receptor-positive breast cancer: ATLAS, a randomised trial', *The Lancet*. Elsevier, 381(9869), pp. 805–816. doi: 10.1016/S0140-6736(12)61963-1.

Deveau, A. P., Bentley, V. L. and Berman, J. N. (2017) 'Using zebrafish models of leukemia to streamline drug screening and discovery', *Experimental Hematology*. ISEH - International Society for Experimental Hematology, 45, pp. 1–9. doi: 10.1016/j.exphem.2016.09.012.

Dhillon, S. (2014) 'Trastuzumab Emtansine: A Review of Its Use in Patients with HER2-Positive Advanced Breast Cancer Previously Treated with Trastuzumab-Based Therapy', *Drugs*, 74(6), pp. 675–686. doi: 10.1007/s40265-014-0201-0.

van de Donk, N. W. C. J. and Dhimolea, E. (2012) 'Brentuximab vedotin.', *mAbs*. Taylor & Francis, 4(4), pp. 458–65. doi: 10.4161/mabs.20230.

Doronina, S. O. et al. (2003) 'Development of potent monoclonal antibody auristatin conjugates for cancer therapy', *Nature Biotechnology*, 21(7), pp. 778–784. doi: 10.1038/nbt832.

Doronina, S. O. et al. (2006) 'Enhanced Activity of Monomethylauristatin F through Monoclonal Antibody Delivery: Effects of Linker Technology on Efficacy and Toxicity', *Bioconjugate Chemistry*, 17(1), pp. 114–124. doi: 10.1021/bc0502917.

Doroshov, J. H. (1986) 'Role of hydrogen peroxide and hydroxyl radical formation in the killing of Ehrlich tumor cells by anticancer quinones.', *Proceedings of the National Academy of Sciences of the United States of America*, 83(12), pp. 4514–8.

Drabsch, Y., Snaar-Jagalska, B. E. and Ten Dijke, P. (2017) 'Fish tales: The use of zebrafish xenograft human cancer cell models', *Histology and Histopathology*, 32(7), pp. 673–686. doi: 10.14670/HH-11-853.

Early Breast Cancer Trialists' Collaborative Group (EBCTCG) et al. (2011) 'Relevance of breast cancer hormone receptors and other factors to the efficacy of adjuvant tamoxifen: patient-level meta-analysis of randomised trials', *The Lancet*, 378(9793), pp. 771–784. doi: 10.1016/S0140-6736(11)60993-8.

Eguiara, A. et al. (2011) 'Xenografts in zebrafish embryos as a rapid functional assay for breast cancer stem-like cell identification', *Cell Cycle*, 10(21), pp. 3751–3757. doi: 10.4161/cc.10.21.17921.

Feitsma, H. and Cuppen, E. (2008) 'Zebrafish as a Cancer Model Cancer Research in Zebrafish', *Mol Cancer Res*, 6(5), pp. 685–94. doi: 10.1158/1541-7786.MCR-07-2167.

Fidler, I. J., Gersten, D. M. and Hart, I. R. (1978) 'The Biology of Cancer Invasion and Metastasis', *Advances in Cancer Research*. Academic Press, 28, pp. 149–250. doi: 10.1016/S0065-230X(08)60648-X.

Fidler, I. J., Kim, S.-J. and Langley, R. R. (2007) 'The role of the organ microenvironment in the biology and therapy of cancer metastasis', *Journal of Cellular Biochemistry*, 101(4), pp. 927–936. doi: 10.1002/jcb.21148.

Fleming, A., Jankowski, J. and Goldsmith, P. (2010) 'In vivo analysis of gut function and disease changes in a zebrafish larvae model of inflammatory bowel disease', *Inflammatory Bowel Diseases*, 16(7), pp. 1162–1172. doi: 10.1002/ibd.21200.

Folkman, J. and Kalluri, R. (2004) 'Cancer without disease', *Nature*, 427(6977), pp. 787–787. doi: 10.1038/427787a.

Fonseka, T. M. et al. (2016) 'Zebrafish models of major depressive disorders', *Journal of Neuroscience Research*, 94(1), pp. 3–14. doi: 10.1002/jnr.23639.

Franceschini, G. et al. (2015) 'New trends in breast cancer surgery: a therapeutic approach increasingly efficacy and respectful of the patient.', *Il Giornale di chirurgia. CIC Edizioni Internazionali*, 36(4), pp. 145–52. doi: 10.11138/GCHIR/2015.36.4.145.

Gaudenzi, G. et al. (2017) 'Patient-derived xenograft in zebrafish embryos: a new platform for translational research in neuroendocrine tumors', *Endocrine*. Springer US, 57(2), pp. 214–219. doi: 10.1007/s12020-016-1048-9.

Gewirtz, D. A. (1999) 'A critical evaluation of the mechanisms of action proposed for the antitumor effects of the anthracycline antibiotics adriamycin and daunorubicin.', *Biochemical pharmacology*, 57(7), pp. 727–41.

Gherzi, D., Wilcken, N. and Simes, R. J. (2005) 'A systematic review of taxane-containing regimens for metastatic breast cancer.', *British journal of cancer*. Nature Publishing Group, 93(3), pp. 293–301. doi: 10.1038/sj.bjc.6602680.

Ghotra, V. P. S. et al. (2012) 'Automated whole animal bio-imaging assay for human cancer



dissemination', PLoS ONE, 7(2). doi: 10.1371/journal.pone.0031281.

Ghotra, V. P. S. et al. (2012) 'Automated Whole Animal Bio-Imaging Assay for Human Cancer Dissemination', PLoS ONE. Edited by L. Rénia. Public Library of Science, 7(2), p. e31281. doi: 10.1371/journal.pone.0031281.

Gianni, L., Salvatorelli, E. and Minotti, G. (2007) 'Anthracycline cardiotoxicity in breast cancer patients: synergism with trastuzumab and taxanes', Cardiovascular Toxicology, 7(2), pp. 67–71. doi: 10.1007/s12012-007-0013-5.

Gu, G. et al. (2017) 'Zebrafish Larvae Model of Dilated Cardiomyopathy Induced by Terfenadine', Korean Circulation Journal, 47(6), p. 960. doi: 10.4070/kcj.2017.0080.

Gualberto, A. (2012) 'Brentuximab Vedotin (SGN-35), an antibody–drug conjugate for the treatment of CD30-positive malignancies', Expert Opinion on Investigational Drugs, 21(2), pp. 205–216. doi: 10.1517/13543784.2011.641532.

Gutierrez, C. and Schiff, R. (2011) 'HER2: biology, detection, and clinical implications.', Archives of pathology & laboratory medicine. NIH Public Access, 135(1), pp. 55–62. doi: 10.1043/2010-0454-RAR.1.

Haldi, M. et al. (2006) 'Human melanoma cells transplanted into zebrafish proliferate, migrate, produce melanin, form masses and stimulate angiogenesis in zebrafish', Angiogenesis, 9(3), pp. 139–151. doi: 10.1007/s10456-006-9040-2.

Hayes, C. L. et al. (1996) '17 beta-estradiol hydroxylation catalyzed by human cytochrome P450 1B1.', Proceedings of the National Academy of Sciences of the United States of America. National Academy of Sciences, 93(18), pp. 9776–81.

He, S. et al. (2012) 'Neutrophil-mediated experimental metastasis is enhanced by VEGFR inhibition in a zebrafish xenograft model', The Journal of Pathology, 227(4), pp. 431–445. doi: 10.1002/path.4013.

Helft, P. R. et al. (2004) 'A phase I study of cantuzumab mertansine administered as a single intravenous infusion once weekly in patients with advanced solid tumors.', Clinical cancer research: an official journal of the American Association for Cancer Research. American Association for Cancer Research, 10(13), pp. 4363–8. doi: 10.1158/1078-0432.CCR-04-0088.

Hershman, D. L. et al. (2011) 'Association between patient reported outcomes and quantitative sensory tests for measuring long-term neurotoxicity in breast cancer survivors treated with adjuvant paclitaxel chemotherapy', Breast Cancer Research and Treatment. Springer US, 125(3), pp. 767–774. doi: 10.1007/s10549-010-1278-0.

Hipol, R., Cariaga, M. and Hipol, R. (2012) 'Anti-inflammatory activities of the aqueous extract of the stem of *Tinospora crispa* (Family Menispermaceae)', Journal of Nature Studies.

Howe, K. et al. (2013) 'The zebrafish reference genome sequence and its relationship to the human

- genome', *Nature. Nature Research*, 496(7446), pp. 498–503. doi: 10.1038/nature12111.
- Hunter, K. W., Crawford, N. P. S. and Alsarraj, J. (2008) 'Mechanisms of metastasis.', *Breast cancer research: BCR. BioMed Central*, 10 Suppl 1(Suppl 1), p. S2. doi: 10.1186/bcr1988.
- Jordan, A. et al. (1998) 'Tubulin as a target for anticancer drugs: agents which interact with the mitotic spindle.', *Medicinal research reviews*, 18(4), pp. 259–96.
- Jordan, M. A. et al. (1993) 'Mechanism of mitotic block and inhibition of cell proliferation by taxol at low concentrations.', *Proceedings of the National Academy of Sciences of the United States of America. National Academy of Sciences*, 90(20), pp. 9552–6.
- Jordan, M. A. (2002) 'Mechanism of action of antitumor drugs that interact with microtubules and tubulin.', *Current medicinal chemistry. Anti-cancer agents*, 2(1), pp. 1–17.
- Jordan, V. C. (1993) 'Fourteenth Gaddum Memorial Lecture. A current view of tamoxifen for the treatment and prevention of breast cancer.', *British journal of pharmacology. Wiley-Blackwell*, 110(2), pp. 507–17.
- Jung, D.-W. et al. (2012) 'A novel zebrafish human tumor xenograft model validated for anti-cancer drug screening', *Molecular BioSystems. The Royal Society of Chemistry*, 8(7), p. 1930. doi: 10.1039/c2mb05501e.
- Kalluri, R. and Zeisberg, M. (2006) 'Fibroblasts in cancer', *Nature Reviews Cancer. Nature Publishing Group*, 6(5), pp. 392–401. doi: 10.1038/nrc1877.
- Kamarazaman, I., Amorn, Z. and Ali, R. (2012) 'Inhibitory properties of *Tinospora crispa* extracts on TNF- $\alpha$  induced inflammation on human umbilical vein endothelial cells (HUVECS)', *Int. J. Trop. Med.*
- Karkampouna, S. et al. (2018) 'CRIPTO promotes an aggressive tumour phenotype and resistance to treatment in hepatocellular carcinoma', *The Journal of Pathology*, 245(3), pp. 297–310. doi: 10.1002/path.5083.
- Kongsaktragoon, B., Tamsiririrkkul, R. and Suvitayavat, W. (1984) 'The antipyretic effect of *Tinospora crispa* Mier ex Hook. f. & Thoms', *Mahidol University Journal*.
- Kupchan, S. M. et al. (1972) 'Tumor inhibitors. LXXIII. Maytansine, a novel antileukemic ansa macrolide from *Maytenus ovatus*', *Journal of the American Chemical Society. American Chemical Society*, 94(4), pp. 1354–1356. doi: 10.1021/ja00759a054.
- Lal, S. et al. (2012) 'Calpain 2 is required for the invasion of glioblastoma cells in the zebrafish brain microenvironment', *Journal of Neuroscience Research*, 90(4), pp. 769–781. doi: 10.1002/jnr.22794.
- Lam, S. H. et al. (2004) 'Development and maturation of the immune system in zebrafish, *Danio rerio*: a gene expression profiling, in situ hybridization and immunological study.', *Developmental*

and comparative immunology, 28(1), pp. 9–28.

De Laurentiis, M. et al. (2008) ‘Taxane-based combinations as adjuvant chemotherapy of early breast cancer: a meta-analysis of randomized trials.’, *Journal of clinical oncology: official journal of the American Society of Clinical Oncology*, 26(1), pp. 44–53. doi: 10.1200/JCO.2007.11.3787.

Lawson, N. D. and Weinstein, B. M. (2002) ‘In Vivo Imaging of Embryonic Vascular Development Using Transgenic Zebrafish’, *Developmental Biology*, 248(2), pp. 307–318. doi: 10.1006/dbio.2002.0711.

Li, D.-M. and Feng, Y.-M. (2011) ‘Signaling mechanism of cell adhesion molecules in breast cancer metastasis: potential therapeutic targets’, *Breast Cancer Research and Treatment*, 128(1), pp. 7–21. doi: 10.1007/s10549-011-1499-x.

Li, M. et al. (2017) ‘Muscular dystrophy modeling in zebrafish’, in *Methods in cell biology*, pp. 347–380. doi: 10.1016/bs.mcb.2016.11.004.

Li, Y. et al. (2015) ‘Genetic depletion and pharmacological targeting of  $\alpha$ v integrin in breast cancer cells impairs metastasis in zebrafish and mouse xenograft models’, *Breast Cancer Research*, 17(1), p. 28. doi: 10.1186/s13058-015-0537-8.

Lin, J.-N. et al. (2015) ‘Development of an Animal Model for Alcoholic Liver Disease in Zebrafish’, *Zebrafish*, 12(4), pp. 271–280. doi: 10.1089/zeb.2014.1054.

Lin, J. et al. (2016) ‘A clinically relevant in vivo zebrafish model of human multiple myeloma to study preclinical therapeutic efficacy.’, *Blood. American Society of Hematology*, 128(2), pp. 249–52. doi: 10.1182/blood-2016-03-704460.

Lin, N. U. (2013) ‘Breast cancer brain metastases: new directions in systemic therapy.’, *Ecanermedicalsience*, 7, p. 307. doi: 10.3332/ecancer.2013.307.

Lin, P., Hu, S.-W. and Chang, T.-H. (2003) ‘Correlation between gene expression of aryl hydrocarbon receptor (AhR), hydrocarbon receptor nuclear translocator (Arnt), cytochromes P4501A1 (CYP1A1) and 1B1 (CYP1B1), and inducibility of CYP1A1 and CYP1B1 in human lymphocytes.’, *Toxicological Sciences: an official journal of the Society of Toxicology*, 71(1), pp. 20–6.

Linenberger, M. L. (2005) ‘CD33-directed therapy with gemtuzumab ozogamicin in acute myeloid leukemia: progress in understanding cytotoxicity and potential mechanisms of drug resistance’, *Leukemia. Nature Publishing Group*, 19(2), pp. 176–182. doi: 10.1038/sj.leu.2403598.

Livak, K. J. and Schmittgen, T. D. (2001) ‘Analysis of Relative Gene Expression Data Using Real-Time Quantitative PCR and the  $2^{-\Delta\Delta CT}$  Method’, *Methods. Academic Press*, 25(4), pp. 402–408. doi: 10.1006/METH.2001.1262.

Ma, Y. et al. (2015) ‘New mouse xenograft model modulated by tumor-associated fibroblasts for human multi-drug resistance in cancer.’, *Oncology reports. Spandidos Publications*, 34(5), pp.

2699–705. doi: 10.3892/or.2015.4265.

Mack, Fiona; Ritchie, Michael; Sapra, P. et al (2014) ‘The Next Generation of Antibody Drug Conjugates’, *Seminars in Oncology*. W.B. Saunders, 41(5), pp. 637–652. doi: 10.1053/J.SEMINONCOL.2014.08.001.

Mansel, R. E., Fodstad, O. and Jiang, W. G. (2007) ‘Metastasis of breast cancer: an introduction’, in, pp. 1–5. doi: 10.1007/978-1-4020-5867-7\_1.

Mantaj, I. et al. (2011) ‘Anti-proliferative and antioxidant effects of *Tinospora crispa* (Batawali)’, *Biomedical Research*. Allied Academies, 22(1).

Mantaj, J. et al. (2015) ‘Crispene E, a cis-clerodane diterpene inhibits STAT3 dimerization in breast cancer cells.’, *Organic & biomolecular chemistry*, 13(13), pp. 3882–6. doi: 10.1039/c5ob00052a.

Marques, I. J. et al. (2009) ‘Metastatic behaviour of primary human tumours in a zebrafish xenotransplantation model’, *BMC Cancer*, 9(1), p. 128. doi: 10.1186/1471-2407-9-128.

Martin, A. M. et al. (2017) ‘Brain Metastases in Newly Diagnosed Breast Cancer: A Population-Based Study.’, *JAMA oncology*. American Medical Association, 3(8), pp. 1069–1077. doi: 10.1001/jamaoncol.2017.0001.

McKay, J. A. et al. (1995) ‘Expression of cytochrome P450 CYP1B1 in breast cancer.’, *FEBS letters*, 374(2), pp. 270–2.

McSherry, E. A. et al. (2007) ‘Molecular basis of invasion in breast cancer’, *Cellular and Molecular Life Sciences*, 64(24), pp. 3201–3218. doi: 10.1007/s00018-007-7388-0.

Mego, M., Mani, S. A. and Cristofanilli, M. (2010) ‘Molecular mechanisms of metastasis in breast cancer—clinical applications’, *Nature Reviews Clinical Oncology*, 7(12), pp. 693–701. doi: 10.1038/nrclinonc.2010.171.

Meshalkina, D. A. et al. (2018) ‘Zebrafish models of autism spectrum disorder’, *Experimental Neurology*, 299(Pt A), pp. 207–216. doi: 10.1016/j.expneurol.2017.02.004.

Mosmann, T. (1983) ‘Rapid colorimetric assay for cellular growth and survival: application to proliferation and cytotoxicity assays.’, *Journal of immunological methods*, 65(1–2), pp. 55–63.

Murray, G. I. et al. (1997) ‘Tumor-specific expression of cytochrome P450 CYP1B1.’, *Cancer research*, 57(14), pp. 3026–31.

Nagini, S. (2017) ‘Breast Cancer: Current Molecular Therapeutic Targets and New Players’, *Anti-Cancer Agents in Medicinal Chemistry*, 17(2), pp. 152–163. doi: 10.2174/1871520616666160502122724.

Newman, D. J. and Cragg, G. M. (2012) ‘Natural Products as Sources of New Drugs over the 30 Years from 1981 to 2010’, *Journal of Natural Products*, 75(3), pp. 311–335. doi:

10.1021/np200906s.

Okuda, K. S. et al. (2016) 'Utilizing Zebrafish to Identify Anti-(Lymph) Angiogenic Compounds for Cancer Treatment: Promise and Future Challenges', *Microcirculation*, 23(6), pp. 389–405. doi: 10.1111/micc.12289.

Otani, M. et al. (2000) 'TZT-1027, an antimicrotubule agent, attacks tumor vasculature and induces tumor cell death.', *Japanese journal of cancer research: Gann*, 91(8), pp. 837–44.

Panowski, S. et al. (2014) 'Site-specific antibody drug conjugates for cancer therapy.', *mAbs*. Taylor & Francis, 6(1), pp. 34–45. doi: 10.4161/mabs.27022.

Parng, C. et al. (2002) 'Zebrafish: A Preclinical Model for Drug Screening', *ASSAY and Drug Development Technologies*, 1(1), pp. 41–48. doi: 10.1089/154065802761001293.

Pasquier, E. and Kavallaris, M. (2008) 'Microtubules: A dynamic target in cancer therapy', *IUBMB Life*. Wiley-Blackwell, 60(3), pp. 165–170. doi: 10.1002/iub.25.

Pathak, A., Jain, D. and Sharma, R. (1995) 'Chemistry and biological activities of the genera *Tinospora*', *International journal of*.

Perez, H. L. et al. (2014) 'Antibody–drug conjugates: current status and future directions', *Drug Discovery Today*, 19(7), pp. 869–881. doi: 10.1016/j.drudis.2013.11.004.

Perou, C. M. et al. (2000) 'Molecular portraits of human breast tumours', *Nature*. Nature Publishing Group, 406(6797), pp. 747–752. doi: 10.1038/35021093.

Pettit, R. K., Pettit, G. R. and Hazen, K. C. (1998) 'Specific activities of dolastatin 10 and peptide derivatives against *Cryptococcus neoformans*.', *Antimicrobial agents and chemotherapy*. American Society for Microbiology, 42(11), pp. 2961–5.

Psaila, B. et al. (2007) 'Priming the "Soil" for Breast Cancer Metastasis: The Pre-Metastatic Niche', *Breast Disease*. Edited by L. Wakefield and K. Hunter. IOS Press, 26(1), pp. 65–74. doi: 10.3233/BD-2007-26106.

Quock, J. et al. (2002) 'Premedication strategy for weekly paclitaxel.', *Cancer investigation*, 20(5–6), pp. 666–72.

Rahman, N. et al. (1999) 'Antimalarial activity of extracts of Malaysian medicinal plants', *Journal of*.

Raimondi, C. et al. (2016) 'A Small Molecule Inhibitor of PDK1/PLC $\gamma$ 1 Interaction Blocks Breast and Melanoma Cancer Cell Invasion', *Scientific Reports*, 6(1), p. 26142. doi: 10.1038/srep26142.

Rivenbark, A. G. et al. (2013) 'Molecular and Cellular Heterogeneity in Breast Cancer', *The American Journal of Pathology*. Elsevier, 183(4), pp. 1113–1124. doi: 10.1016/j.ajpath.2013.08.002.

Roche, H. and Vahdat, L. T. (2011) 'Treatment of metastatic breast cancer: second line and beyond', *Annals of Oncology*. Oxford University Press, 22(5), pp. 1000–1010. doi: 10.1093/annonc/mdq429.

Sacco, A. et al. (2016) 'Cancer Cell Dissemination and Homing to the Bone Marrow in a Zebrafish Model', *Cancer Research*, 76(2), pp. 463–471. doi: 10.1158/0008-5472.CAN-15-1926.

Sawka, C. A. et al. (1986) 'Role and mechanism of action of tamoxifen in premenopausal women with metastatic breast carcinoma.', *Cancer research*. American Association for Cancer Research, 46(6), pp. 3152–6.

Schiff, P. B. and Horwitz, S. B. (1980) 'Taxol stabilizes microtubules in mouse fibroblast cells.', *Proceedings of the National Academy of Sciences of the United States of America*. National Academy of Sciences, 77(3), pp. 1561–5.

Scully, O. J. et al. (2012) 'Breast cancer metastasis.', *Cancer genomics & proteomics*. International Institute of Anticancer Research, 9(5), pp. 311–20.

Siegel, R. L., Miller, K. D. and Jemal, A. (2018) 'Cancer statistics, 2018', *CA: A Cancer Journal for Clinicians*. American Cancer Society, 68(1), pp. 7–30. doi: 10.3322/caac.21442.

Sissung, T. M. et al. (2006) 'Pharmacogenetics and Regulation of Human Cytochrome P450 1B1: Implications in Hormone-Mediated Tumor Metabolism and a Novel Target for Therapeutic Intervention', *Molecular Cancer Research*, 4(3), pp. 135–150. doi: 10.1158/1541-7786.MCR-05-0101.

Spink, D. C. et al. (1997) 'Induction of cytochrome P450 1B1 and catechol estrogen metabolism in ACHN human renal adenocarcinoma cells', *The Journal of Steroid Biochemistry and Molecular Biology*. Pergamon, 62(2–3), pp. 223–232. doi: 10.1016/S0960-0760(97)00024-1.

Stierle, A., Strobel, G. and Stierle, D. (1993) 'Taxol and taxane production by *Taxomyces andreaeanae*, an endophytic fungus of Pacific yew.', *Science (New York, N.Y.)*, 260(5105), pp. 214–6.

Stoletov, K. et al. (2007) 'High-resolution imaging of the dynamic tumor cell vascular interface in transparent zebrafish', *Proceedings of the National Academy of Sciences*, 104(44), pp. 17406–17411. doi: 10.1073/pnas.0703446104.

Sullivan, C. et al. (2017) 'Infectious disease models in zebrafish', in, pp. 101–136. doi: 10.1016/bs.mcb.2016.10.005.

Sutter, T. R. et al. (1994) 'Complete cDNA sequence of a human dioxin-inducible mRNA identifies a new gene subfamily of cytochrome P450 that maps to chromosome 2.', *The Journal of biological chemistry*, 269(18), pp. 13092–9.

Teicher, B. A. and Chari, R. V. J. (2011) 'Antibody Conjugate Therapeutics: Challenges and Potential', *Clinical Cancer Research*, 17(20), pp. 6389–6397. doi: 10.1158/1078-0432.CCR-11-

1417.

Thorn, C. F. et al. (2011) ‘Doxorubicin pathways: pharmacodynamics and adverse effects’, *Pharmacogenet Genomics*, pp. 440–446. doi: 10.1097/FPC.0b013e32833ffb56.

Tobia, C. et al. (2013) ‘Zebrafish embryo as a tool to study tumor/endothelial cell cross-talk’, *Biochimica et Biophysica Acta - Molecular Basis of Disease*. Elsevier B.V., 1832(9), pp. 1371–1377. doi: 10.1016/j.bbadis.2013.01.016.

Tovar, E., Essenburg, C. and Graveel, C. (2017) ‘In vivo Efficacy Studies in Cell Line and Patient-derived Xenograft Mouse Models’, *BIO-PROTOCOL*, 7(1). doi: 10.21769/BioProtoc.2100.

Veinotte, C. J., Dellaire, G. and Berman, J. N. (2014) ‘Hooking the big one: the potential of zebrafish xenotransplantation to reform cancer drug screening in the genomic era’, *Dis Model Mech*, 7(7), pp. 745–754. doi: 10.1242/dmm.015784.

Venghateri, J. B. et al. (2013) ‘Ansamitocin P3 Depolymerizes Microtubules and Induces Apoptosis by Binding to Tubulin at the Vinblastine Site’, *PLoS ONE*. Edited by L. Kurgan, 8(10), p. e75182. doi: 10.1371/journal.pone.0075182.

Vittori, M., Motaln, H. and Turnšek, T. L. (2015) ‘The Study of Glioma by Xenotransplantation in Zebrafish Early Life Stages’, *Journal of Histochemistry & Cytochemistry*. SAGE PublicationsSage CA: Los Angeles, CA, 63(10), pp. 749–761. doi: 10.1369/0022155415595670.

Vredenburg, M. R. et al. (2001) ‘Effects of orally active taxanes on P-glycoprotein modulation and colon and breast carcinoma drug resistance.’, *Journal of the National Cancer Institute*, 93(16), pp. 1234–45.

Wayne C. Widdison et al. (2006) ‘Semisynthetic Maytansine Analogues for the Targeted Treatment of Cancer’. American Chemical Society. doi: 10.1021/JM060319F.

Wehmas, L. C. et al. (2016) ‘Developing a Novel Embryo–Larval Zebrafish Xenograft Assay to Prioritize Human Glioblastoma Therapeutics’, *Zebrafish*, 13(4), pp. 317–329. doi: 10.1089/zeb.2015.1170.

Weigelt, B., Peterse, J. L. and van’t Veer, L. J. (2005) ‘Breast cancer metastasis: markers and models’, *Nature Reviews Cancer*. Nature Publishing Group, 5(8), pp. 591–602. doi: 10.1038/nrc1670.

White, R. M. et al. (2008a) ‘Transparent Adult Zebrafish as a Tool for In Vivo Transplantation Analysis’, *Cell Stem Cell*, 2(2), pp. 183–189. doi: 10.1016/j.stem.2007.11.002.

White, R. M. et al. (2008b) ‘Transparent Adult Zebrafish as a Tool for In Vivo Transplantation Analysis’, *Cell Stem Cell*. BioMed Central, 2(2), pp. 183–189. doi: 10.1016/j.stem.2007.11.002.

White, R., Rose, K. and Zon, L. (2013) ‘Zebrafish cancer: the state of the art and the path forward’, *Nature Reviews Cancer*, 13(9), pp. 624–636. doi: 10.1038/nrc3589.

- Wilson, L. and Jordan, M. A. (1995) 'Microtubule dynamics: taking aim at a moving target', *Chemistry & Biology*. Cell Press, 2(9), pp. 569–573. doi: 10.1016/1074-5521(95)90119-1.
- Wo, Y. Y., Stewart, J. and Greenlee, W. F. (1997) 'Functional analysis of the promoter for the human CYP1B1 gene.', *The Journal of biological chemistry*, 272(42), pp. 26702–7.
- Xie, H. et al. (2004) 'Pharmacokinetics and biodistribution of the antitumor immunoconjugate, cantuzumab mertansine (huC242-DM1), and its two components in mice.', *The Journal of pharmacology and experimental therapeutics*. American Society for Pharmacology and Experimental Therapeutics, 308(3), pp. 1073–82. doi: 10.1124/jpet.103.060533.
- Yang, X. et al. (2013) 'A Novel Zebrafish Xenotransplantation Model for Study of Glioma Stem Cell Invasion', *PLoS ONE*. Edited by D. Ribatti. Public Library of Science, 8(4), p. e61801. doi: 10.1371/journal.pone.0061801.
- Yen Jennifer, White Richard, S. D. (2014) 'Zebrafish models of cancer: progress and future challenges', *Current Opinion in Genetics & Development*. Elsevier Current Trends, 24, pp. 38–45. doi: 10.1016/J.GDE.2013.11.003.
- Yin, H.-C. et al. (2008) 'Influence of TCDD on Zebrafish CYP1B1 Transcription during Development', *Toxicological Sciences*, 103(1), pp. 158–168. doi: 10.1093/toxsci/kfn035.
- Zhao, S., Huang, J. and Ye, J. (2015) 'A fresh look at zebrafish from the perspective of cancer research.', *Journal of experimental & clinical cancer research: CR*. BioMed Central, 34(1), p. 80. doi: 10.1186/s13046-015-0196-8.
- Zhou, Q. (2017) 'Site-Specific Antibody Conjugation for ADC and Beyond.', *Biomedicines*. Multidisciplinary Digital Publishing Institute (MDPI), 5(4). doi: 10.3390/biomedicines5040064.
- Zon, L. I. and Peterson, R. T. (2005) 'In vivo drug discovery in the zebrafish', *Nature Reviews Drug Discovery*, 4(1), pp. 35–44. doi: 10.1038/nrd1606.
- Zulhairi, A., Abdah, M. and Kamal, N. (2008) 'Biological Properties of *Tinospora crispa* (Akar Patawali) and Its Antiproliferative Activities on Selected Human Cancer Cell Lines.', *Malaysian journal of*.



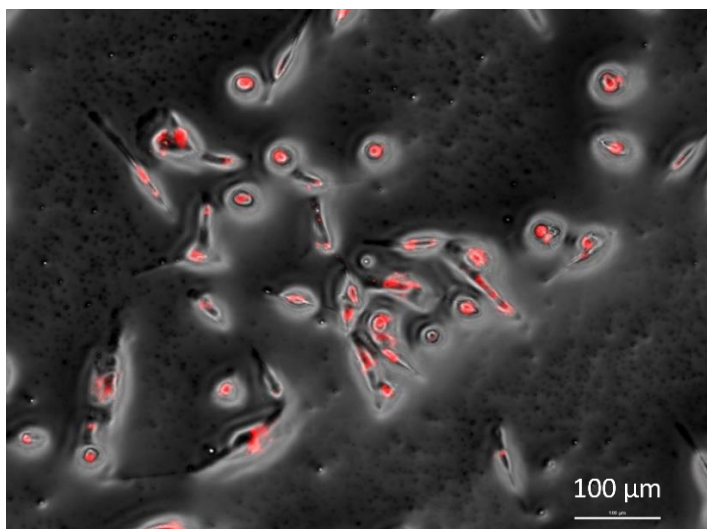
## **APPENDIX**

## OPTIMIZATION

### 1.6 In vitro optimization

#### 1.6.1 Transfection vs. Lypophilic dye

For visualization of BC cells in the xenografts, the cancer cells were fluorescently tagged. Initially, the cells were transfected with a red fluorescent protein plasmid pCMV DsRed Express 2. Upon visualization under a fluorescence microscope, we observed that a small percentage of the transfected cells did not exhibit fluorescence. Moreover, the MTS assays performed in transfected cells vs parental control cells showed significant sensitivity among the two sets of cells. Therefore, we decided to use CM-DiI to label the cells and cells showed fluorescence up to nine days after they were labeled (Figure 1).



**Figure 21:** MDA-MB-231 cells labeled with CM-DiI visualized under TRITC filter.

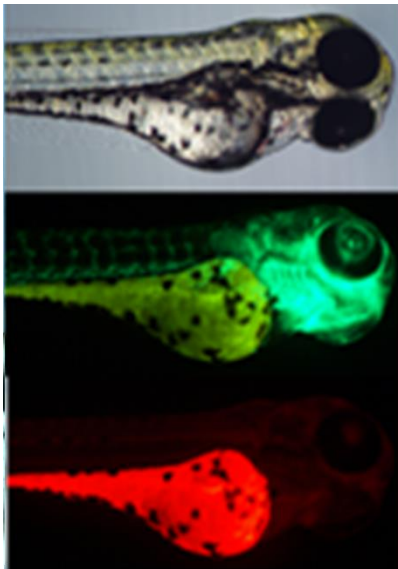
#### 1.6.2 Effect of media on growth of different cancer cells:

To determine the effect of media on the three different cell lines, BT-474 and MDA-MB-231 were grown in DMEM supplemented with 10% FBS and 1% P/S 37° C for a period of one

week and compared the growth (number of cells) with the BT-474 growing in Hybri-Care Medium (ATCC® 46-X™) media supplemented with 10% FBS and 1% P/S and MDA-MB-231 cells growing in DMEM F12 supplemented with 10% FBS and 1% P/S. We did not observe any significant changes in the number of cells growing in the two flasks. Therefore, to eliminate the variables, we maintained MCF-7, BT-474, and MDA-MB-231 cell cultures in DMEM supplemented with 10% FBS and 1% P/S.

### **1.6.3 Effect of Doxorubicin in zebrafish larvae**

Zebrafish larvae were exposed to different concentrations of DOX (0.5-25 $\mu$ M) over a period of 96 hours with replacement of doses every 24 hour and observation for deformities (Figure 12). At 6.5  $\mu$ M or higher concentrations, there was an accumulation of DOX in the intestinal cavity of the larvae starting as soon as 24 hours post treatment. The accumulation was observed to be more in larvae exposed to higher concentrations. The larvae exposed to a concentration of 25 $\mu$ M were deformed and did not survive. Moreover, we observed that larvae exposed to DOX, when observed under a fluorescence filter (TRITC) exhibited red fluorescence as shown in Figure. This was an indication of uptake of DOX by the larvae and provides support to our waterborne exposures in the larvae. However, this contradicted with the fluorescence of the CM-DiI labeled BC cells and we decided not to use DOX as our positive control.



**Figure 20** Pictomicrographs of 4-day old zebrafish larvae after exposure to 12.5  $\mu$ M DOX for 24 hours. Image acquired at 10x magnification using brightfield, FITC, and TRITC filters

## **1.7 In vivo optimization**

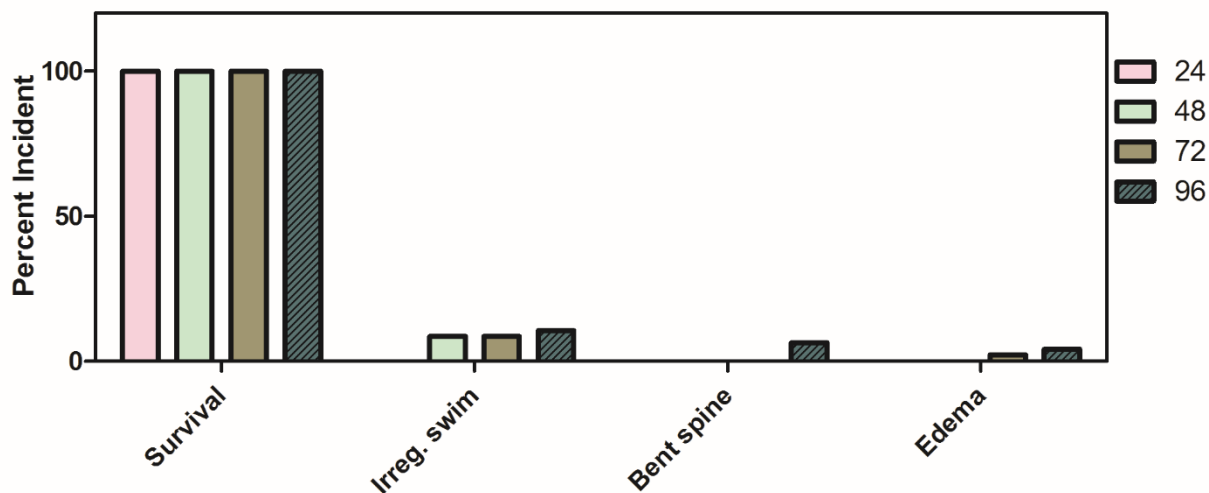
### **1.7.1 Preparation of agar coated petridish for microinjection:**

For injecting zebrafish larvae at 2 and 3 dpf the larvae were placed in a plastic petridish positioned dorsally against a glass slide. The larvae were unstable and low survival rate after injection was observed. The larvae require an appropriate setup to survive the microinjection and at the same time, be stably positioned so the microinjection procedure can be efficiently carried out. Therefore, we used low-melting agarose gel (0.1%) to coat the petridish and before the gel solidified completely, we used capillaries to make indentations in the gel for positioning the embryos for microinjection. This method ensured successful orientation of larvae and microinjection in the yolk sac. The larvae were easily transferred to a petridish containing embryo water for revival.

#### **1.7.1.1 Determination of optimum temperature for zebrafish and human BC cells:**

Human cell lines are incubated at a temperature of 37°C, at which they grow and proliferate normally. Zebrafish embryos, on the other hand, are incubated at a temperature of 28°C for the initial five days of their life until they reach the stage where they require an external food source. Zebrafish larvae xenografted with human cells cannot survive because of the increase in temperature by 9°C and the cells also cannot survive a temperature which is approximately 9°C lower than the human body temperature. So, for normal proliferation of BC cells in the fish, and normal growth of the larvae, we incubated the larvae and the cells separately at different temperatures. We observed that at 34°C, both the fish and the cells grew normally, without any deformities in the fish, and normal proliferation of the BC cells. The BC cells, MCF-7, BT-474, and MDA-MB-231, were plated in T25 flasks and the cell counts were measured after incubating the cells at 37°C and 34°C for 72 hours. No significant differences were observed in the cell

numbers. For zebrafish, we incubated zebrafish eggs at 28°C and 34°C and observed the embryos after every 24 hours to determine if there were any deformities associated with the increased temperature. We observed no deformities at 34°C but the embryos hatched at 2dpf as opposed to 3 dpf at 28°C.



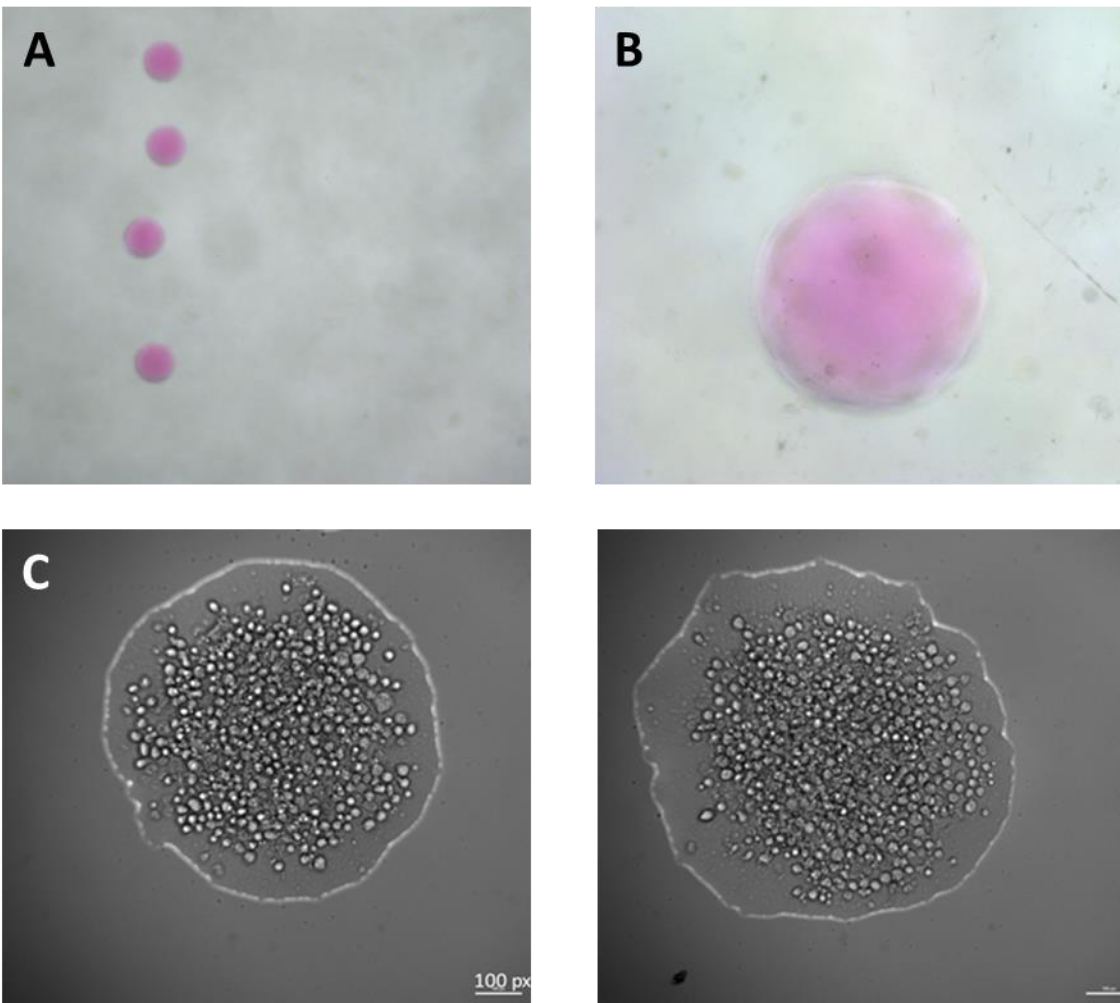
**Figure 21:** Percent incidence of larvae incubated at 34 for a period of 4 days for different parameters was evaluated. The larvae (n = 48) were placed in a 48 well plate and evaluated for survival and deformities such as irregular swimming, curved body axis (bent spine), and pericardial and yolk sac edemas.

## 1.7.2 Xenotransplant optimization

### 1.7.2.1 Injection cell volume:

The number of cells required per mL to get 100-150 cell in 5 nl cell suspension were calculated to be  $1 \times 10^6$ /ml. The cell suspension was injected from the microneedle on a droplet of oil placed on a glass slide and averaged the number of cells in 3 injections from each microneedle. The diameter of the injection droplets was measured using a stage micrometer. The image of the stage micrometer was captured at the same focus and magnification as the injection droplet. The required diameter of the injection diameter to make the injection volume to be approximately 5 nL

was 106 mm. The volume was calculated using the formula  $\frac{4}{3} \pi r^3$ . Additionally, the number of cells in each droplet were also manually counted from images of the injection droplet under higher magnification (20x) using Nikon Eclipse Ti2 (Figure 22). The number of cells observed from both methods were compared to confirm the number of cells/injection.



**Figure 22:** Pictomicrographs of injection droplets in oil. A) Image of four consecutive injections acquired at 4x magnification. B) Image of injection acquired at 10 x magnification. C) Image of two injections acquired at 20x magnification using bright field

### **1.7.2.2 Injection time determination:**

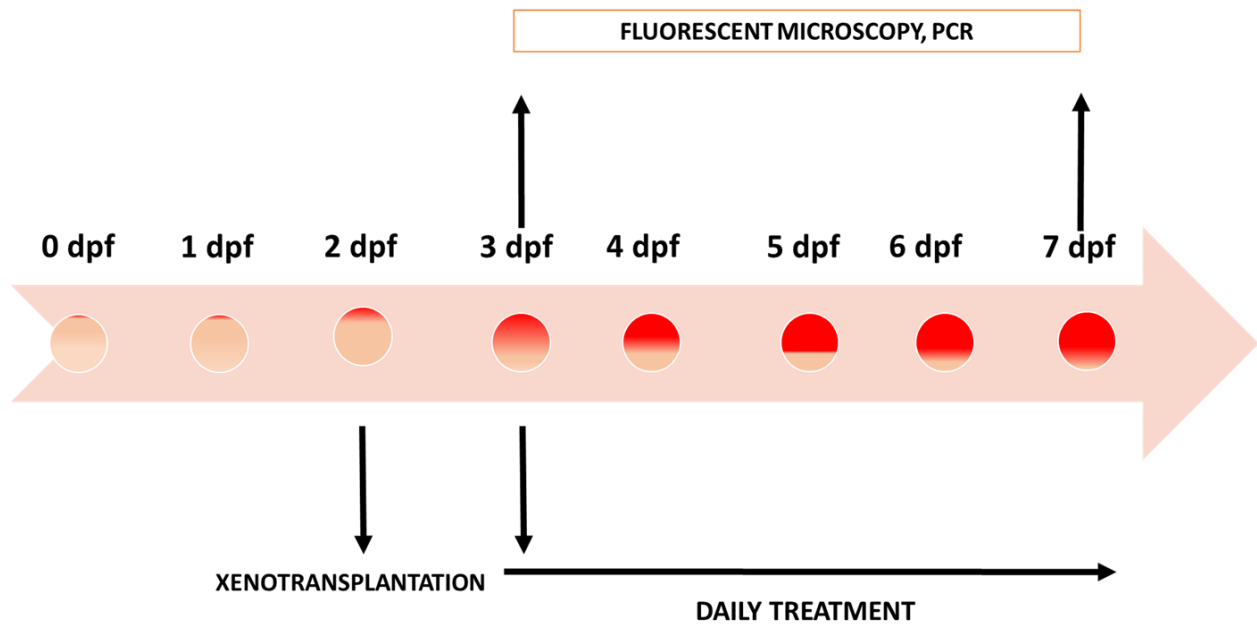
To determine the optimum survival of the fish and its ability to sustain the microinjection, microinjections in the zebrafish were performed at 0, 1, and 2 dpf. At 0 dpf, the dechorionated embryos immediately died from the injections. The larvae were injected at 2 and 3 dpf, and observed the xenografted larvae for 6 days post injection. At 3 dpf the larvae were challenging to inject as yolk sac was harder to penetrate with the microneedle and most of the injected larvae did not retain the cancer cells (upon observation under the fluorescence filter). Whereas the larvae injected at 2 dpf exhibited the ability to retain the BC cells and exhibited higher survival rate post injection. Therefore, all subsequent microinjections were carried out at 2 dpf.

### **1.7.2.3 Xenotransplant assay timeline:**

To study the proliferation of BC cells and to determine the effects of treatment on the larvae post injection, the survival of the larvae post injection was observed up to 9 dpf. It was observed that after 7 dpf, the larvae had a higher mortality rate. And as described in the previous section, 2 dpf was determined as the optimum time to inject the larvae. Hence, we decided to inject the fish at 2 dpf and conduct our evaluation studies until 5 dpi or 7 dpf. The xenotransplantation assay



timeline is illustrated in Figure 23.



**Figure 23:** Timeline of the Xenotransplant Assay

### 1.7.3 Microscopy optimization

#### 1.7.3.1 Mounting medium:

Imaging individual larvae requires proper mounting material in order to keep the anaesthetized larvae in place. Initially, anaesthetized larvae were inserted in warm 1% agarose gel (not solidified) and then a drop of the agarose gel along with the larvae was sucked up and placed on the glass slide. After imaging several larvae, autofluorescence of agarose gel was observed and added a lot of background to the fluorescent images. Thereafter, alternate materials such as gelatin and 2% noble agar gel were tested as the mounting gel and observed for autofluorescence. Gelatin exhibited autofluorescence. For noble agar, a 2% noble agar gel solidified within an immunohistology chamber was used and a groove was carved in the gel to house the anaesthetized larvae for imaging. However, the volume of tricaine around the fish had to be optimized to ensure

that the tricaine did not dry up from the heat emanating from the laser of the microscope lens. We observed that noble agarose did not autofluoresce and did not interfere with the fluorescence signal of the fish. Additionally, as suggested by Dr. Joshua Bloomekatz, we utilized electric tape to construct an elevation on a coverslip and cut out the tape forming a rectangular space (Figure 5) and anaesthetized larvae was placed onto the space in tricaine and covered using another coverslip. This provided an enclosure for the larvae and provided the opportunity to enhance our field of view of the larvae. We obtained much clearer images using this technique.

With the arrival of Nikon Eclipse Ti2, we were able to image fish in a 48 well plate using (0.08%) low melt agarose. This was much faster, had better image quality, and we were able to image more fish in the same period of time.



**Figure 24:** Elevation created using electrical tape on a coverslip for mounting anaesthetized zebrafish larvae for imaging under fluorescence microscope. The anaesthetized larvae were stable in this setting for 4-5 hours

## 1.8 Quantification of breast cancer cell proliferation via PCR

### 1.8.1.1 Real Time PCR in cells

For our studies, it was important to identify a gene that is expressed by BC cells but not

constitutively expressed by normal zebrafish cells to compare the effect of treatment with candidate compounds versus controls. As CYP1B1 is frequently expressed in human BC, we chose this as our gene of interest. The CYP1B1 primers used were previously published (Lin et al. 2003). In zebrafish, two types of CYP1 family genes have been characterized. *cyp1a* is expressed in liver and *cyp1b1*, *cyp1c1* and *cyp1c2* are transcribed in the heart and eye in adult zebrafish. During development, *cyp1b1* is expressed maximally within 2-3 dpf, with specific expression in ocular cells, diencephalon, and the midbrain-hindbrain boundary determined by whole-mount RNA in situ hybridization analysis (Yin et al. 2008). So, we selected human CYP1B, specifically expressed in the three cancer cell lines, as a marker of tumor cell expression and proliferation in zebrafish larvae xenotransplanted with human breast cancer cells.

To detect the expression of CYP1B1 in MCF-7, BT-474, and MDA-MB-231 cells, the cells were plated in 12 well plates at the density of  $2.5 \times 10^5$  cells/well in 1 mL of DMEM and incubated at 37°C supplemented with 5% CO<sub>2</sub>. At 90% confluence, cells were detached using tryPLE EXPRESS (ThermoFisher Scientific, CA). TryPLE was neutralized using equal volume of DMEM and cells were centrifuged at 4000 rpm (2670 x g) for 5 minutes. Cells were counted, and  $1 \times 10^6$  cells were used for mRNA extraction. Cell pellet was lysed with lysis buffer (Thermo Scientific, CA) supplemented with 2% β-mercaptoethanol. Further extraction of mRNA was conducted using GeneJET RNA purification kit and as instructed by manufacturer (Thermo Scientific, CA). The concentration of mRNA quantified using Nanodrop 2000, and the purity of mRNA was determined by assessing the  $A_{260}/A_{280}$  ratio and samples with values >2 were used for further experimentation. The RNA samples were reverse-transcribed to cDNA using Taqman® Reverse Transcription reagents (Applied Biosystems, CA): random hexamers, Multiscribe Reverse Transcriptase, RNase inhibitor, deoxyNTP mix, 25 mM MgCl<sub>2</sub>, 10xRT buffer in 25 μL

reaction. The temperature program used was 25 °C for 10 min, 37 °C for 60 min and 95 °C for 5 min. RT-qPCR was performed in Applied Biosystems 7200 using SYBR Green (Applied Biosystems, Massachusetts) and the parameters used were: 95 °C for 10 min, then 40 cycles of 95 °C for 15 sec and 60 °C for 1 min, followed by 95 °C for 15 sec, 60 °C for 1 min, 95 °C for 15 sec dissociation curve. CYP1B1 and 18S were amplified in duplicate in separate reactions on the same plate. The fold induction of CYP1B1 mRNA in xenotransplanted zebrafish relative to non-injected larvae were normalized to 18S given by formula  $=2^{-\Delta\Delta C_T}$  as described by (Livak and Schmittgen, 2001), where  $C_T$  was the threshold cycle indicating the fractional cycle number corresponding to the threshold attained by the amplified CYP1B1.

**Table 7:** RT-qPCR primers

CYP1B1	F: 5'-GCTGCAGTGGCTGCTCCT-3' R: 5'-CCCACGACCTGATCCAATTCT-3'
18S	F: 5'-TGG TTA ATT CCG ATA ACG AAC GA-3' R: 5'-CGC CAC TTG TCC CTC TAA GAA-3'

#### 1.8.1.2 RT-qPCR in zebrafish

To detect CYP1B1 in xenografted larvae and to confirm that human CYP1B1 was not expressed in un-injected larvae, zebrafish larvae xenotransplanted with the breast cancer cells were pooled (20 fish per vial repeated twice) at 1 dpi and 5 dpi in RNA later and stored at -80 °C until we performed RNA isolation on them. RNA was isolated from the larvae using TRIzol (Invitrogen, Massachusetts), RNase-Free DNase set (Qiagen, California), and RNeasy mini kit (Qiagen, California) using manufacturer's protocol. The extracted RNA was then quantified on a NanoDrop

2000 (ThermoFisher Scientific, Massachusetts) and samples were evaluated for acceptable  $A_{260}/A_{280}$  ratio. Further reverse-transcription and RT-qPCR were performed as described above. The statistical significance from RT-qPCR results was analyzed using one-way ANOVA and Tukey's post hoc test where statistical significance was found to be at  $p \leq 0.05$ . RT-qPCR results.

Human CYP1B1 was measured using RT-qPCR in the three cancer cell lines MCF-7, BT-474, and MDA-MB-231, and in zebrafish xenografted with MCF-7 and MDA-MB-231 cells. Un-injected zebrafish larvae were also quantified to detect any expression. Expression of CYP1B1 was detected in all three cell lines and the xenograft larvae, but not detected in un-injected larvae.

To our knowledge, the expression of a gene as a quantitative method to determine the effect of anti-cancer compounds has not been done before and represents an additional method that can be used to validate the effect of treatment. Although, high concentration of mRNA from zebrafish xenografts could not be extracted, the expression of CYP1B1 in the breast cancer cell lines and the xenografted fish was detected.

## VITA

### EDUCATION

---

- 08/2013 – present**      **Ph.D.** in Pharmaceutical Sciences (Pharmacology), **The University of Mississippi**, University, Mississippi, USA  
Dissertation: Developing Zebrafish as an In Vivo Model to Screen Compounds for Human Breast Cancer, under the supervision of Dr. Kristine L. Willett.
- 08/2008 – 08/2012**      **Bachelor of Pharmacy**, **Punjab Technical University**, Punjab, India

### WORK EXPERIENCE

---

- 08/2013 – present**      **Graduate Student Investigator**, The University of Mississippi, University, MS, USA
- Zebrafish Assays
- Developed *in vivo* safety assays to determine maximally tolerated dose of anti-cancer compounds for screening, evaluated developmental deformities.
  - Optimized microinjection techniques for volume of injection; number of cancer cells injected, location of injection, age of injection, and survival of larvae post injection.
  - Utilized fluorescent microscopy for live fish imaging to monitor metastasis of breast cancer cells, acquire z stacks for an accurate quantification, analyzed images using NIS Elements (Nikon).
  - Performed sectioning and staining of adult zebrafish for histology to determine the multigenerational effects of benzo[a]pyrene (B[a]P) on reproduction in the offspring of parents exposed to B[a]P.
  - Developed transgenic zebrafish crosses using adult Casper and Tg(*fli1:egfp*) transgenic strains of zebrafish to obtain transparent zebrafish larvae with GFP labeled vasculature.
- In vitro Assays
- Screened anti-cancer compounds using MTS assay, determined sensitivity imparted by transfection/staining of cancer cells in response to anti-cancer compounds.
  - Optimized incubation temperature of human breast cancer cells for xenotransplantation assays.
  - Determined the effect of treatment with anti-cancer compounds on the expression of CYP1B1 gene in human breast cancer cell lines.

- 09/2012 – 05/2013**     **Executive Manager under training**, ION Healthcare LTD. (a medium scale pharmaceutical products manufacturer and supplier), Quality Control/Quality Assurance, Himachal Pradesh, India
- Learned fundamentals of Quality Assurance, Quality Control and Production; Handling Artwork, Batch Manufacturing Record/Batch Procedures (BMR & BPR), Regulatory Documentation
  - Conducted quality control tests on raw materials, semi-finished and finished tablets, capsules and liquid formulations

## SKILLS

- 
- Zebrafish Expertise**     Raising, maintenance, and spawning of zebrafish; Development of transgenic zebrafish lines; Safety and Toxicity assays in zebrafish larvae; RNA isolation; Xenotransplantation of human cancer cells in zebrafish (microinjection technique); RT-qPCR, Mounting and imaging live zebrafish larvae, Sectioning adult zebrafish; H&E staining (histology).
- Other Techniques**     Cell culture techniques (thawing, freezing, plating), Transfection, Staining, *In vitro* cytotoxicity assays, *In vitro* drug screening (selection of potent compounds with anti-cancer activity based on IC<sub>50</sub>), RNA isolation, RT-qPCR, Gel Permeation Chromatography, HPLC, Centrifugation Microbial culture techniques, Protein Extraction-Purification & Quantification.

## TEACHING EXPERIENCE

- 
- 08/2013 – present**     *Teaching Assistant*, The University of Mississippi, University, MS
- Pathophysiology
  - Advanced Pathophysiology
  - Basic and Clinical Pharmacology

## PROJECTED PUBLICATIONS

- 
1. T. Dhawan, K. Willett. **Zebrafish as drug discovery screen for novel chemotherapeutics for treatment of human breast cancer**. Scientific Reports (In Preparation)

## PRESENTATION/CONFERENCE PROCEEDINGS

- 
1. Dhawan T., Ashpole N., Willett K. **Using Transgenic Zebrafish Larvae for Xenotransplantation of Human Breast Cancer Cells and Screening of Natural Compounds for Anti-Cancer Activity**. SOT Annual meeting and Exposition, San Antonio, Texas, USA, March 2018.
  2. Dhawan T., Anderson A., Brooks T., Willett K. **Xenotransplantation of Human Breast Cancer Cells in Zebrafish for Screening of Chemotherapeutic Compounds**. SOT Annual meeting and Exposition, Baltimore, Maryland, USA, March 2017.
  3. Dhawan T. **Fighting Breast Cancer: The Natural Way**. Graduate School Three Minute Thesis Competition, UM, October 2016
  4. Dhawan T., Anderson A., Brooks T., Willett K. **Developing An In Vivo Screen To Test The Efficacy And Safety Of Curcumin Against MCF-7 Breast Cancer Cells**. SOT Annual meeting and Exposition, New Orleans, Louisiana, USA, March 2016.

5. Dhawan T., Fang X., Corrales J., Thornton C., Scheffler B., Willett K., **Transcriptomic Changes in Zebrafish Embryos and Larvae Following Benzo[A]Pyrene Exposure**. AAPS Annual meeting and Exposition, San Diego, California, USA, March 2015.
6. Dhawan T., Thornton C., Corrales J., Burkett A., Shore J., White M.B, and Willett, K.L. **Reproductive Effects of Dietary Benzo[a]pyrene Exposure in Zebrafish drugs**. South Central Chapter of SOT Annual meeting, Oxford, MS, October 2015.
7. Dhawan T., **DNA Methylation and Gene Expression in Fish Liver Tumorigenesis**. BioMolecular Sciences Department Seminar Series, University of Mississippi, MS April 2014.
8. Dhawan T., Khan N., **Anxiolytic Effects of Eucalyptus Leaf Extracts in Mice**. 15th Science Congress held at Guru Nanak Dev University, Amritsar February 2012.

## SCIENTIFIC AND PROFESSIONAL OUTREACH

---

<b><u>Reviewer</u></b>	Manuscript reviewer for Drug and Chemical Toxicology Journal
<b><u>Volunteer</u></b>	Continuing Education Course, SOT Annual meeting and Exposition, March 2017 <u>Course</u> : “Reproductive Toxicity: Challenges and Practical Approaches to Determine Risk in Drug Development”
<b><u>Sponsorship Commit Member</u></b>	American Scientists of Indian Origin Special Interest Group (SIG), SOT, January 2015 - March 2016 <ul style="list-style-type: none"> <li>▪ Brainstormed ideas for inviting sponsorships for awards and reception</li> <li>▪ Drafted invitation letters for sponsorships from Pharmaceutical companies</li> </ul>
<b><u>Cultural Secretary</u></b>	▪ Indian Association of North Mississippi, January 2015- 2017
<b><u>Co-author</u></b>	▪ Civil Society report on Status of Right to Education ACT implemented in Delhi (in collaboration with a NGO “JOSH”) December 2012- March 2013
<b><u>Educator</u></b>	▪ Educated underprivileged school children (grades 1-9) November 2011- March 2013
<b><u>Judge</u></b>	▪ Lower Science Fair (grades 5-8), University of Mississippi, 2016-2017 ▪ Mississippi State Science Fair (grades 10-12), University of Mississippi, April 2016
<b><u>Social Liaison</u></b>	BioMolecular Sciences Journal Club, University of Mississippi, May 2016- January 2017
<b><u>Coordinator</u></b>	International Olympics for Special Children, Chandigarh, India, August 2008
<b><u>Certification</u></b>	Epigenetic Control of Gene Expression by The University of Melbourne on Coursera. September 2015

## AWARDS & HONORS

- 
- 2018** ▪ Dissertation Writing Fellowship



- 2017** ■ Edith Pritchard Graduate Student Award  
■ South Central Chapter Travel Award for Society of Toxicology Annual Meeting, Baltimore, Maryland, USA
- 2016** ■ Graduate Student Council Research Grant, The University of Mississippi, University, Mississippi, USA  
Project: Developing an in vitro and in vivo model to screen chemotherapeutic compounds for the treatment of human breast cancer.  
Role: PI  
■ Graduate School Council Travel award for SOT Annual Meeting, New Orleans, Louisiana, USA
- 2015** ■ Best Graduate Student Poster award for Graduate School Council Research Forum poster presentation  
■ Reproductive and Developmental Toxicology Specialty Section (RDTSS) Travel award for SOT Annual Meeting, San Diego, California, USA  
■ Graduate School Council Travel award for SOT Annual Meeting, San Diego, California, USA
- 2011** ■ Winning Team, National Pharmacy Quiz, Punjab, India